AD NUMBER

AD803262

NEW LIMITATION CHANGE

TO

Approved for public release, distribution unlimited

FROM

Distribution authorized to U.S. Gov't. agencies and their contractors; Administrative/Operational Use; OCT 1966. Other requests shall be referred to Army Electronics Command, Fort Monmouth, NJ.

AUTHORITY

USAEC ltr 27 Jul 1971

UNCLASSIFIED

AD_____

TECHNICAL REPORT ECOM-01241-F

WAVE PROPAGATION STUDIES RELATED TO THE THEORY OF NEAR 1 CPS MAGNETIC EFFECTS OF HIGH ALTITUDE NUCLEAR DETONATIONS

FINAL REPORT VOLUME II

BY
ROBERT F. SMILEY

OCTOBER 1966

ECOM

UNITED STATES ARMY ELECTRONICS COMMAND · FORT MONMOUTH, N. J.
CONTRACT NO. DA28-043-AMC 01241(E)
GEOPHYSICS DIVISION
ALLIED RESEARCH ASSOCIATES, INC.
CONCORD, MASSACHUSETTS

UNCLASSIFIED

3

UNCLASSIFIED

AD_____

TECHNICAL REPORT ECOM-01241-F

WAVE PROPAGATION STUDIES RELATED TO THE THEORY OF NEAR 1 CPS MAGNETIC EFFECTS OF HIGH ALTITUDE NUCLEAR DETONATIONS

REPORT NO. 15
CONTRACT DA-28-043-AMC 01241(E)
(Continuation of Contract DA-36-039-SC-89177)
FINAL REPORT VOLUME II
28 FEBRUARY 1965 TO 22 APRIL 1966

BY
ROBERT F. SMILEY

"The work prepared under this contract was made possible by the support of the Advanced Research Projects Agency under ARPA Order No. 163-61, Amendment No. 9 dated 16 July 1964, Project Code No. 4820, which provides for an additional project in the Vela Sierra Program, through the United States Army Electronics Laboratories."

OCTOBER 1966

ECOM
UNITED STATES ARMY ELECTRONICS COMMAND · FORT MONMOUTH, N. J.
DA PROJECT NO. 5011.11.854.01.33
GEOPHYSICS DIVISION
ALLIED RESEARCH ASSOCIATES, INC.
CONCORD, MASSACHUSETTS

BLANK PAGE

ABSTRACT

Results are presented from a group of theoretical studies of wave propagation in horizontally stratified media representative of the ionosphere and the sub-ionosphere. The report contains: four studies of the transient three-dimensional magnetic fields produced by magnetic dipoles in various combinations of horizontally stratified isotropic plasma and vacuum regions; and six studies of one-dimensional hydromagnetic wave propagation in horizontally stratified plasma and vacuum regions. Also included are bibliographies concerning natural ULF magnetotelluric effects, ULF lightning effects, reflection and refraction of hydromagnetic waves, and hydromagnetic wave propagation in the ionosphere.

FOREWORD

This volume describes and presents results of theoretical studies of electromagnetic and hydromagnetic wave propagation in horizontally stratified plasma and un-ionized regions. These studies were performed for the United States Army Electronics Laboratories as a part of a more general study of the ULF magnetotelluric effects of high altitude nuclear detonations. Volume I of this report presents a summary of this research program, performed under USAEL Contract No. DA-28-043-AMC-01241(E), and presents these results of this program which pertain more directly to experimental ULF magnetotelluric measurements of nuclear detonations and to their theoretical interpretation.

TABLE OF CONTENTS

TABLE OF CONTENTS (cont)

LIST OF ILLUSTRATIONS

LIST OF ILLUSTRATIONS (cont)

LIST OF TABLES

LIST OF COMMON SYMBOLS

$A(t)$	Response of a linear system to a unit step function
$\overline{B}$	Time-dependent component of magnetic induction vector
$\overline{B}_o$	Constant vector component of a magnetic field
B_x, B_y, B_z	Components of $\overline{B}$ in rectangular cartesian coordinates
B_ρ, B_θ, B_ψ	Components of $\overline{B}$ in spherical polar coordinates
c	Speed of light in vacuum
C	Dipole moment times $\mu/4\pi$
Ci	Cosine integral
erf	Error function
erfc	Complementary error function
$\overline{E}$	Electric Field vector
E_x, E_y, E_z	Rectangular cartesian components of $\overline{E}$
f	Frequency in cycles per second
$\overline{F}$	Vector potential
h	Height above sub-ionosphere or vacuum cavity
$h(t)$	Response of a linear system to a unit impulse
h_2	Height of plasma slab above a vacuum cavity
H	Height of sub-ionosphere or vacuum cavity
$H(i\omega)$	Frequency response function of a linear system
I	Modified Bessel function of the first kind
J, J'	Bessel function of the first kind and its first derivative
$\overline{J}$	Current density vector
J^*	Asymptotic expression for J (See Eqs. (D.17) and (D.18))
k	Wave number
K	Modified Bessel function of the second kind
m	Dipole moment

p	Scale distance associated with Alfven speed variation in the upper ionosphere
r	Radial distance
R	Reflection coefficient
R(x)	Designates real part of x
s	Transformed variable of the Laplace transform
sgn (x)	Sign of x (+ 1 for x > 0; - 1 for x < 0)
S(t)	Step function (S (t) = 0 for t < 0 and S (t) = 1 for t > 0)
Si	Sine integral
t	Time
T	Period or characteristic time
$\bar{v}$	Plasma velocity
V	Wave propagation speed
V_a	Alfvén speed
V_m	Wave front speed in a hydromagnetic plasma
w	Function defined by Equation (B.2.22)
W	Function defined by Equation (B.8.35)
x	Horizontal distance
y	Horizontal distance perpendicular to X-axis
z	Vertical distance
α	Damping parameter (Eq. (2.1))
γ	Propagation constant ($\gamma = ik$)
$\delta(t)$	Delta or impulse function of t (see Appendix E)
δ_n	n'th derivative of the delta function (see Appendix E)

θ	Polar angle
μ	Permeability in vacuum
ν	Collision or damping frequency
ρ	Horizontal distance
σ	Conductivity
σ_o	Real part of conductivity
τ	Non-dimensional time
φ	Acute angle between geomagnetic field vector and the vertical
Φ	Flux
$\bar{\Phi}$	Divergence of vector potential in Appendix A
ψ	Azimuthal angle
ω	Frequency, rad/sec

SUBSCRIPTS

p	Plasma
v	Vacuum
x	X-component
y	Y-component
z	Z-component

SECTION I

INTRODUCTION

The subject of ultra-low-frequency (ULF) magnetohydrodynamic wave propagation has recently become of importance because of its relationships to solar induced geomagnetic disturbances and to near 1 cps magnetotelluric effects of high altitude nuclear detonations. However, the present understanding of this subject is quite limited because of the considerable mathematical difficulties involved in solving any problem of hydromagnetic wave propagation through complex plasma media, except for the simplest cases where the plasma is completely uniform or has slowly varying properties (so that a WKB approach may be used). In order to improve present understanding of hydromagnetic wave propagation in the ionosphere, two groups of related theoretical wave propagation studies were made under USAECOM sponsorship, the results of which are summarized in Sections II and III of this report. The first group of studies, summarized in Section II and described in detail in Appendix A, considers the three-dimensional electromagnetic fields produced by magnetic dipoles in various combinations of horizontally stratified isotropic plasma regions. The second group of studies, summarized in Section III and described in detail in Appendix B considers various one-dimensional problems of hydromagnetic wave propagation. Section IV discusses the application of these study results to ionospheric wave propagation problems.

A bibliography is included covering four groups of topics associated with the subject of ULF wave propagation in horizontally stratified media representative of the ionosphere.

BLANK PAGE

SECTION II

SUMMARY OF THREE-DIMENSIONAL WAVE PROPAGATION STUDIES

2.1 INTRODUCTION

Appendix A of this report presents a theoretical analysis of four three-dimensional problems concerned with the steady-state and transient magnetic fields produced by magnetic dipoles in various types of horizontally stratified plasma and un-ionized media. The principal results of these studies are summarized below, details being given in Appendix A.

It is assumed throughout this section that Maxwell's equations are applicable with an isotropic conductivity law and that the displacement current may be neglected in vacuum regions. This assumption of isotropic conductivity is, of course, not generally exactly applicable to hydromagnetic wave propagation studies, which are our principal concern in this report. However, to a considerable degree, both qualitatively and quantitatively, a study of these problems offers considerable insight into the corresponding hydromagnetic problems.

In this section the term perfect plasma is used to refer to a plasma with purely imaginary conductivity; the term complex plasma for a complex conductivity; and the term ohmic plasma for a real conductivity (see Sec. A. 2).

2.2 MAGNETIC DIPOLE IN A UNIFORM PLASMA

Section A. 3 of Appendix A presents a derivation of the steady-state and step-function-response electromagnetic fields produced by a magnetic dipole in an infinite uniform plasma. These results are exactly applicable to the analogous case of a hydromagnetic plasma, provided that the dipole axis is parallel to the ambient magnetic field for the hydromagnetic case.

Considering only the magnetic fields produced by a suddenly created magnetic dipole, the transient magnetic fields are shown in Figures 2.1 through 2.3, where the following symbols are used

α is a damping parameter
r is distance from dipole to observer
ν is a characteristic collision damping frequency
σ_o is the real component of conductivity
V is the phase speed
μ is the permeability in vacuum

$$\alpha = \tfrac{1}{2} \nu \, r / V = \tfrac{1}{2} \mu \sigma_o V r \qquad (2.1)$$

and where B_r and B_θ are radial and tangential components of the transient magnetic field in polar coordinates with respect to the dipole axis in a plane through the dipole axis. The azimuthal component of the transient magnetic field is zero.

For a perfect plasma, the transient magnetic field takes the form of a wave front moving into the plasma at the phase speed V, with the magnetic field ahead of the front being zero (for $Vt/r < 1$) and behind the front being equal to that for the static dipole condition (see curve for $\alpha = 0$ in Fig. 2.1). Both of the magnetic field components B_r and B_θ contain infinite impulses at the wave front (see Eqs. (A.3.13) and (A.3.14)).

For the case of a complex plasma ($\alpha > 0$) with small to moderate value of damping ($\alpha \lesssim 1$), a similar behavior occurs (see curves for $\alpha = 1$ in Fig. 2.1), except that the initial peak field strength (just behind the wave front) for the radial component (B_r) is somewhat smaller than the static value and is larger for the tangential component. Both components vary monotonically toward the static value.

For greater values of damping ratios, the magnetic field at the wave front varies as indicated in Figure 2.2, according to Equations (A.3.7) and (A.3.8). The radial component decreases monotonically with increased damping; the tangential component increases with increased damping up to a damping ratio of about $\alpha = 3$, and decreases thereafter.

Time histories of the magnetic field for a large value of damping are shown in Figure 2.1 for $\alpha = 5$. It may be noted that the tangential magnetic field increases above the initial values at the wave front to a maximum before

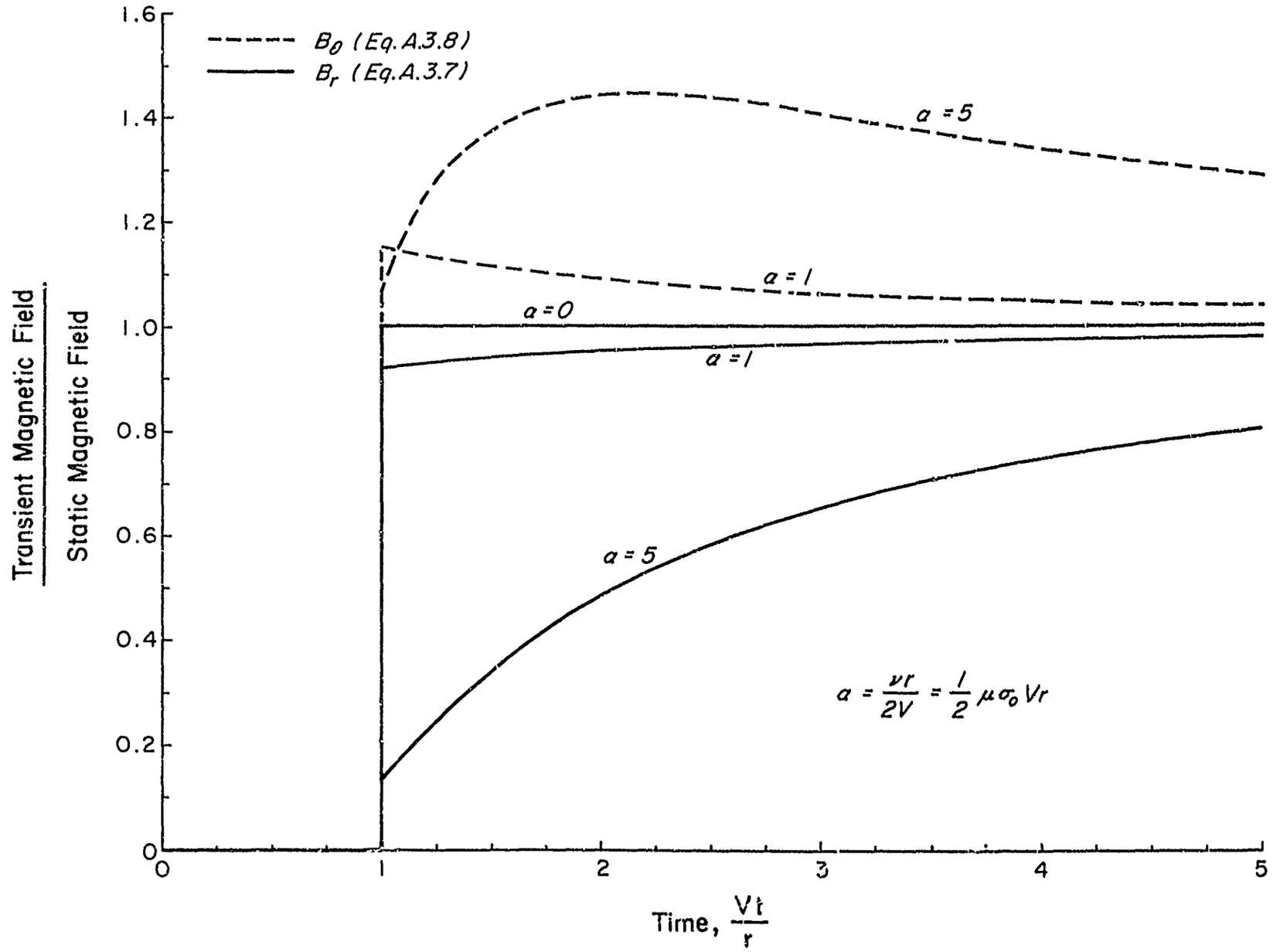

Fig. 2.1 Transient Magnetic Field for a Dipole in a Complex Plasma

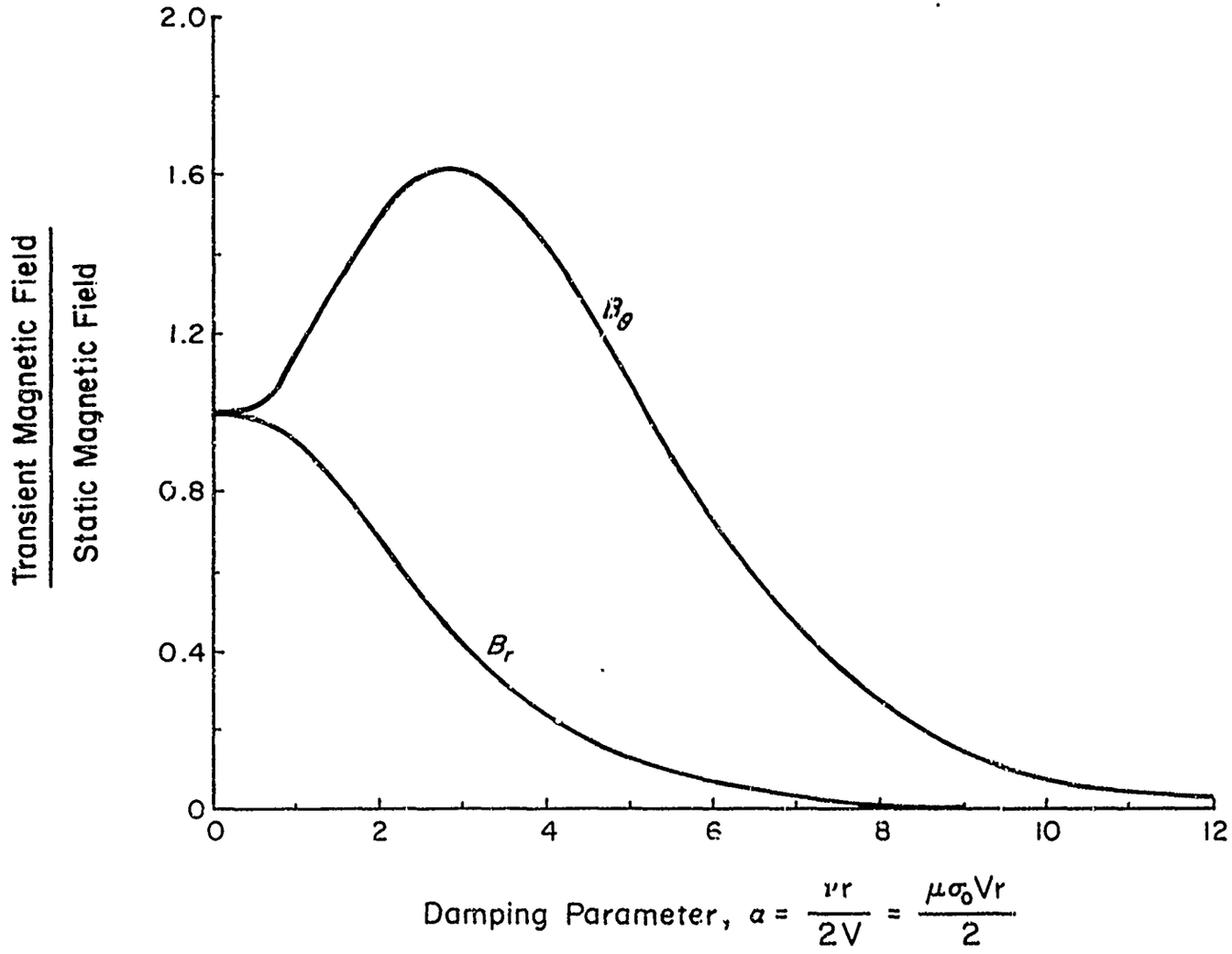

Fig. 2.2 Magnetic Field at the Wave Front (Eqs. (A.3.7) and (A.3.8))

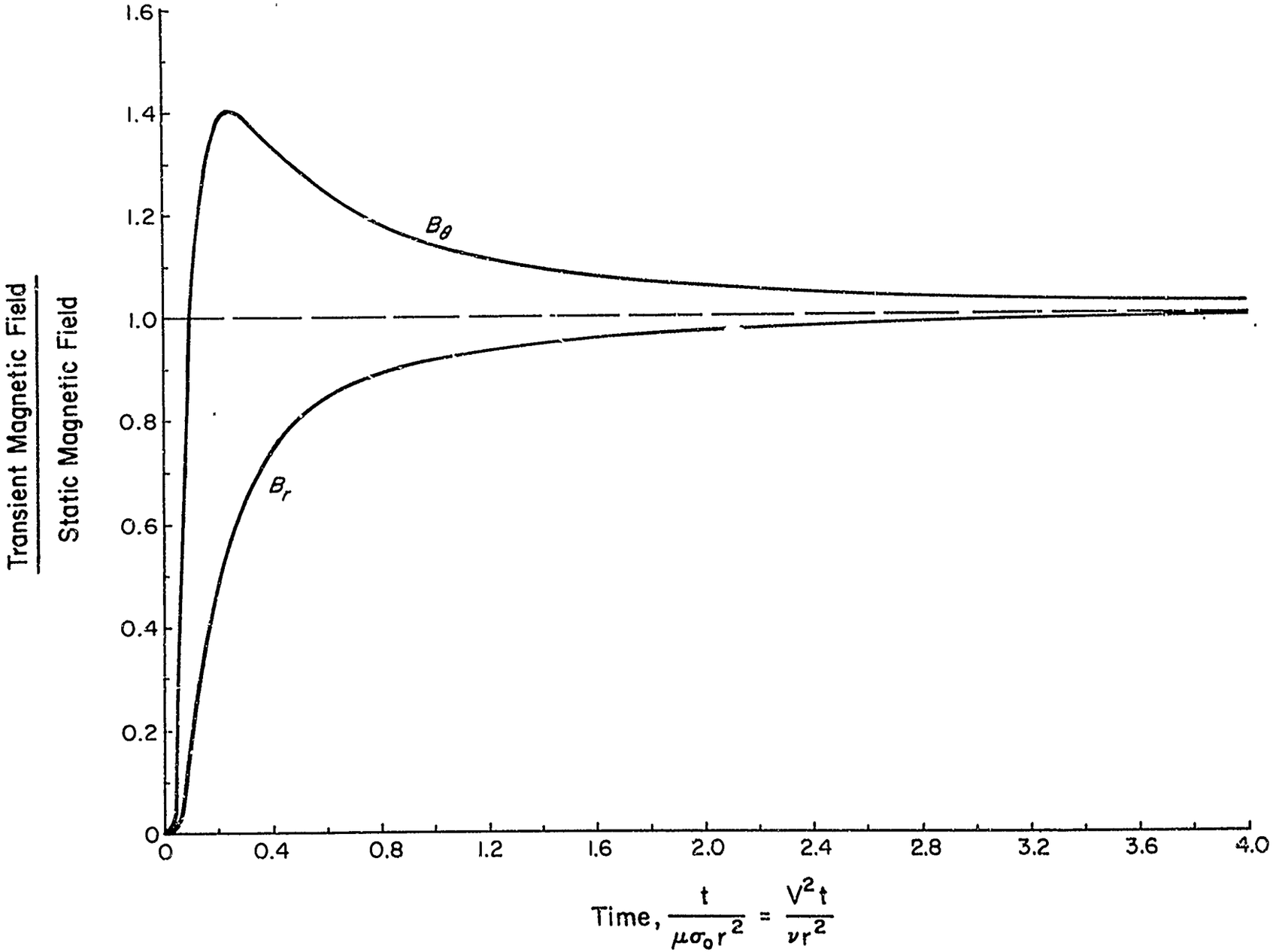

Fig. 2.3 Transient Magnetic Field for a Dipole in an Ohmic Plasma (Eqs. (A.3.15) and (A.3.16))

approaching the static condition; the radial compcnent increases monotonically from the initial value toward the static value.

Considering finally the case of an ohmic plasma, Figure 2.3 presents time histories of the corresponding magnetic field components. These curves correspond to the complex case where $a \to \infty$ and are similar to the above discussed curves for $a = 5$, except that the initial value is zero for the ohmic case, there being no distinct finite-amplitude wave front in this case.

2.3 HORIZONTAL MAGNETIC DIPOLE IN A SEMI-INFINITE PLASMA

Section A.4 of Appendix A considers the transient magnetic fields produced by a horizontal magnetic dipole located at a height h above a horizontal interface separating a plasma above from a vacuum below.

The following reciprocity law, indicated in Figure 2.4, is found to be

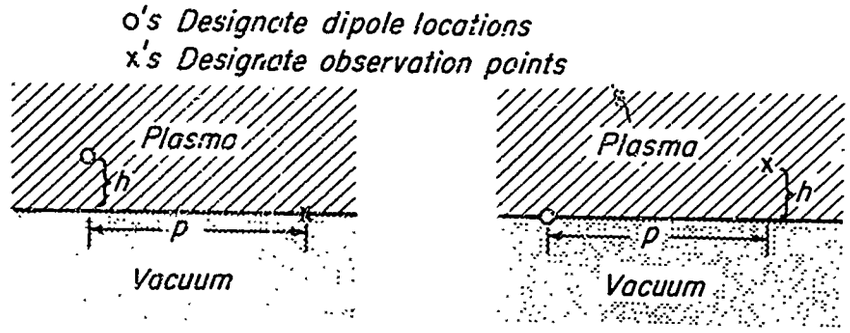

Fig. 2.4 Two Equivalent Problems

5563 b

valid in the plasma. The magnetic field at the plasma-vacuum interface created by a dipole at the height h (Fig. 2.4a) is the same as the magnetic field created at the height h by a dipole at the interface (Fig. 2.4b).

For the special case where both dipole and observation points are located in the plane of the interface, the transient magnetic fields produced by a suddenly created (step-function) magnetic dipole vary as indicated in Figure 2.5. This figure presents time histories of the horizontal magnetic field components for a perfect plasma and an ohmic plasma, where B_ρ and B_θ are the radial and tangential components of the horizontal magnetic field.

For both perfect and ohmic plasmas, the magnetic field of the dipole immediately fills the vacuum half-space (since displacement current is neglected), but requires a finite time to penetrate into the plasma. Hence, the plasma region initially acts as a perfect reflector, creating twice the static magnetic field at time zero in the vacuum region (and at the interface). With increasing time, the doubled magnetic field at the interface then begins to decrease as the excess dipole field penetrates into the plasma. For a perfect plasma, the magnetic field components eventually reverse their polarity, reaching a large negative peak at the time $t = r/V$ (Fig. 2.5a), which is the time required for the dipole disturbance to travel in the plasma from the dipole to an observer point. The magnetic field components then abruptly reverse their direction and reach their static values. For the case of an ohmic plasma, the transition from the initial doubled field to the final static state is almost a simple monotonic decay (Fig. 2.5b), with a characteristic time constant on the order of $0.1\mu\sigma_o r^2$.

2.4 VERTICAL MAGNETIC DIPOLE IN A SEMI-INFINITE PLASMA

Section A.5 of Appendix A considers the transient magnetic fields produced by a vertical magnetic dipole located above a horizontal interface separating a plasma above from a vacuum below. These results are exactly applicable to the analogous case of a hydromagnetic plasma, provided that the ambient magnetic field vector for the hydromagnetic plasma is a vertical vector.

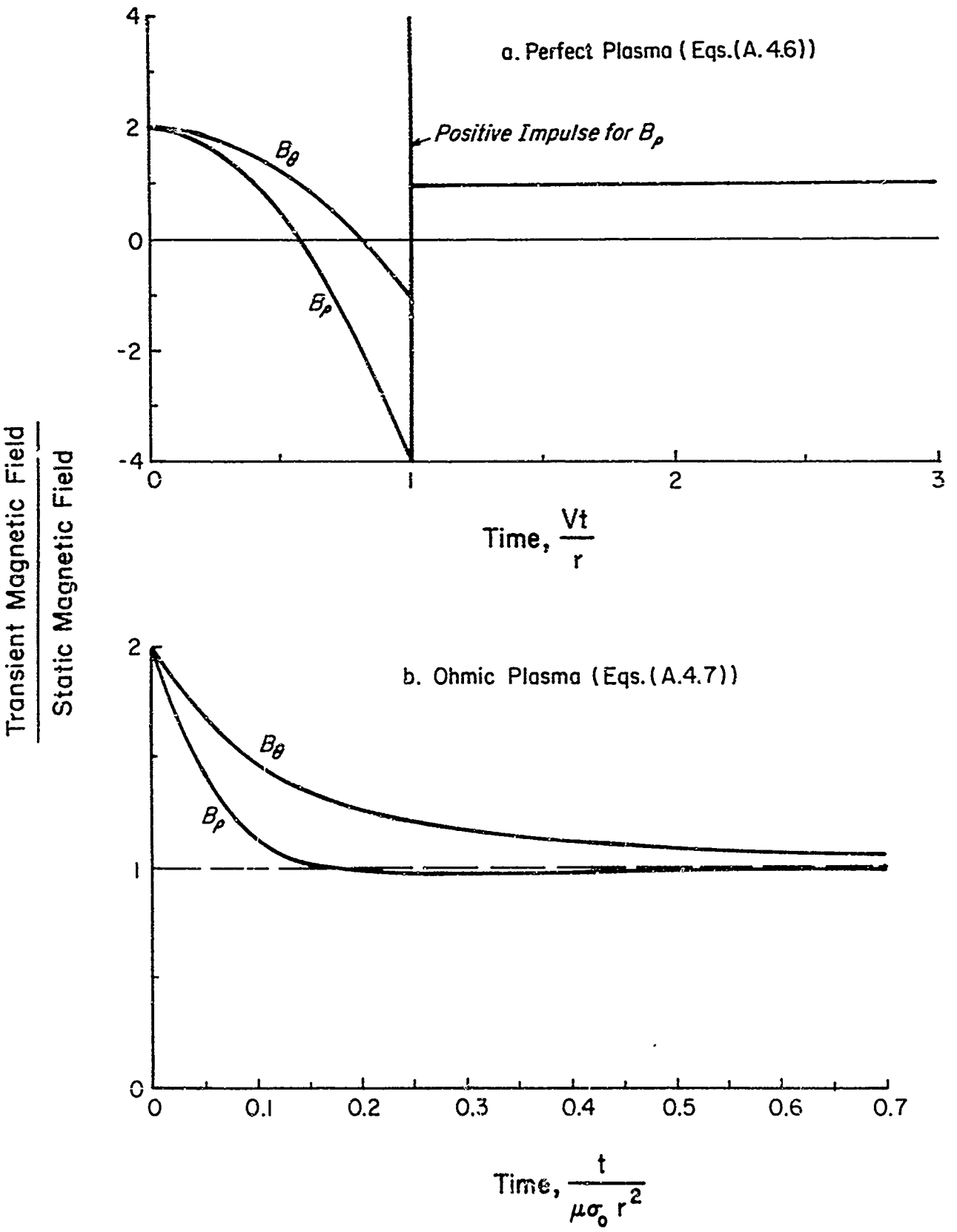

Fig. 2.5 Magnetic Fields for a Horizontal Dipole in a Semi-infinite Plasma

For the special case of a perfect plasma where both dipole and observation points are located in the plane of the interface, the transient magnetic fields produced by a suddenly created (step-function) magnetic dipole vary as indicated in Figure 2.6, where B_ρ and B_z are the radial and vertical magnetic field components, the other component being zero. The initial magnetic field components are zero, since the plasma region initially acts as a perfect reflector (see Sect. 2.3), thereby creating an image dipole canceling the applied dipole. As time increases, the magnetic field components increase to large multiples of the static dipole field, reaching infinity at the time $t = \rho/V$, which is the time required for the dipole-produced wave front to travel in the plasma from dipole to observer. For larger times, the vertical component of the magnetic field immediately reaches the static dipole value and the horizontal component decreases rapidly toward zero.

2.5 HORIZONTAL DIPOLE ABOVE A VACUUM CAVITY

Section A.6 of Appendix A considers the problem where a horizontal magnetic dipole is placed in a plasma at an attitude h above a horizontal vacuum cavity of depth H, the lower edge of the cavity being the surface of a perfect conductor. For the case of a suddenly applied (step-function) dipole in the plasma, the transient magnetic field in the cavity at the surface of the perfect conductor behaves as follows for perfect, dissipative, and ohmic plasma.

Time histories of the transient magnetic fields at the surface of the perfect conductor, according to Equation (A.6.29), are shown in Figures 2.7 and 2.8 for perfect and ohmic plasma, respectively, for the parameter ratios:

$$h/H = 1 \; ; \; H/\rho = 0.1 \qquad \text{(A.6.41)}$$

where

ρ is the horizontal distance between dipole and observation point

Considering first the perfect plasma, it may be seen from Figure 2.7 that the transient magnetic field is zero until the time $t = h/V$, which is the

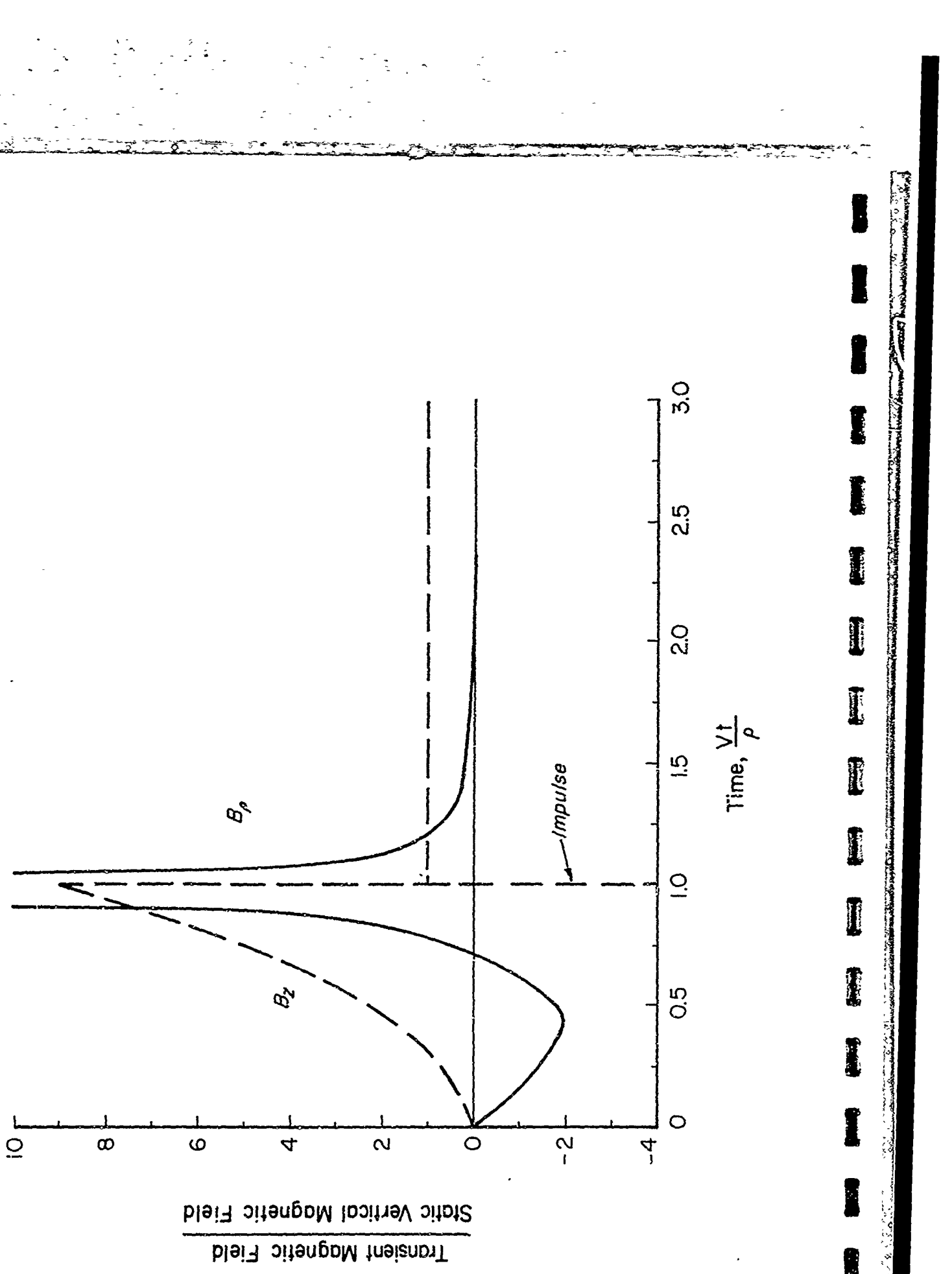

Figure 2.6 Magnetic Field for a Vertical Dipole in a Semi-Infinite Plasma (Eqs. (A.5.12))

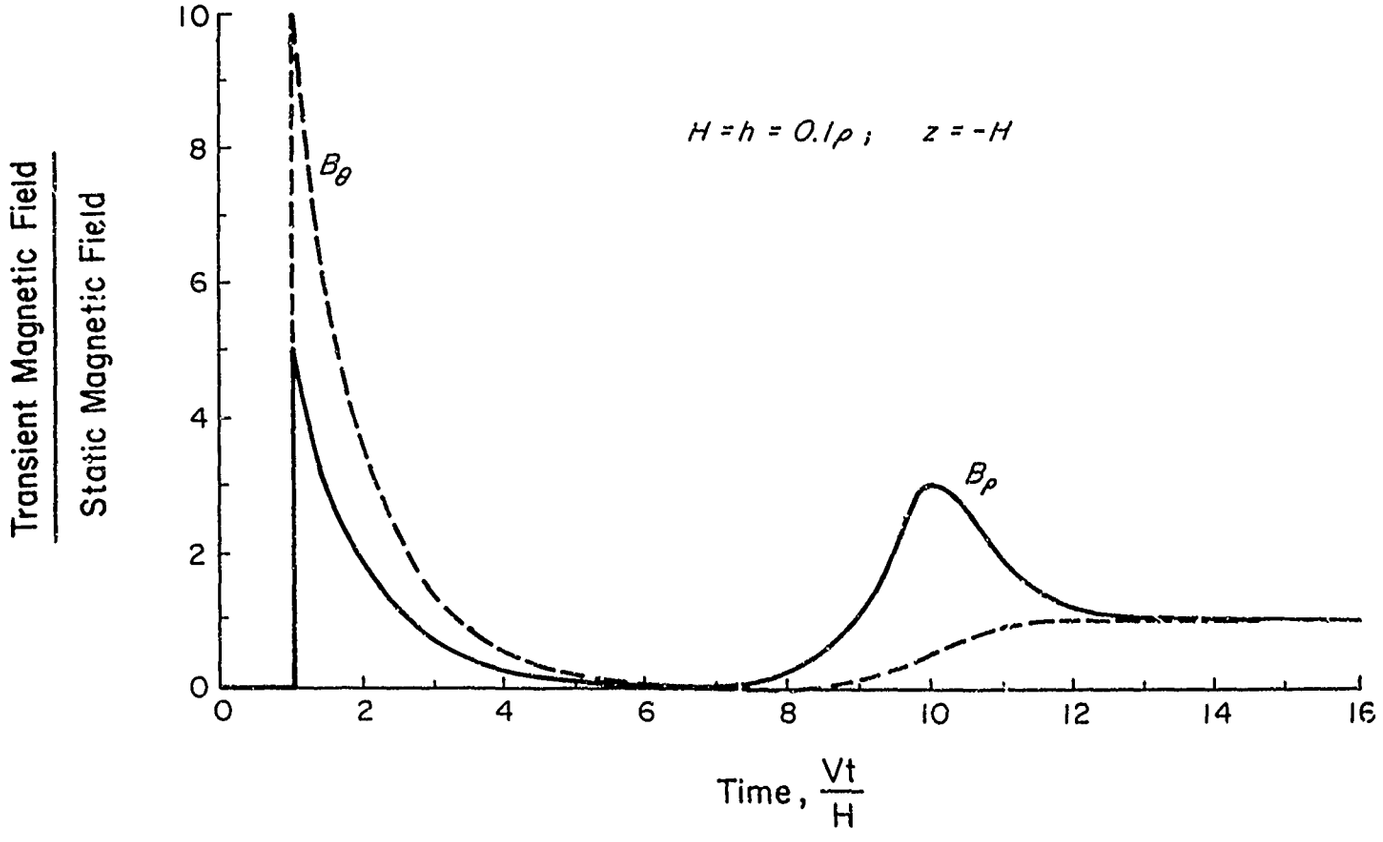

Fig. 2.7 Magnetic Field in a Cavity Below a Perfect Plasma (Eqs. (A. 6. 29), (A. 6. 30), (A. 6. 33) and (A. 6. 34))

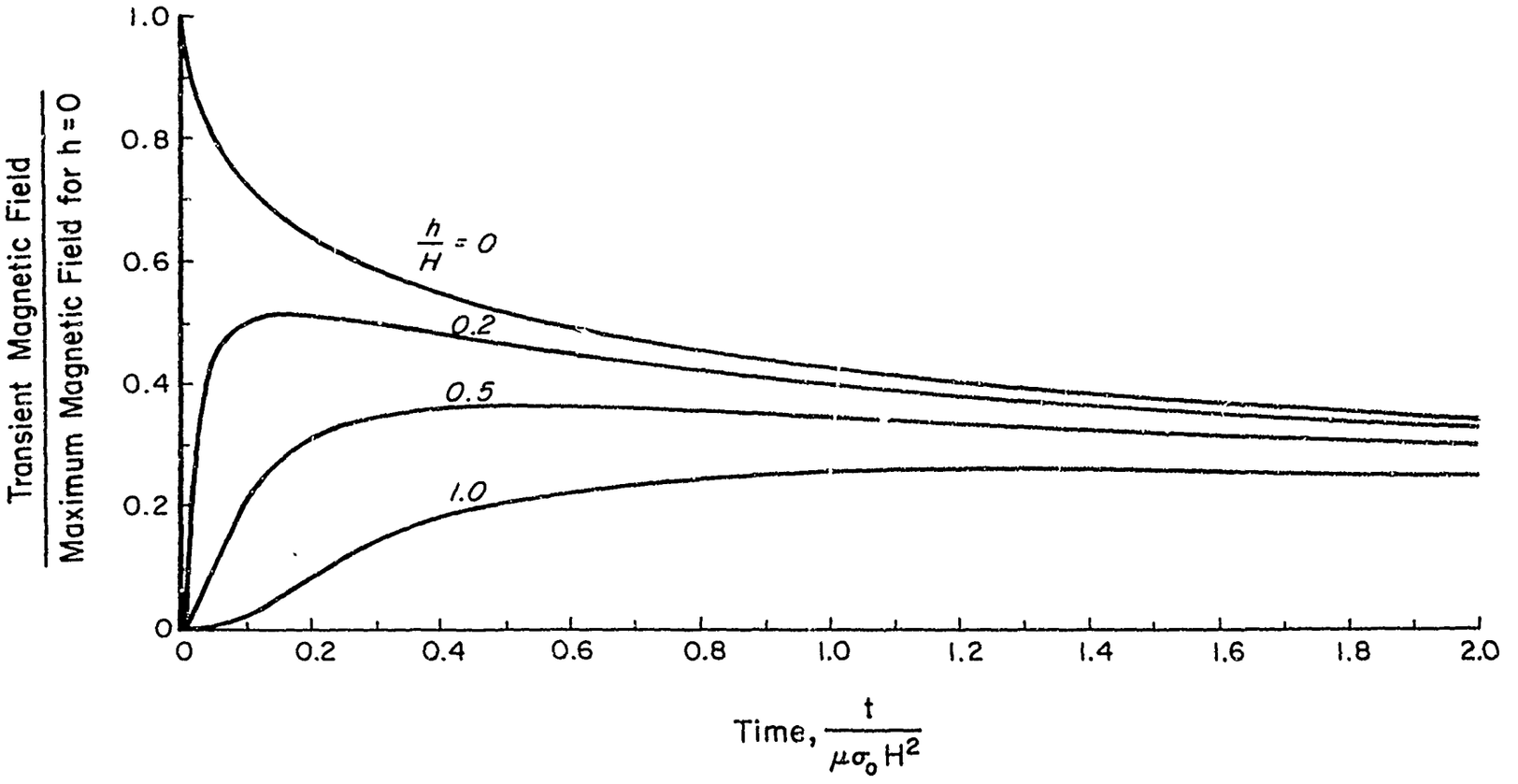

Figure 2.8 Magnetic Field in a Cavity Below an Ohmic Plasma (a) Early Time Variation (Eqs. (A. 6. 29), (A. 6. 36), (A. 6. 37) and (A. 6. 38))

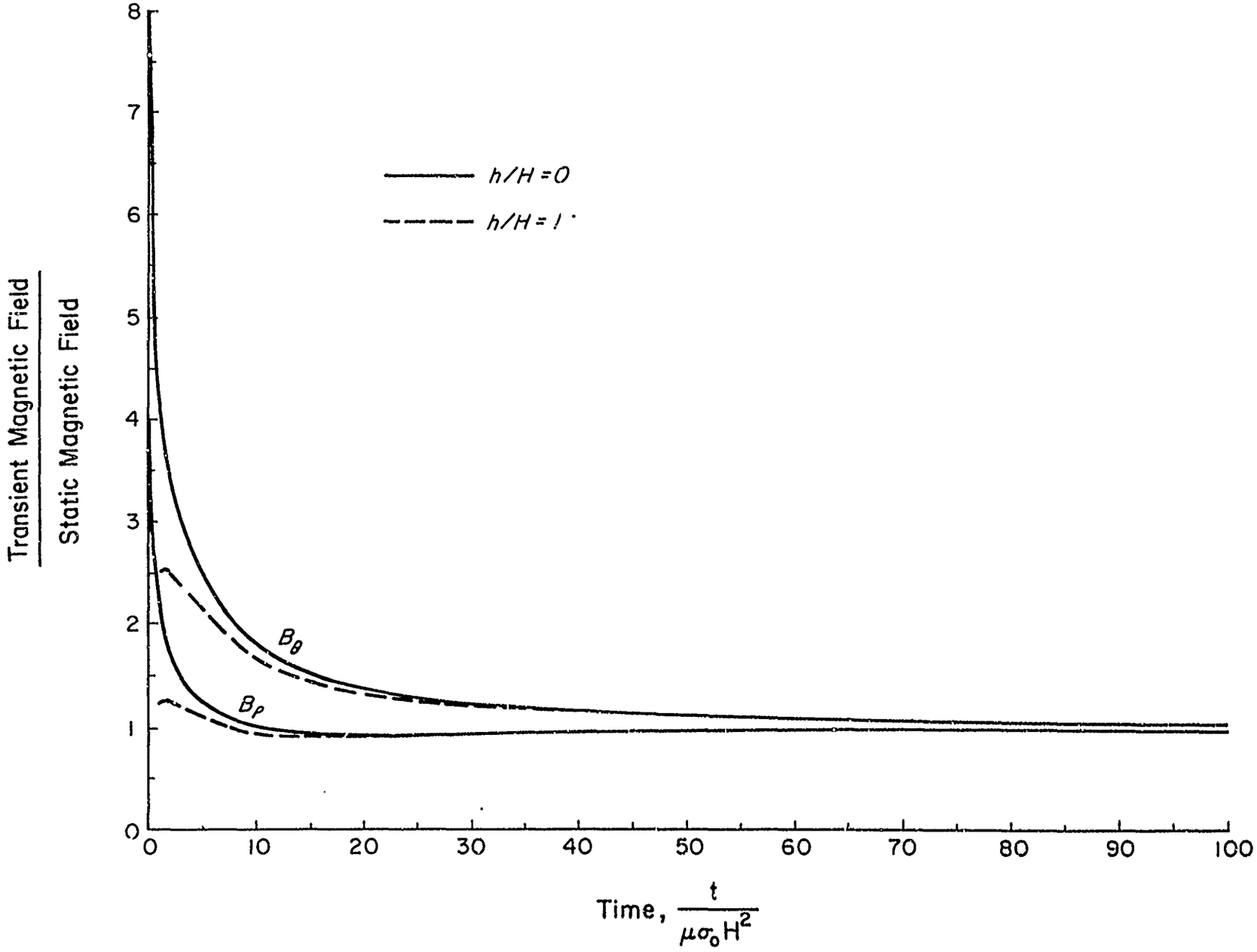

Fig. 2.8 (Cont'd) Magnetic Field in a Cavity Below an Ohmic Plasma
(b) Late Time Variations

time required for the wave front to travel vertically downward from the dipole altitude to the upper edge of the vacuum cavity. At this time, the magnetic field suddenly jumps to the large multiple ρ/H of the static value of the dipole field for the θ-component of the magnetic field and to the multiple $\frac{1}{2}\rho/H$ for the radial component. The magnetic field then decays exponentially toward zero as the magnetic field in the cavity decays into the plasma (see Section B.3 of Appendix B). The characteristic decay time here is H/V. For large values of time, near $t = \rho/V$, the magnetic field in the cavity rises again and, after a short transient period, reaches the static dipole field configuration. This second disturbance corresponds to direct travel of the electromagnetic wave through the plasma to the observation point ρ, as contrasted to the early time peak at $Vt = h$ which corresponds to a more rapid travel via the vacuum cavity.

Next, consider the case of a cavity below an ohmic plasma (Fig. 2.8). If the dipole is located at the upper edge of the cavity or in the cavity ($h/H = 0$), the initial magnetic field is the same as for a perfect plasma, and subsequently decays slowly toward the static field configuration (Fig. 2.8b). There is no conspicuous second peak or rapid transition here of the type noted above for a perfect plasma, because of the large dissipation of transients experienced by waves traveling any large distance inside an ohmic plasma.

For dipoles located above the cavity in an ohmic plasma, the peak magnetic field strength decreases with increasing altitude (see Fig. 2.8 and solid line in Fig. 2.9) and occurs at progressively later times as the altitude h is increased.

For dipoles located in a dissipative plasma above a vacuum cavity, the magnetic field behavior will be intermediate between that for a perfect and for an ohmic plasma. More specifically, there will be an initial delay until the wave front travels from the dipole to the upper surface of the cavity. The magnetic field in the cavity will then jump suddenly to the value given by Equation (A.6.35), which is plotted as dashed lines in Figure 2.9. If the dissipation is large, the magnetic field will subsequently increase to a maximum and then decay toward the static value; otherwise, for small dissipation, the trends of Figure 2.7 for a perfect plasma will be followed. The peak value of the magnetic field transient may be calculated from Equation (A.6.35) for small dissipation (dashed lines in Fig. 2.9) and may be estimated from the solution for an ohmic plasma for large values of dissipation (solid line in Fig. 2.9).

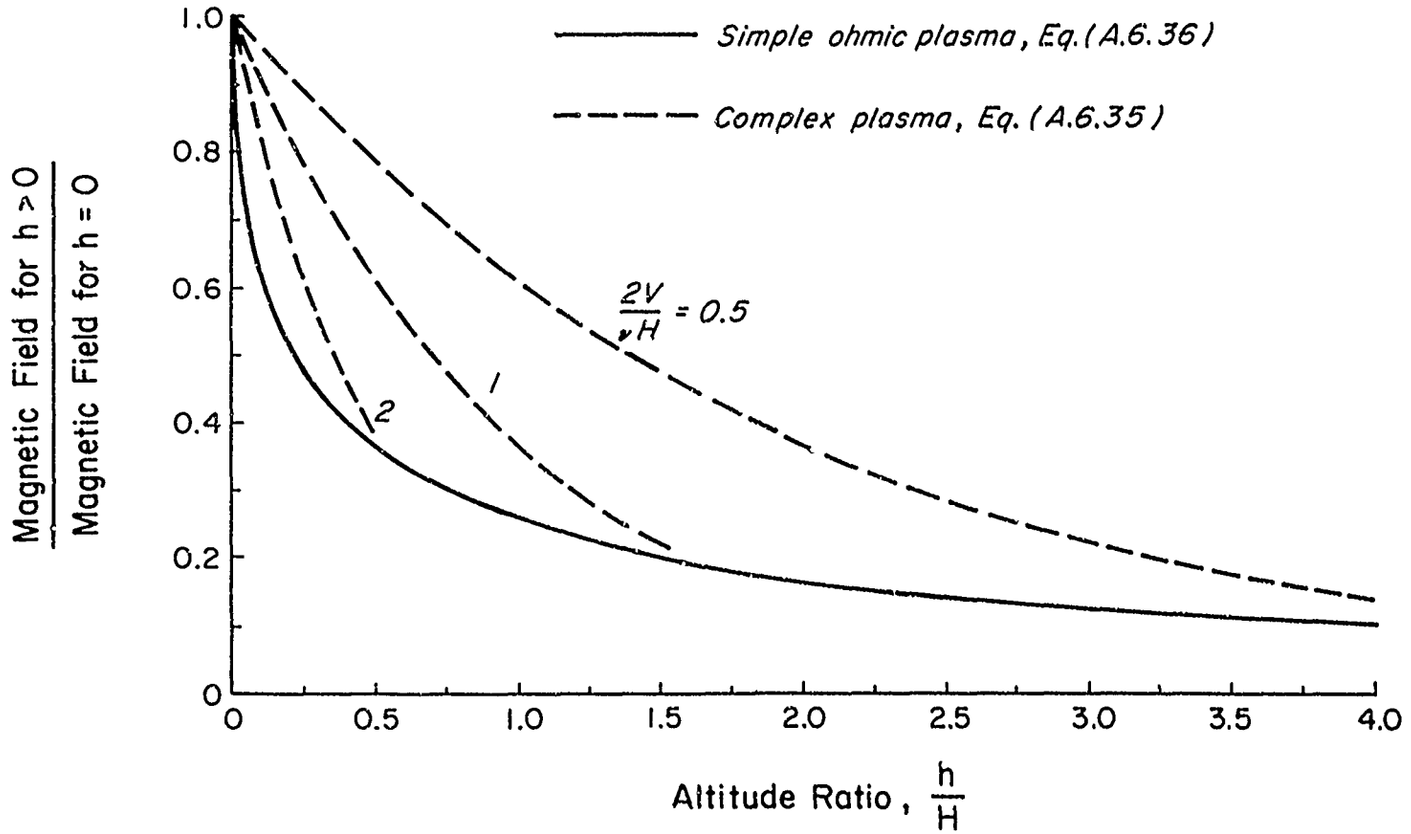

Fig. 2.9 Peak Magnetic Field in a Cavity

BLANK PAGE

SECTION III

SUMMARY OF ONE-DIMENSIONAL HYDROMAGNETIC WAVE PROBLEMS

3.1 INTRODUCTION

This Section presents a summary of a group of theoretical studies, presented in Appendix B, which are concerned with one dimensional hydromagnetic wave propagation in stratified plasma and vacuum regions. These studies are considered relevant to an understanding of near 1 cps fluctuations in the earth's magnetic field in and below the ionosphere, which may be initially excited by hydromagnetic or electromagnetic waves created by distant high altitude nuclear detonations. They are also relevant to an understanding of the ultra-low-frequency worldwide effects of lightning discharges.

Five types of plasma and vacuum regions are considered in this section, which are designated as perfect plasma, complex plasma, ohmic plasma, Hall-effect plasma, and vacuum. Precise definitions of the properties of these regions are given by the equations of Section B.2 and are briefly outlined below.

A perfect plasma is defined herein as a conventional cold collision-free hydromagnetic plasma without Hall effects present (Eqs. (B.2.5) and (B.2.6)).

A complex plasma is defined as a cold hydromagnetic plasma with collision damping present, but without Hall effects (Eqs. (B.2.7) and (B.2.8)). This type of plasma simulates the F-layer of the ionosphere.

An ohmic plasma is defined as a plasma whose ratio of current density to electric field intensity is given by the scalar Ohm's law expression for an simple conductor ($\bar{J} = \sigma \bar{E}$) with a real scalar conductivity constant.

A Hall-effect plasma is defined as a hydromagnetic plasma characterized by finite real Pedersen and Hall conductivity constants (Eq. (B.2.9)), and infinite parallel conductivity. This type of plasma simulates the E-layer of the ionosphere.

A vacuum is defined as a non-conducting region wherein Maxwell's displacement current may be neglected. For frequencies near or below 1 cps, this type of region simulates the behavior of the atmosphere and ionosphere up to about 90 km altitude in the daytime, and up to about 290 km at night.

Throughout this section it is assumed that all plasma regions are permeated by a uniform ambient geomagnetic field, whose field vector $\overline{B}_o$ lies in the YZ-plane of a rectangular cartesian coordinate system having a horizontal XY-plane

3.2 ESCAPE FROM A VACUUM CAVITY INTO A SEMI-INFINITE PLASMA

3.2.1 Step Function Response

Section B.3 of Appendix B considers the escape of a magnetic pulse from a vacuum cavity of height H, which is bounded below by a perfect conductor and above by a semi-infinite hydromagnetic plasma containing an ambient constant magnetic field vector $\overline{B}_o$ (Fig. 3.1). It is assumed that at time zero a uniform small horizontal magnetic field of strength B_{vo} and total flux $\Phi = B_{vo}H$ is suddenly applied to the cavity and is then permitted to relax into the plasma.

For the case of a perfect hydromagnetic plasma (see Section B.2 of Appendix B), the initial magnetic field in the cavity decays exponentially with increasing time t (see Eq. (B.3.15)) as

$$B(t) = B_{vo} \exp(-V_m t/H) \qquad (3.1)$$

where

B is the transient magnetic field strength in the cavity
H is the cavity depth

and where V_m is the phase velocity in the hydromagnetic plasma, which is (from Eq. (B.2.20))

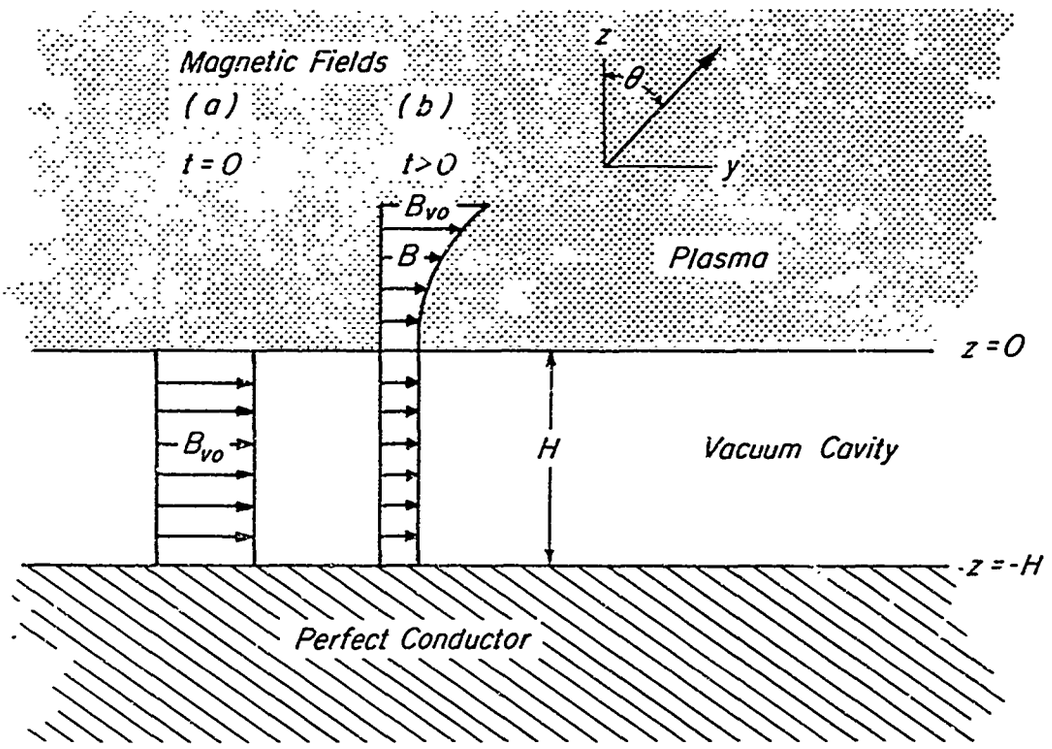

Fig. 3.1 Escape of a Magnetic Field from a Vacuum Cavity into a Semi-Infinite Plasma

$$V_m = \begin{cases} V_a \text{ for modified Alfven waves} \\ V_a \cos\theta \text{ for Alfven waves} \end{cases} \qquad (3.2)$$

where

V_a is the Alfven speed ($V_a = B_o/\sqrt{\mu\rho}$)

B_o is the ambient magnetic field strength

θ is the acute angle between the ambient magnetic field vector $\bar{B}_c$ and the vertical.

and where the component of the magnetic field in the plane formed by the ambient magnetic field vector and the vertical behaves as a modified Alfvén wave and the component perpendicular to this plane vehaves as an Alfvén wave wave (see Section B.2). The corresponding transient magnetic field in the plasma consists of a shock front of amplitude B_{vo} with a spatially exponentially decaying wake moving into the plasma from the cavity wall, traveling at the phase speed V_m, as is shown in Figure 3.2, according to Equation (B.3.15).

For a complex plasma, more complicated equations apply (see Eq. (B.3.11)), but the behavior will be qualitatively the same for small values of the damping ratio $\nu H/V_m$, where ν is a characteristic ion collision frequency. For large damping ratios ($\nu H/V_m >> 1$), the behavior approaches that for a simple ohmic plasma in that the shock front vanishes, the magnetic field in the cavity B_v decays as (from Eq. (B.3.21))

$$B_v = B_{vo}\, w\,(i\sqrt{t/T}) \qquad (3.3)$$

where

$$T = \mu\sigma H^2 \qquad (3.4)$$

$$w(z) = \exp(-z^2)\,\mathrm{erfc}(-iz) \qquad (3.5)$$

σ is the conductivity

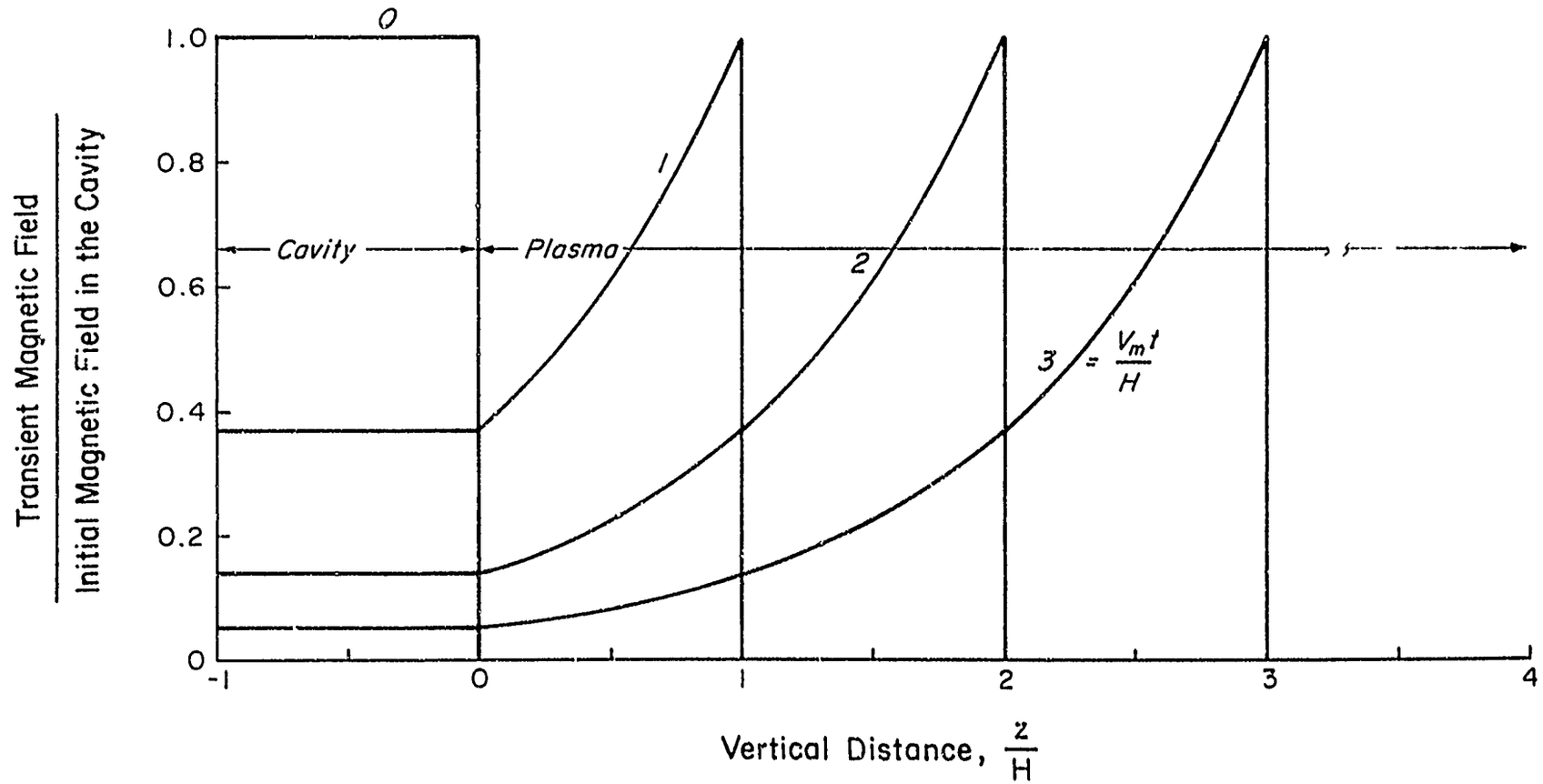

Figure 3.2 Escape of a Magnetic Field from a Vacuum Cavity into a Perfect Plasma; Spatial Distribution for Several Times (Eq. (B. 3. 15))

(see upper curve in Fig. 3.3), and the wave in the plasma takes the form indicated in Figures 3.3 and 3.4 (See Eq. (B.3.19)).

It may be noted here that the characteristic time associated with the decay of the magnetic field in the cavity below the perfect plasma is H/V_m, which is of the order of one second for the nighttime sub-ionosphere cavity (e.g., for H~300 km, V_m~300 km per sec). The characteristic decay time for an ohmic plasma is $\mu\sigma H^2$, which is of the order of one second for the daytime sub-ionosphere cavity (e.g., using a Pederson conductivity for the E-layer of about 2×10^{-4} MKS units with an ionosphere height of 80 km).

For escape into an Hall effect plasma, the magnetic field in the cavity obeys a relationship of the form (see Eq. (B.3.34)

$$\left.\begin{aligned} B_{vx}(t) &= C_{11}\, w_+ + C_{12}\, w_- \\ B_{vy}(t) &= C_{21}\, w_+ + C_{22}\, w_- \end{aligned}\right\} \qquad (3.6)$$

where

$$w_\pm = w\left(i\sqrt{t/T_\pm}\right)$$

and where the $T_\pm$'s are complex constants (Eq. (B.3.32)) and where the C's are each linear functions of both of the initial components B_{vxo} and B_{vyo} of the magnetic field in the cavity (see Eq. (B.3.34)). Figures 3.5 and 3.6 illustrate this magnetic field variation and its rate of change for parameters appropriate to the daytime E-layer of the ionosphere for the case where the ambient magnetic field is vertical (high latitude condition) and where the initial magnetic field is polarized in the Y-direction ($B_{xo} = 0$). The magnetic field in the Y-direction decays in about the same manner as for an ohmic plasma (Fig. 3.3). A substantial X-component is seen to come into existence in less than a second and subsequently decays at a rate similar to that for the Y-component.

3.2.3 Frequency Response

Next, consider the cavity frequency response to a steady state sinusoidal input of magnetic flux. For the cases of a plasma without Hall effects, this is given by Equation (B.8.17) as

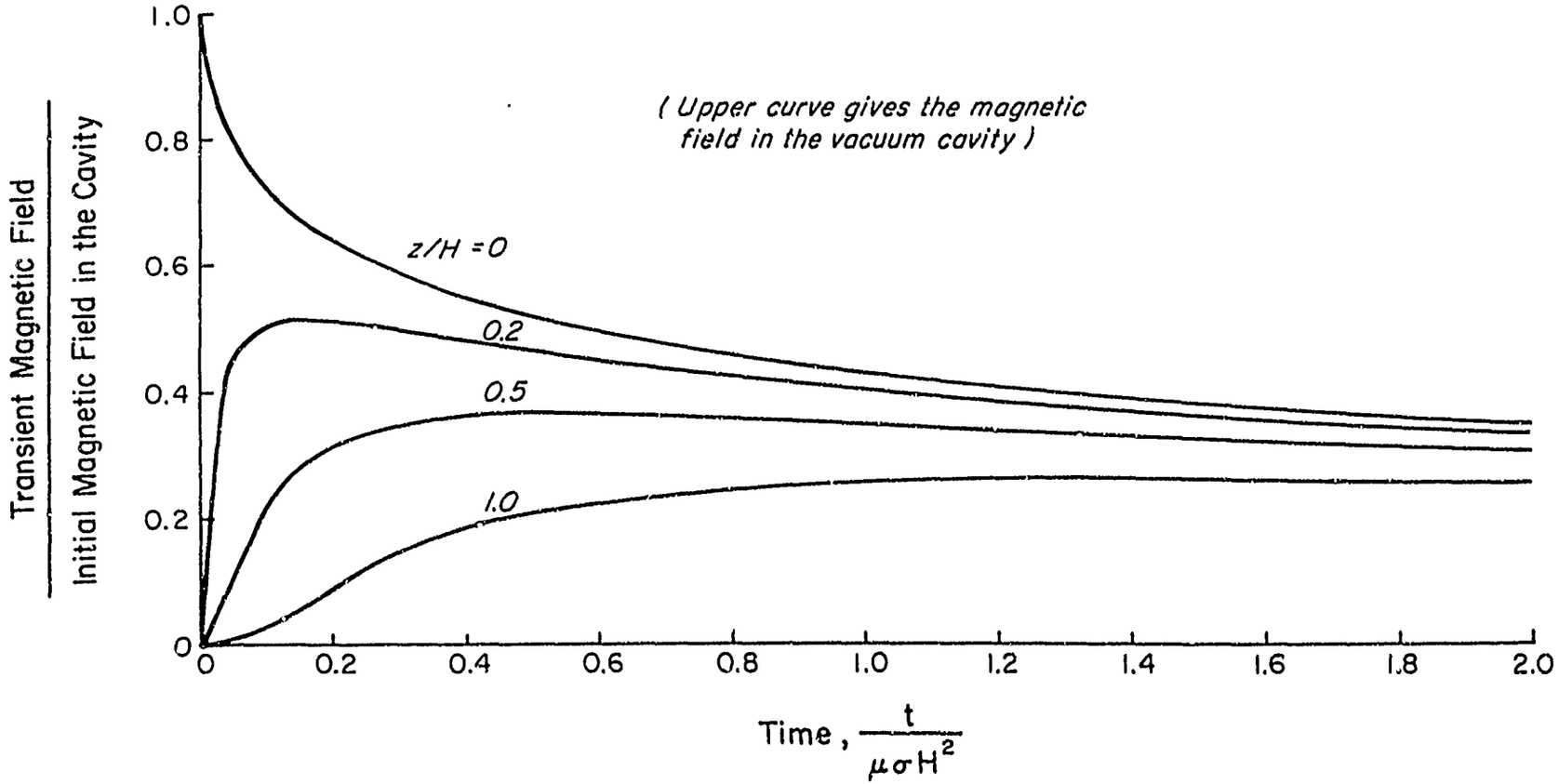

Figure 3.3 Escape of a Magnetic Field from a Vacuum Cavity into an Ohmic Plasma, Time Histories of the Magnetic Field

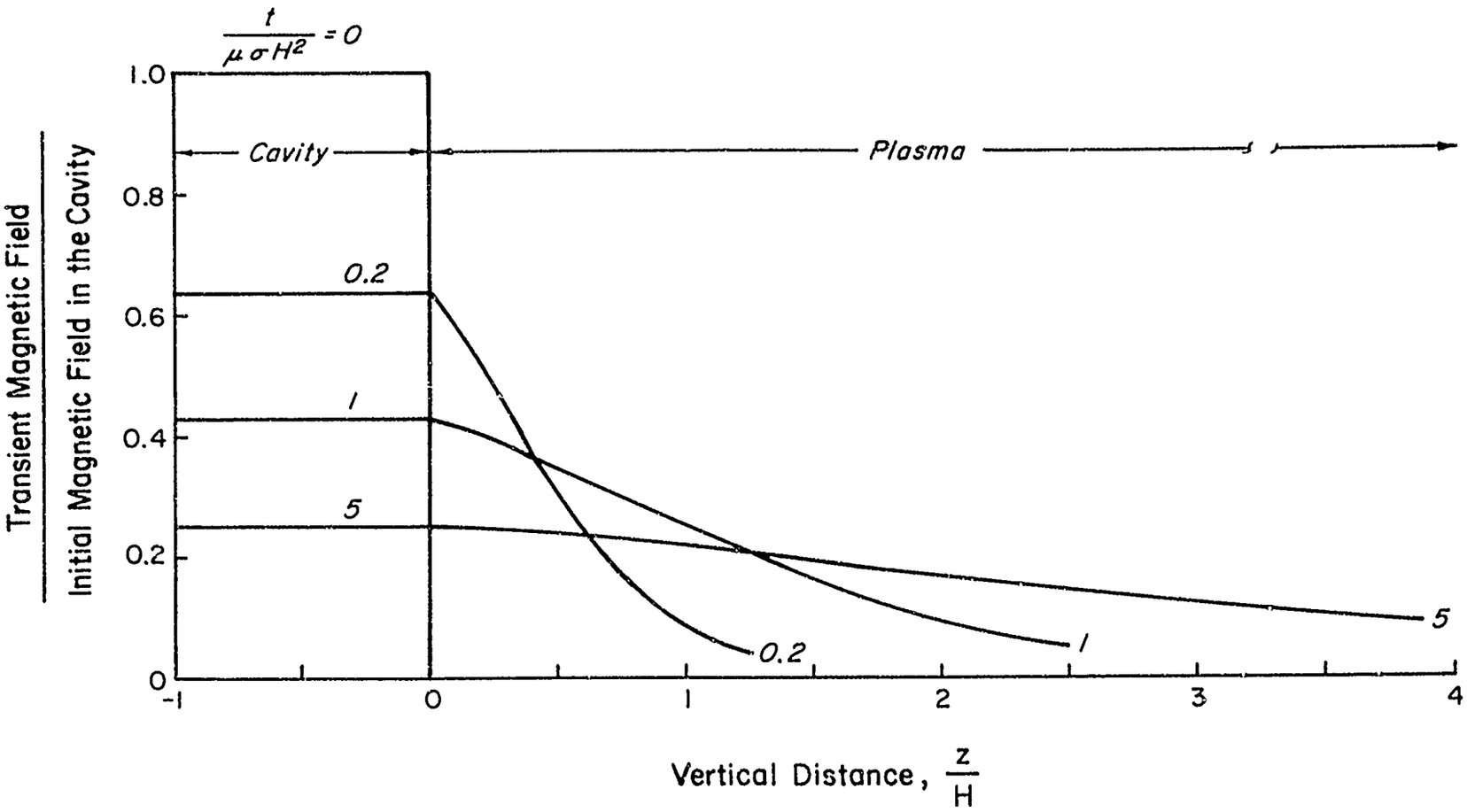

Figure 3.4 Escape of a Magnetic Field from a Vacuum Cavity into an Ohmic Plasma; Spatial Distribution for Several Times

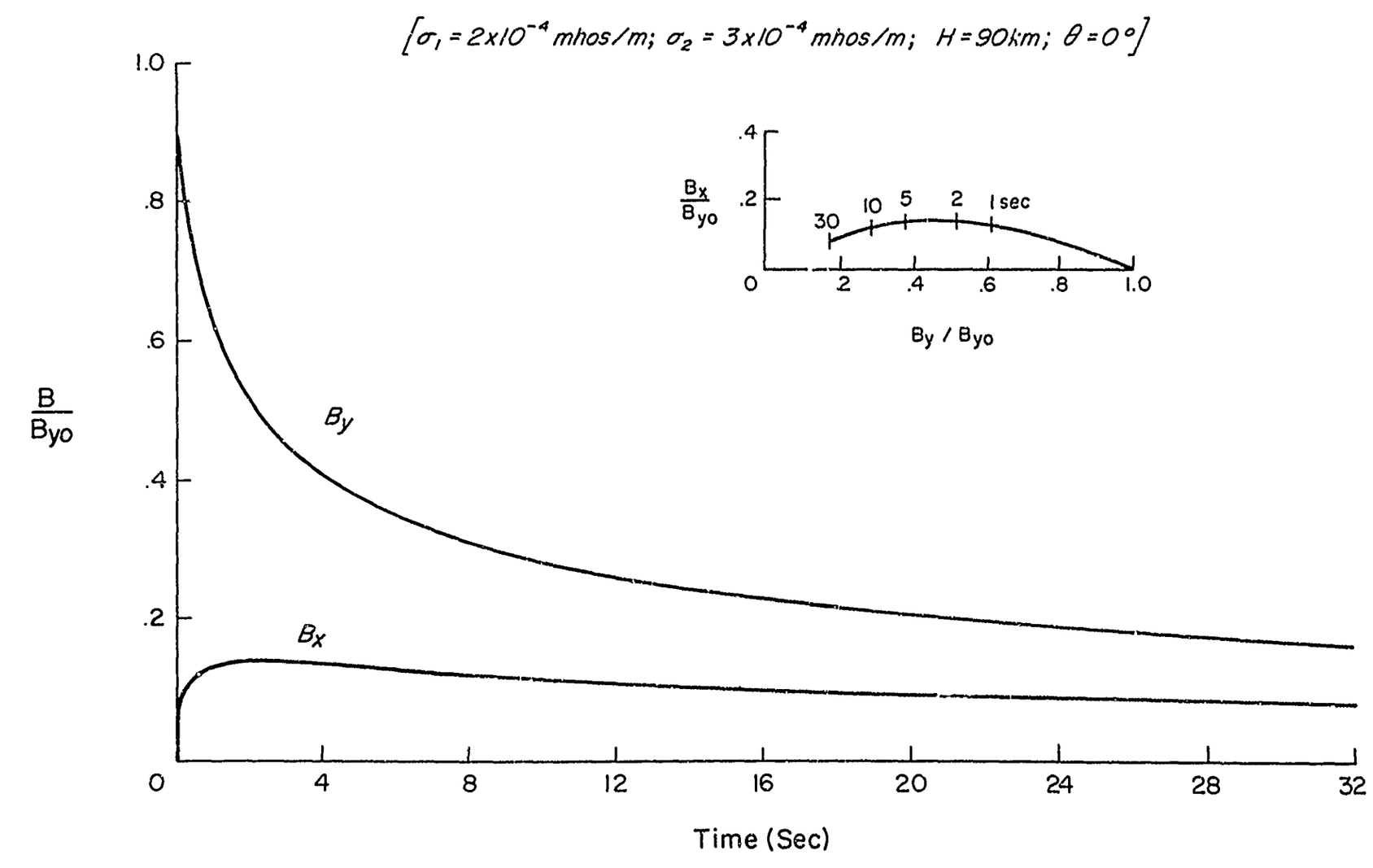

Fig. 3.5 Time History and Polarization of Magnetic Field Escaping from a Vacuum Into a Hall-Effect Plasma

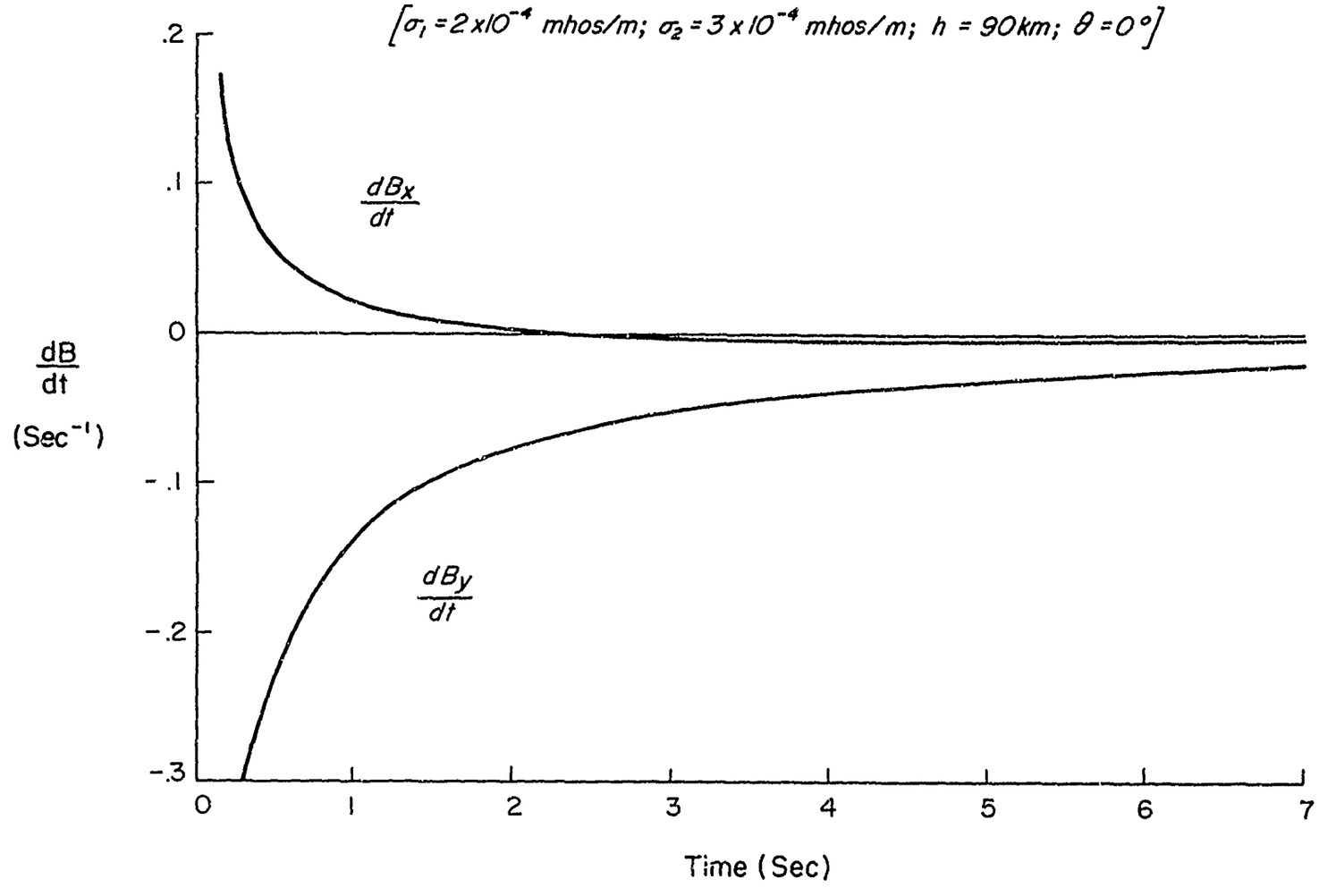

Fig. 3.6 Time History of Rate of Change of Magnetic Field Escaping from a Vacuum Cavity Into a Hall-Effect Plasma.

$$H(i\omega) = ikH/(1 + ikH) \qquad (3.7)$$

where

$H(i\omega)$ is the frequency response function

k is the wave number in the plasma

and from Equations (B.2.28) through (B.2.30)

$$ik = \begin{cases} \sqrt{(i\omega)^2 + (i\omega)\nu}/V_m & \text{(complex plasma)} \\ i\omega/V_m & \text{(perfect plasma)} \\ \sqrt{i\omega\mu\sigma} & \text{(ohmic plasma)} \end{cases}$$

3.3 ESCAPE FROM A VACUUM CAVITY THROUGH A FINITE PLASMA SLAB

Section B.8.3 of Appendix B considers the problem of the escape of a magnetic pulse from a vacuum cavity of height H, which is bounded below by a perfect conductor (where $\bar{E} = 0$) and is bounded above by a finite height dense plasma slab of height h_2, and which is in turn bounded above by a rarefied plasma region (Fig. 3.7). Also considered is the response of the cavity to a sinusoidal application of magnetic flux to the cavity.

3.3.1 Step Function Response

First consider the case of the step-function response of the cavity. It is assumed that at time zero a uniform small horizontal magnetic field of unit strength ($\bar{B}_{vo} = 1$) and total flux $\Phi = B_{vo}H$ is suddenly applied to the cavity and is then permitted to relax into the plasma.

Complex plasma

For the case of a complex plasma, the magnetic field in the cavity varies as

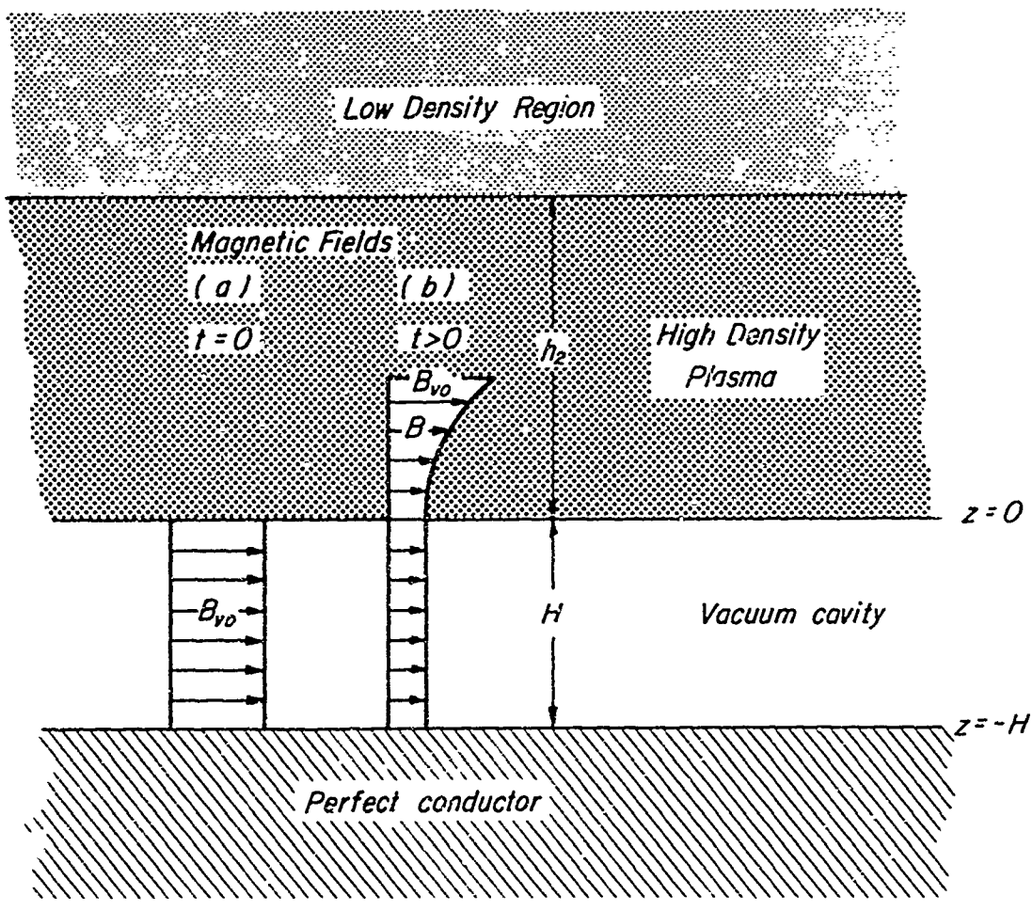

Fig. 3.7 Escape of a Magnetic Field from a Vacuum Cavity Through a Finite Plasma Slab

$$B_v(t) = 1 - 2\sum_n C_n\left(1 - \exp\left(-\tfrac{1}{2}\nu t\right)\left[\cos\omega_n t + \tfrac{1}{2}(\nu/\omega_n)\sin\omega_n t\right]\right) \qquad \text{(B.8.30a)}$$

$$= 2\Sigma C_n \exp\left(-\tfrac{1}{2}\nu t\right)\left[\cos\omega_n t + \tfrac{1}{2}(\nu/\omega)\sin\omega_n t\right] \qquad \text{(B.8.30b)}$$

where

ν is a collision damping frequency

and where the C_n's and ω_n's are numerical constants defined in Section B.8.3 of Appendix B. (Table I gives the first few values of $2C_n$ for $a = H/h_2 = \frac{2}{3}$ and 2.) The response behavior consists of a superimposition of damped oscillations at the characteristic frequencies ω_n.

Perfect plasma

For a perfect plasma, the magnetic field in the cavity varies according to Equation (B.8.30) above with $\nu = 0$, or

$$B_v(t) = 2\Sigma C_n \cos\omega_n t \qquad (3.8)$$

where

$$\omega_n = \xi_n V_m/h_2 \ , \qquad (3.9)$$

where the ξ_n's are the positive roots of the equation

$$a\xi_n \tan\xi_n = 1 \qquad (3.10)$$

(see Table I for the first few values of ξ_n for $a = \frac{2}{3}$ and 2), where

$$a = H/h_2 \qquad (3.11)$$

h_2 is the height of the finite plasma slab

V_m is the phase speed in the plasma

The response behavior is seen to consist of a superimposition of continuous oscillations at the various characteristic frequencies ω_n at the amplitudes $2C_n$ (see Eq. (3.8); also Table I for the first four values of $2C_n$ for $a = \frac{2}{3}$ and 2).

TABLE I

VALUES OF CONSTANTS FOR AN OHMIC PLASMA

$[\mu \sigma H^2 = 1.26 \text{ sec}]$

H/h_2	n	ξ_n	$2C_n$	T_{n_1} (sec)
2/3	1	.99	.635	2.900
	2	3.54	.184	.226
	3	6.51	.065	.067
	4	9.58	.031	.031
2	1	.65	.851	0.740
	2	3.29	.086	.029
	3	6.36	.024	.008

* Listed values of ξ_n and $2C_n$ also apply for complex and perfect plasmas

Ohmic plasma

For an ohmic plasma (see Sect. B.8.3.3):

$$B_v(t) = 2\sum_n C_n \exp(-t/T_{n1}) \tag{3.12}$$

where

$$T_{n1} = \mu\sigma H^2/(a^2\xi_n^2) \tag{3.13}$$

and where the first few values of C_n and ξ_n are given in Table I for $a = H/h_2 = \frac{1}{3}$ and 2 and the corresponding values of T_{n1} are given for $\mu\sigma H^2 = 1.26$ sec (for $\sigma = 10^{-4}$ mhos/m, H = 90 km). These numerical values for a = 2 are considered representative of the daytime near-equatorial ionosphere. Time histories of the magnetic field in the cavity are shown in Figure 3.8 for this value of $\mu\sigma H^2$ for $H/h_2 = 0$, $\frac{1}{3}$ and 2. It is seen that for $H/h_2 = 2$, a substantial decay occurs in a time of about one second.

Hall-effect plasma

For the case of a Hall effect plasma, the magnetic field varies according to a relationship of the form given by Equation (3.6), with the w-functions being replaced by W-functions as defined by Equation (B.8.35).

3.3.2 Frequency Response

The cavity frequency response to a steady state sinusoidal input of magnetic flux, for the case of a plasma slab without Hall effects, is given by Equation (B.8.21) as

$$H(i\omega) = (1 - [kH\tan kh_2]^{-1})^{-1} \tag{B.8.21}$$

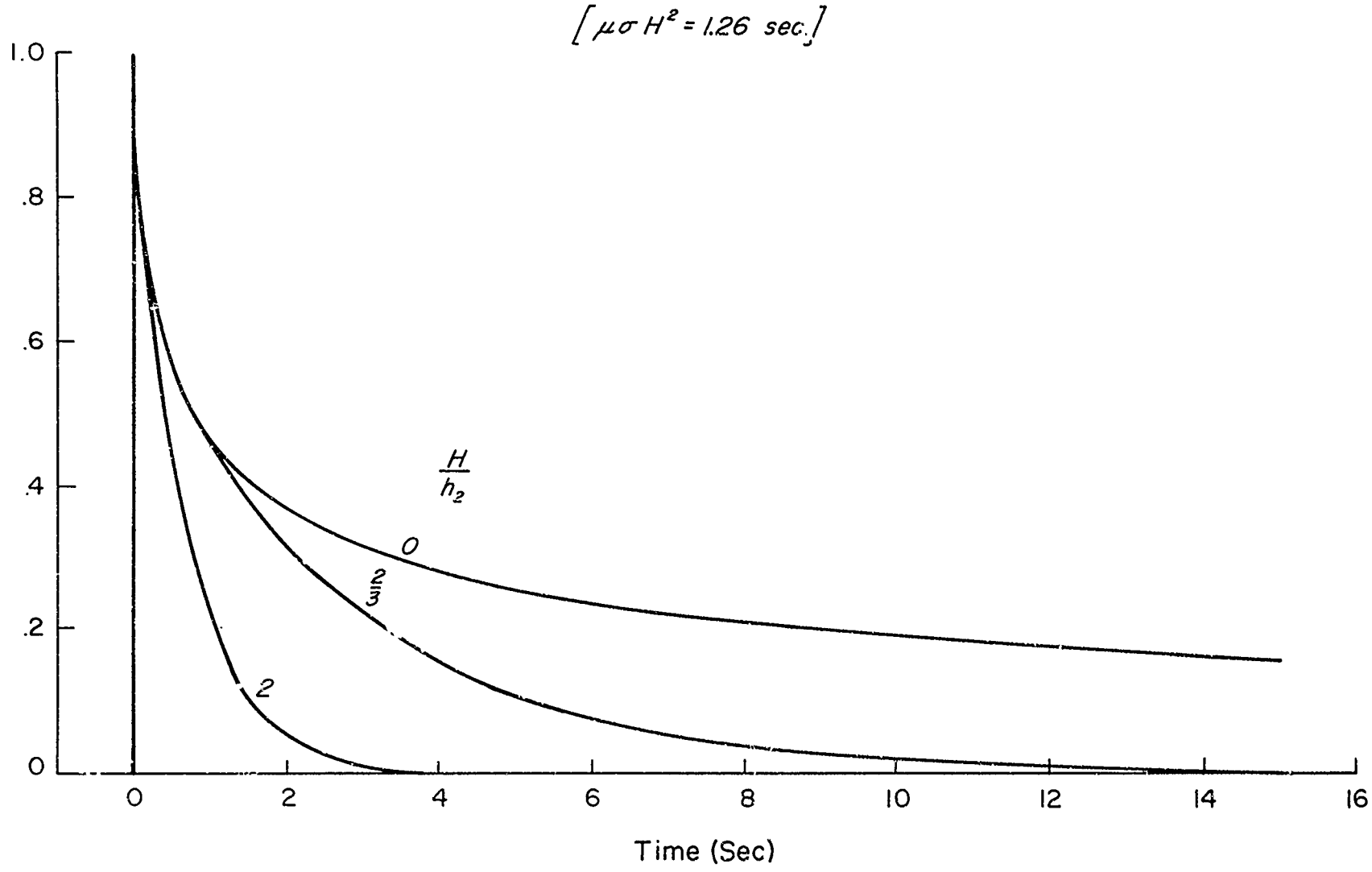

Fig. 3.8 Decay of the Magnetic Field in a Cavity Below a Finite Ohmic Slab

where the wave number k is given by Equations (B.2.28) through (B.2.30) for complex, perfect and ohmic plasma slabs. For a plasma slab with Hall effects, Equation (B.8.21) above is replaced by a four-component tensor with each component obeying an equation similar to this equation (see Eq. (B.8.37)).

3.4 ESCAPE FROM A VACUUM CAVITY INTO AN EXPONENTIAL PLASMA REGION

Section B.8.4 of Appendix B considers the problem of the escape of a magnetic pulse from a vacuum cavity of height H, which is bounded below by a perfect conductor (where $\overline{E} = 0$) and is bounded above by a perfect plasma whose properties simulate the nighttime ionosphere as follows (see Fig. 3.9). This perfect plasma consists of a lower part of height h_2, which is a uniform perfect plasma with phase speed V_{mo}. Above this is a semi-infinite horizontally stratified perfect plasma region whose phase speed first increases exponentially with increasing altitude (with the scale height 2p) and then eventually approaches a constant uniform condition at the phase speed V_{m1}, where $V_{m1} \gg V_{mo}$. (See Eq. (B.6.1)).

3.4.1 Step-Function Response

First consider the step function response of the cavity to a unit magnetic flux applied at time zero. This step function response is given by Equation (B.8.55) as

$$B_v = 2\, R\left[\sum_n C_m \exp(i\omega_n t)\right] \tag{3.14}$$

where

$$\omega_n = \tfrac{1}{2}\xi_n V_{mo}/p \tag{3.15}$$

$R[\ ]$ designates the real part of the function,

and the C_m's and ξ_n's are complex coefficients of H/h_2 and V_{mo}/V_{m1} (see Sec. B.8.4). Numerical values of parameters for these equations were computed for $V_{mo}/V_{m1} = 0.05$ and $a = H/(2p) = 0.968$ (from H = 290 km and p = 150 km); these values for the first four modes are shown in Table II.

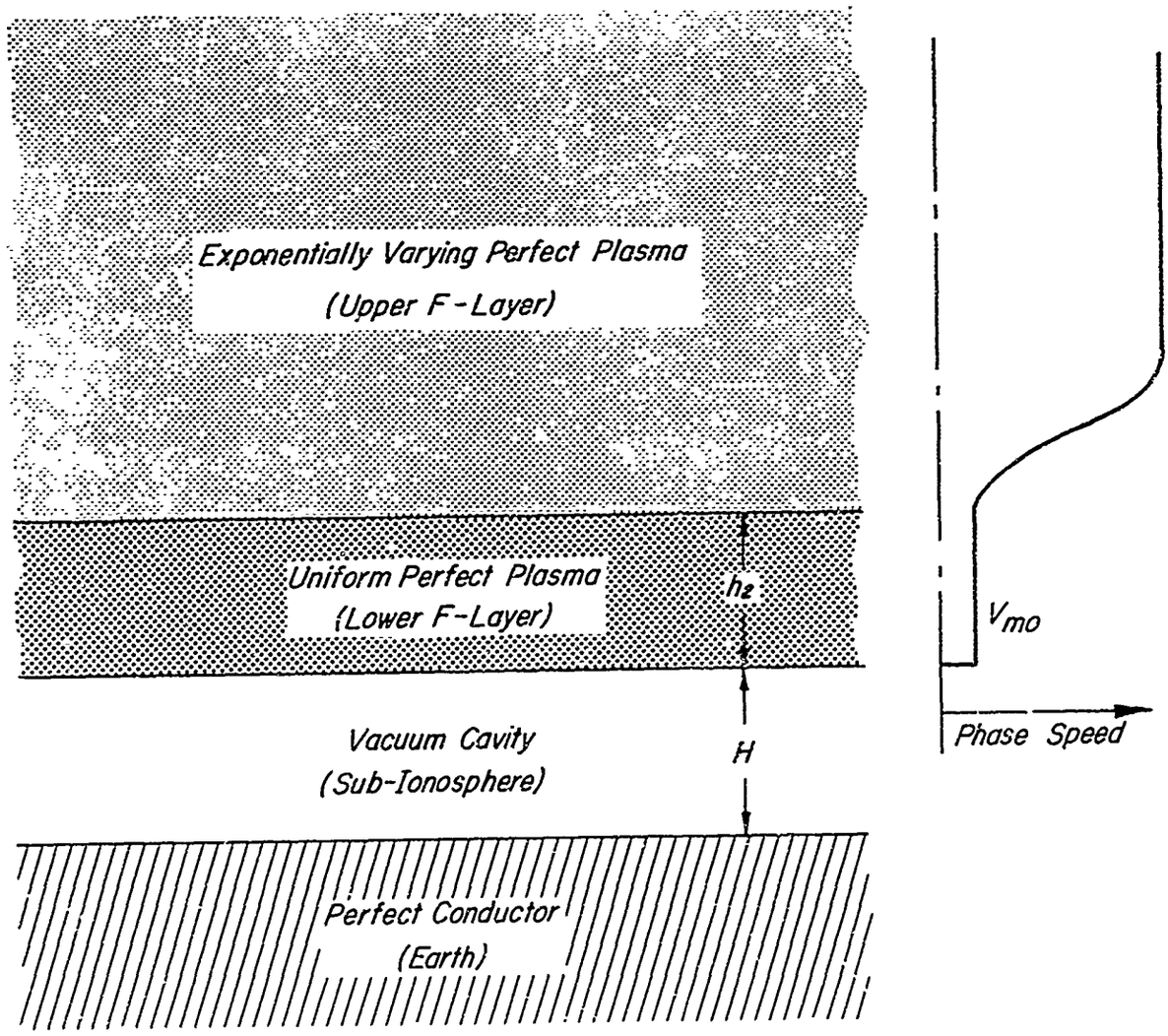

Fig. 3.9 Escape of a Magnetic Field Through An Exponential Plasma Region

TABLE II

VALUES OF CONSTANTS FOR EXPONENTIAL PLASMA PROBLEM

[V_{mo}/V_{m1} = 0.05 ; H/(2p) = 290/300 = 0.968]

$h_2/2p$	mode	1	2	3	4
0.733	ξ_n (real part)*	0.755	2.51	4.16	6.14
	ξ_n (imag. part)	0.0312	0.103	0.190	0.262
	$2C_n$*	0.662	0.146	0.065	0.029
	A_n*	0.250	0.184	0.136	0.089
	f_n** (cps)	0.124	0.414	0.685	1.01
0.367	ξ_n (real part)*	0.94	3.09	5.32	7.54
	ξ_n (imag. part)	0.051	0.187	0.306	0.447
	$2C_n$*	0.726	0.149	0.052	0.027
	A_n*	0.341	0.230	0.137	0.101
	f_n** (cps)	0.155	0.508	0.875	1.24

* Computed for V_{mo}/V_{m1} = 0 , an approximation which is accurate enough for small values of V_{mo}/V_{m1}.

** Assuming $2p/V_{mo}$ = 300/310 = 0.968 sec.

A time history of the magnetic field decay is shown in Figure 3.10 for $a = h_2/(2p) = 220 \text{ km}/300 \text{ km} = 0.73$. Two abscissa scales are shown, one for a generalized time scale $V_{mo}t/H$ and one for an absolute time scale based on the characteristic time $(2p)/V_{mo} = 300 \text{ km}/310 \text{ km/sec} = 0.97 \text{ sec.}$, which is representative of a low latitude nighttime ionospheric condition. The magnetic field is seen to initially decay exponentially (Eq. (3.1) applies here), and then tends to oscillate and decay more slowly at the lowest characteristic frequency. After only one or two cycles of this oscillation, all higher modes die out and the subsequent response varies simply as

$$B = 0.662 \exp(-\tau/32) \cos(0.755\,\tau) \tag{3.16}$$

where

$$\tau = \tfrac{1}{2} V_{mo} t/p \tag{3.17}$$

The characteristic time T for this final exponential decay is seen to correspond to $\tau = 32$ or

$$T = 64p/V_{mo} \tag{3.18}$$

It is interesting to note that while the magnetic field response occurs predominately in the lowest frequency mode, the same is not true for the rate of change of the magnetic field since the series obtained by differentiating Equation (3.14) converges much more slowly than the series in Equation (3.14). The first term in the differentiated series remains the largest term, but is not much larger than the second term for moderately long time durations.

3.4.2 Frequency Response

The frequency response function for the vacuum cavity for a steady-state sinusoidal application of magnetic flux is given approximately by Equation (B.8.50) as

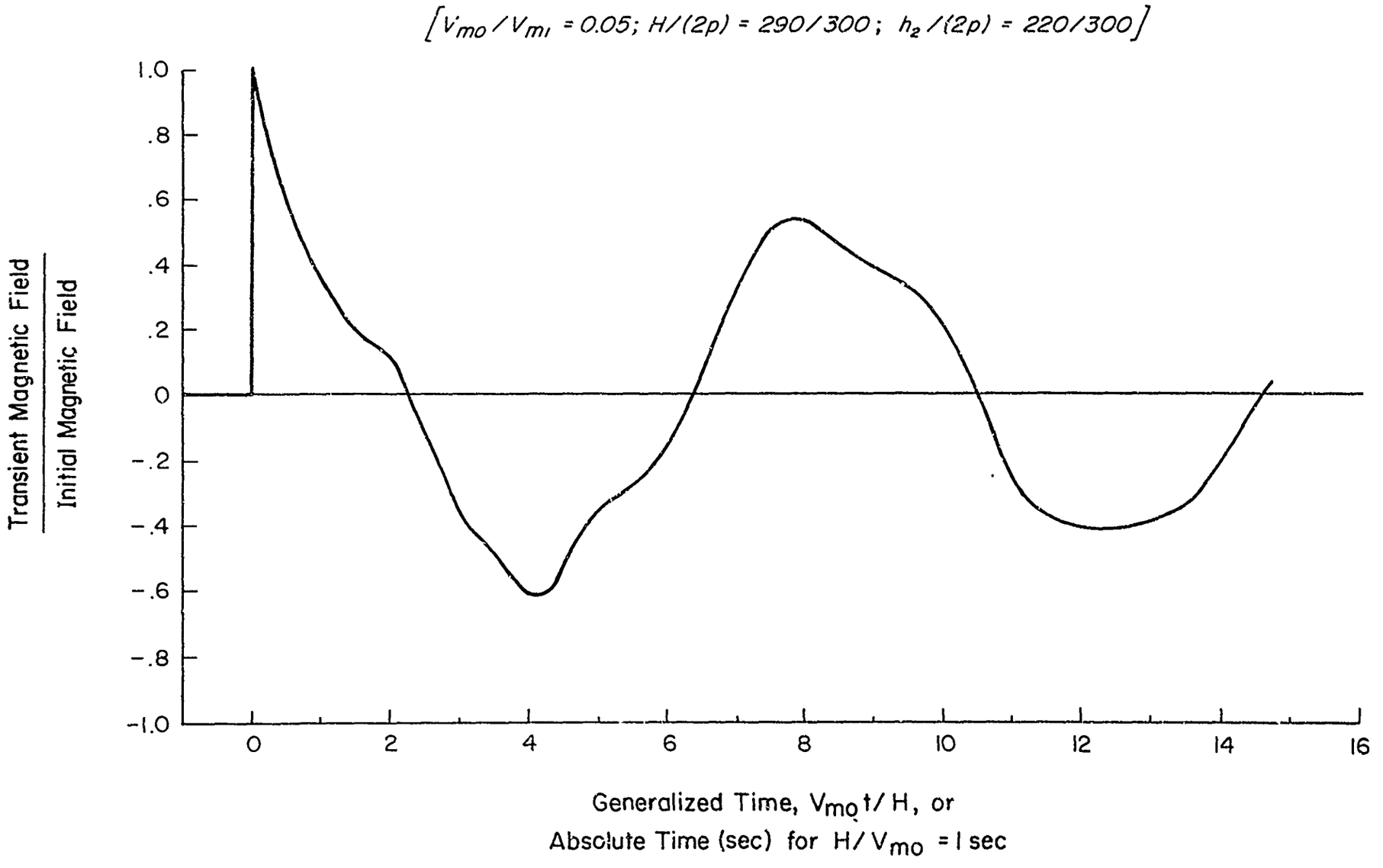

Fig. 3.10 Cavity Magnetic Response To a Step-Function Input

$$H(i\omega) = 1 + \left[a\xi \tan(\alpha + b\xi) - 1\right]^{-1} \qquad \text{(B.8.50)}$$

where

$$\xi = 2\omega p/V_{mo} \qquad \text{(B.6.3)}$$

$$\alpha = \tan^{-1}\left[J_1(\xi)/J_0(\xi)\right] \qquad \text{(B.5.6)}$$

$$a = \tfrac{1}{2} H/p \qquad \text{(B.8.48)}$$

$$b = \tfrac{1}{2}(h_e/p \mp i\pi\epsilon);\ \omega \gtrless 0 \qquad \text{(B.8.43)}$$

$$\epsilon = V_{mo}/V_{mi} \ll 1 \qquad \text{(B.8.44)}$$

This variation is shown in Figure 3.11 as a function of the generalized frequency parameter $\xi = 2\omega p/V_{mo}$ for $a = h_e/(2p) = 220/300 = 0.73$ and for $a = 0$. (The curve for $a = 0$ corresponds to the problem of Section 3.2 for escape into a semi-infinite perfect plasma.) Also shown in this figure is an absolute frequency scale for the characteristic time $(2p)/V_{mo} = 300$ km/310 km/sec, representative of a low latitude nighttime ionospheric condition.

It is seen from Figure 3.11 that there is a conspicuous near-resonant condition at the generalized frequency $\xi = 2\omega p/V_{mo} \approx 0.755$ and that there are a sequence of other higher frequency progressively more strongly damped resonant conditions. The first four characteristic frequencies are listed in Table II according to Equation (B.8.47). In order to interpret these frequencies in terms of nighttime ionosphere variations, they are plotted against geomagnetic latitude in Figure 3.12, under the assumption that the Alfvén speed varies with geomagnetic latitude in the same manner as does the geomagnetic field for a simple dipole representation, i.e., for

$$V_a = V_{ae}\sqrt{\sin^2\lambda + \tfrac{1}{4}\cos^2\lambda} \qquad (3.19)$$

where

λ is geomagnetic latitude

V_{ae} is the Alfven speed at the equator ($\lambda = 0$)

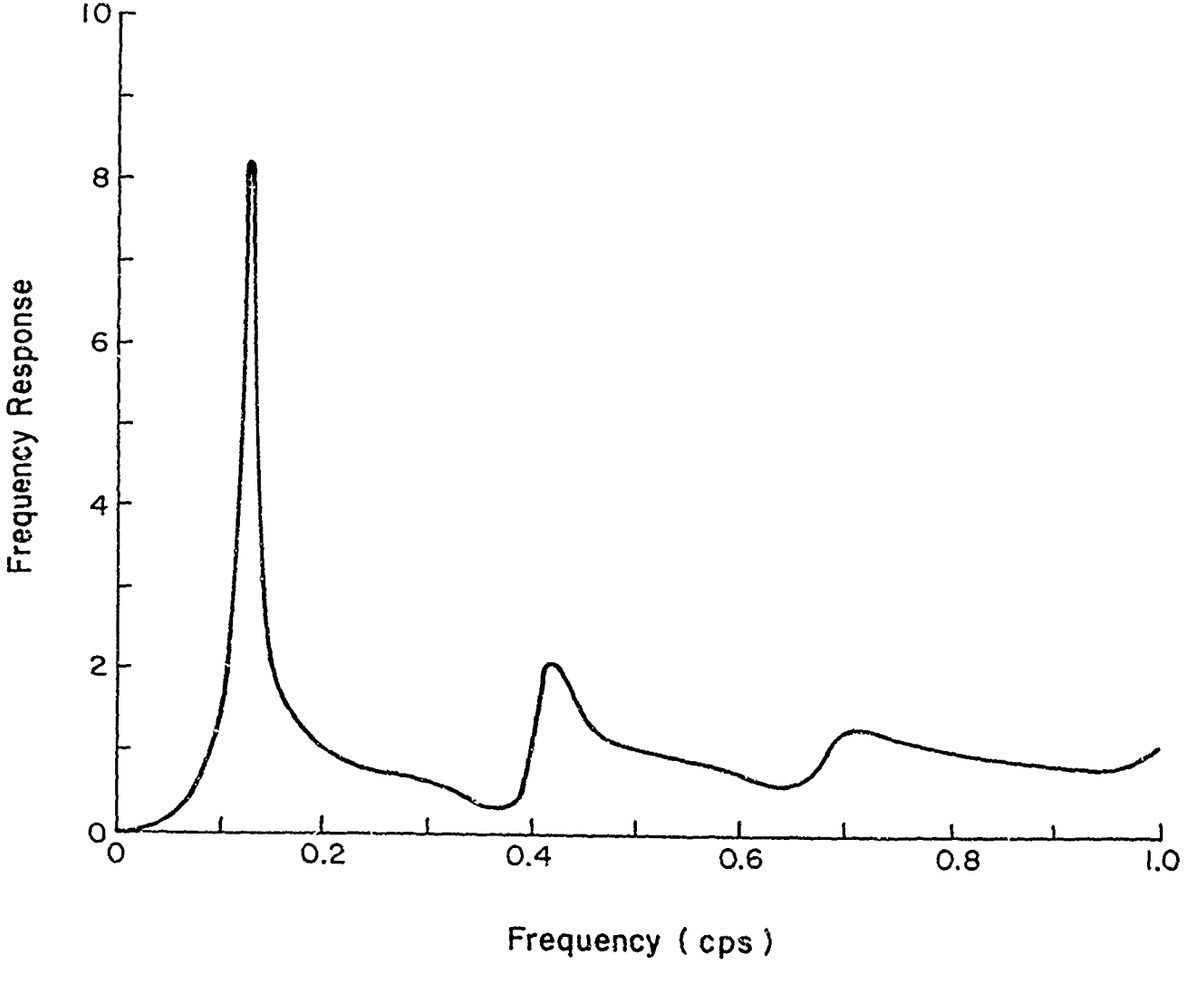

Fig. 3.11 Frequency Response Variations

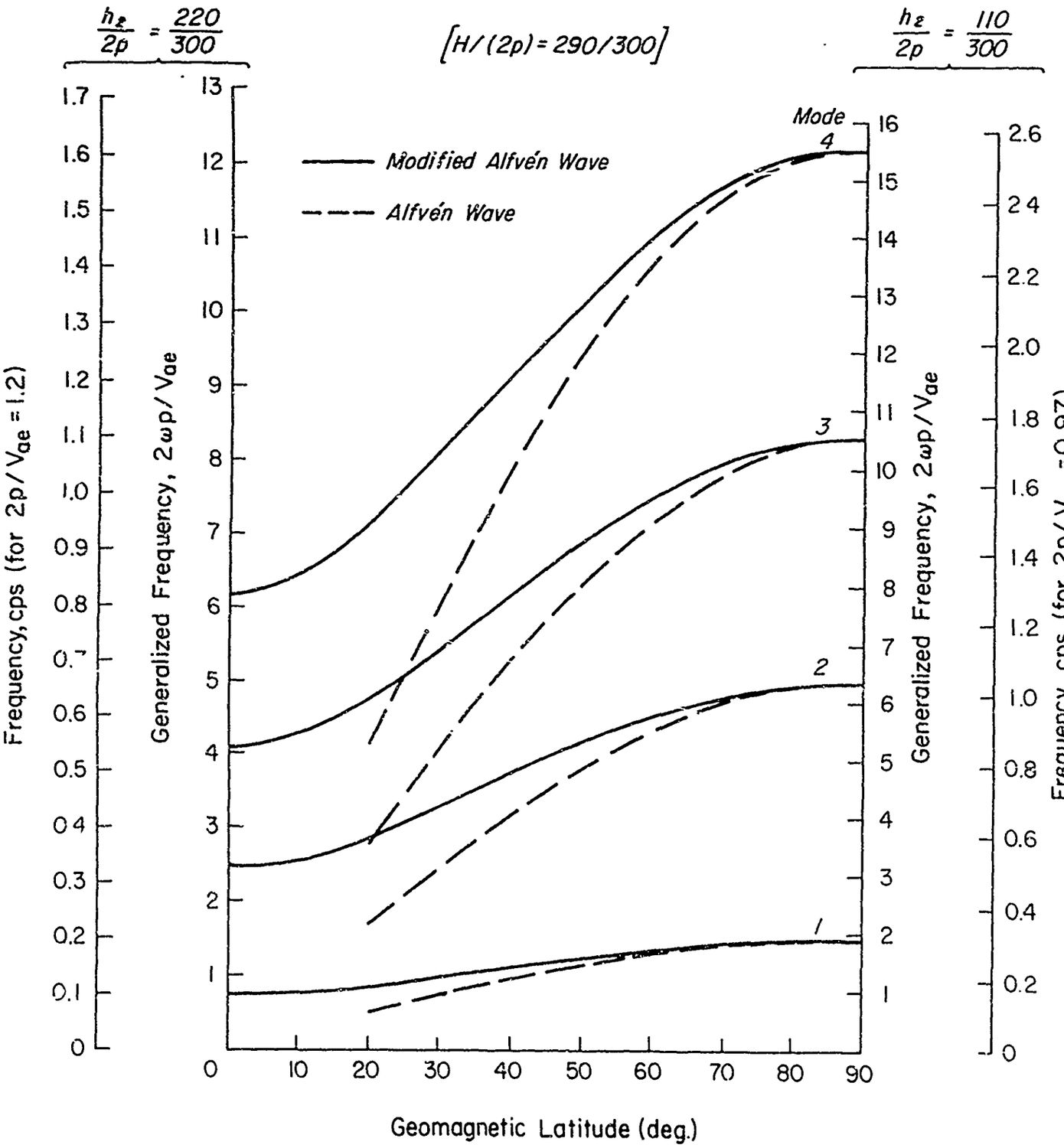

Fig. 3.12 Characteristic Frequencies of the Nighttime Ionosphere

Both generalized and absolute* frequency scales are shown in this figure for $h_2/(2p) = 220/300$ and $110/300$†, and frequency variations are shown for both Alfvén and modified Alfvén waves. (No curves are shown for the Alfvén made at low latitudes since the present model is not applicable there.) It is noted that the frequencies increase with geomagnetic latitude, and are moderately larger for the modified Alfvén mode at intermediate latitudes. The absolute frequencies for the first four modes are seen to range from about 0.1 to 2.5 cps.

3.5 DESCENT OF A HYDROMAGNETIC WAVE INTO A VACUUM CAVITY

Section B.4 of Appendix B considers the problem where a semi-infinite rectangular hydromagnetic wave front, descending through a perfect hydromagnetic plasma, encounters a vacuum cavity, the lower edge of which is bounded by a perfect conductor (Fig. 3.13). The initial descent speed of the wave front depends on the polarization of the incident magnetic field. If its magnetic vector is in the plane formed by the ambient magnetic field vector ($\bar{B}_o$) and the vertical, the wave is a modified Alfvén wave traveling at the Alfvén speed V_a; if its magnetic vector is perpendicular to this plane, the wave is an Alfvén wave, traveling at the phase speed $V_a \cos\varphi$, where φ is the acute angle between the ambient magnetic field vector and the vertical.

In either case, the magnetic field produced in the cavity by the descending wave increases with time as shown in Figure 3.14, according to the equation

$$B_v = 2B_i[1 - \exp(-V_m t/H)] \qquad (B.4.6)$$

where V_m is given by Equation (3.2) and B_i is the strength of the incident magnetic field.

Descent of the incident wave into the cavity also produces a reflected wave, whose time history is of the form indicated in Figure 3.15. It may be noted that the reflected wave initially has a negative peak, followed by an exponential transition to an eventual reflection coefficient of plus unity.

---

* For $2p/V_{ae} = 300$ km/300 km/sec

† The ratio $h_2/(2p) = 110/300$ is believed to be more realistic for the nighttime ionosphere.

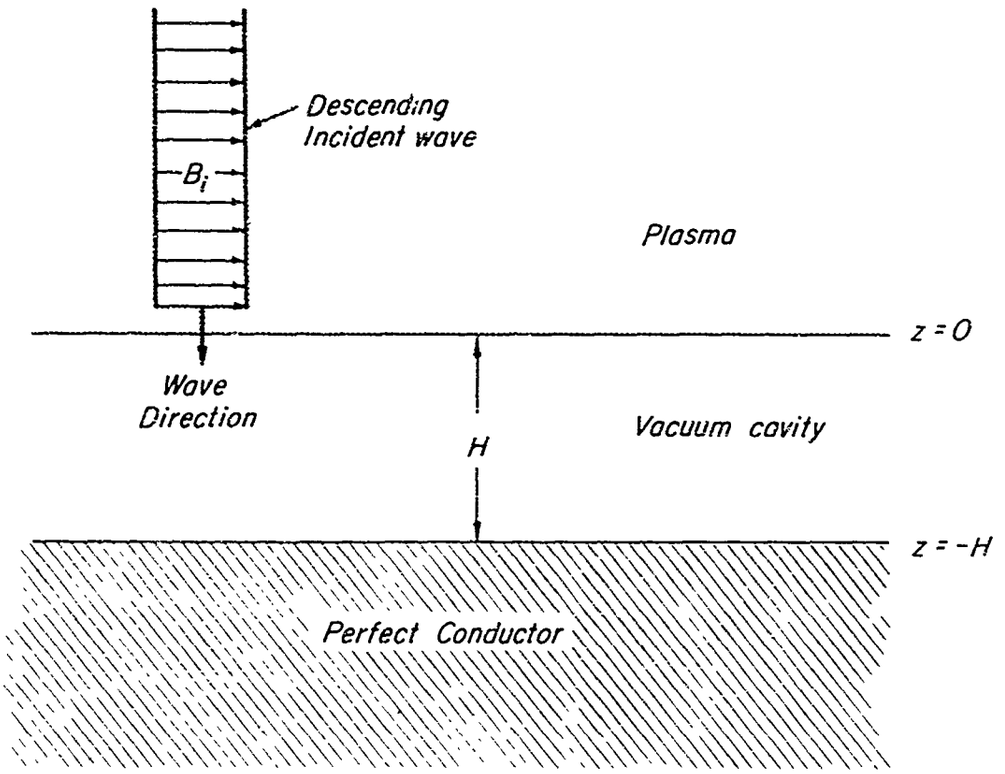

Fig. 3.13 Descent of a Hydromagnetic Wave into a Vacuum Cavity

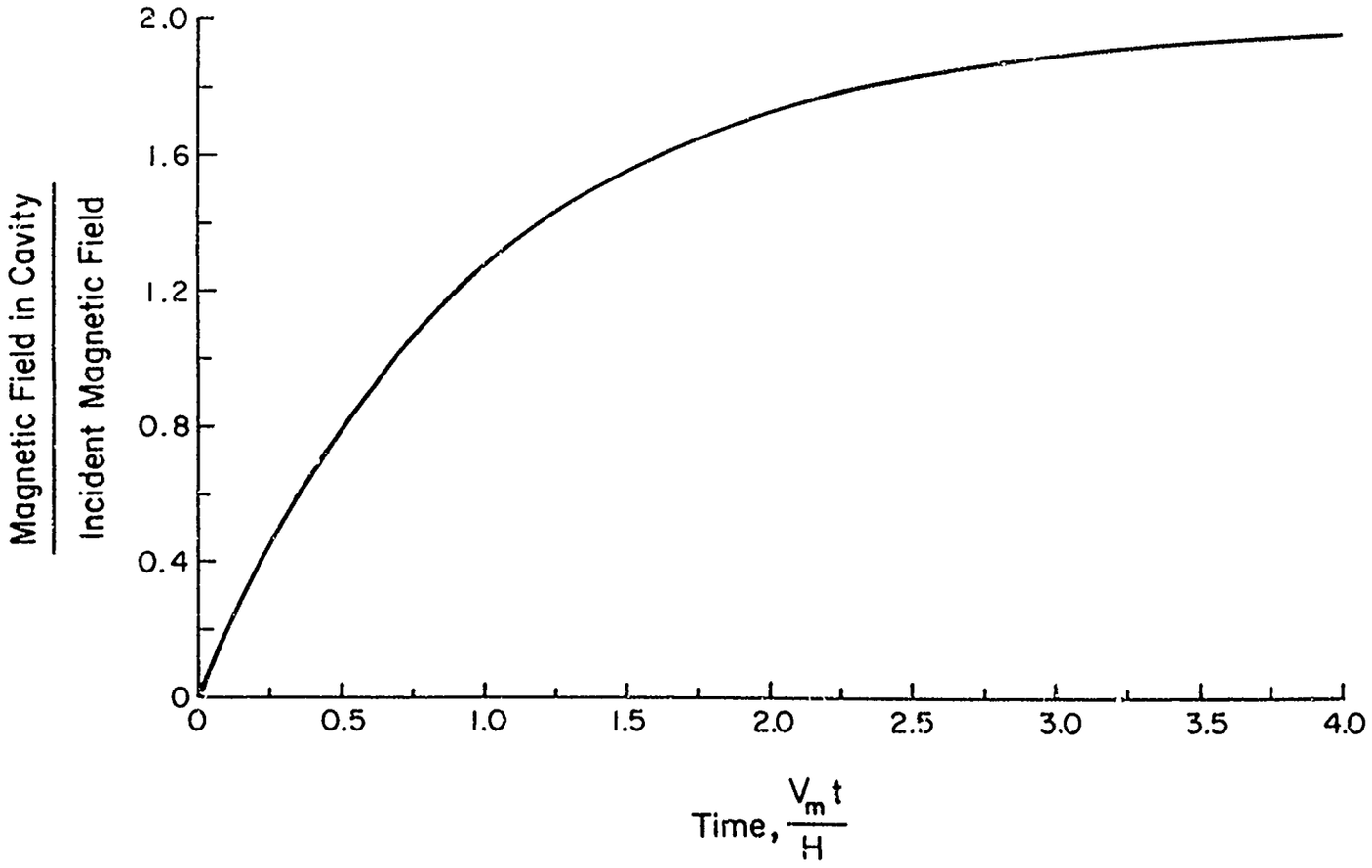

Figure 3.14 Growth of the Magnetic Field in the Cavity

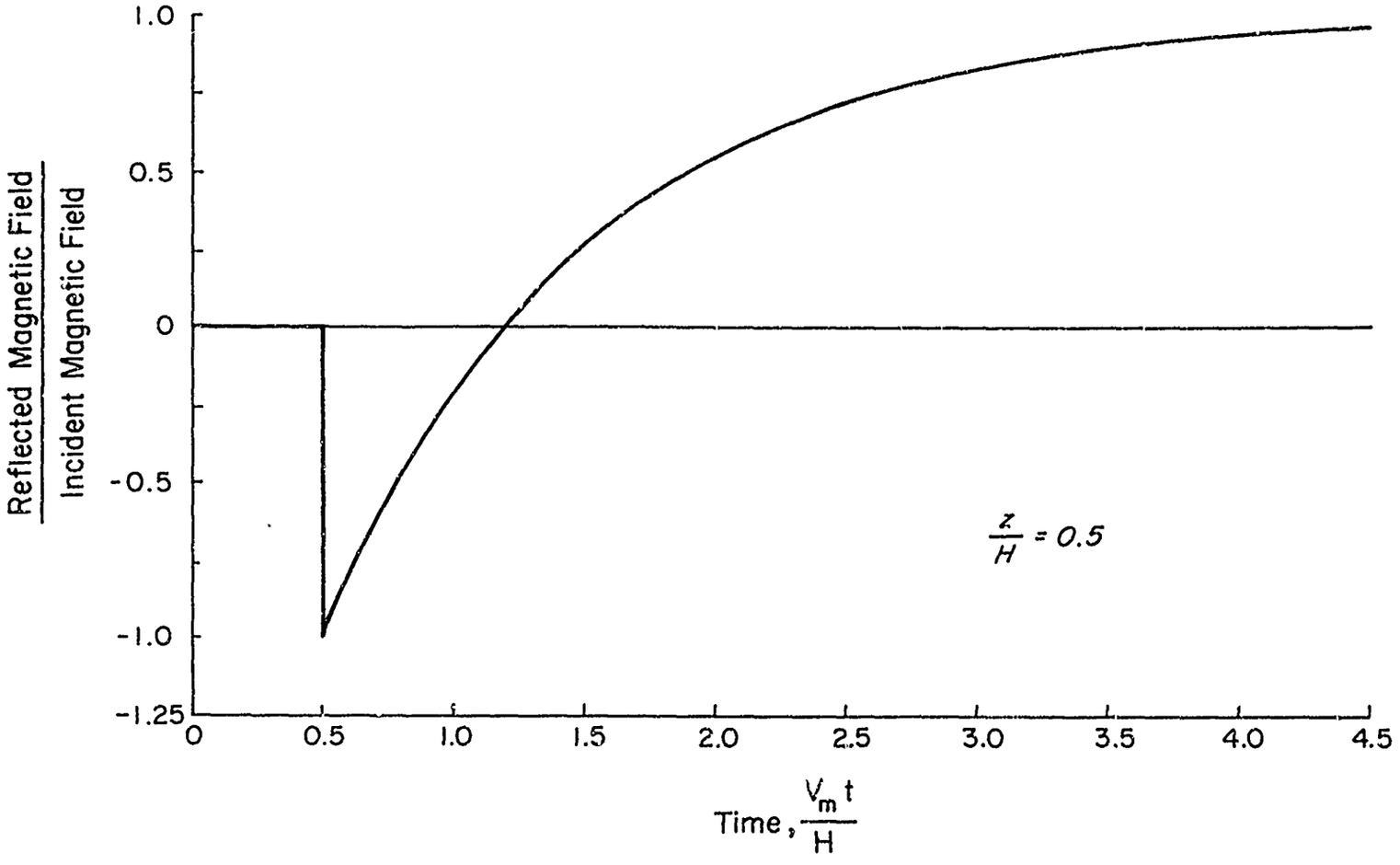

Figure 3.15 Reflected Magnetic Field

3.6 REFLECTION FROM EXPONENTIAL BARRIERS

Section B.5 and B.6 of Appendix B consider two similar problems, where a hydromagnetic wave, traveling in a uniform perfect hydromagnetic plasma, suddenly encounters a region of exponentially increasing Alfven speed (Figs. 3.16 and 3.17). In Section B.5, the Alfven speed is assumed to increase without limit (Fig. 3.16), and in Section B.6 is assumed to have a finite upper limit (Fig. 3.17). In either case, the incidence of a semi-infinite rectangular wave front on the exponential barrier produces a reflected wave of the form shown in Figure 3.18, where

V_{mo} is the initial phase speed (Fig. 3.16)

$2p$ is a scale distance associated with the phase speed variation (Eq. (B.5.3))

If the final Alfven speed is considered unlimited (Section B.5), the conspicuous peak in this figure is infinite; if the final Alfven speed is limited (Section B.6), this peak becomes finite.

It may be noted in Figure 3.18 that the polarity of the reflected wave is reversed from that of the incident wave, this behavior being characteristic of reflection from regions of greater phase speeds. The reflected wave intensity is seen to increase with time up to a peak value at the time $4p/V_{mo}$, after which time the wave rapidly approaches the endpoint condition of a reflection coefficient of minus unity.

Also considered in Appendix B is the energy transmitted through the exponential barrier for the case of incident steady-state sinusoidal waves. The fraction of the incident energy transmitted through the barrier is zero if the final Alfven speed is unlimited; is equal to $4V_{mo}/V_{m1}$ for a finite phase speed limit with frequency approaching zero (from the limiting value of Eq. (B.6.5)), and increases with increasing frequency as indicated in Figure 3.19.

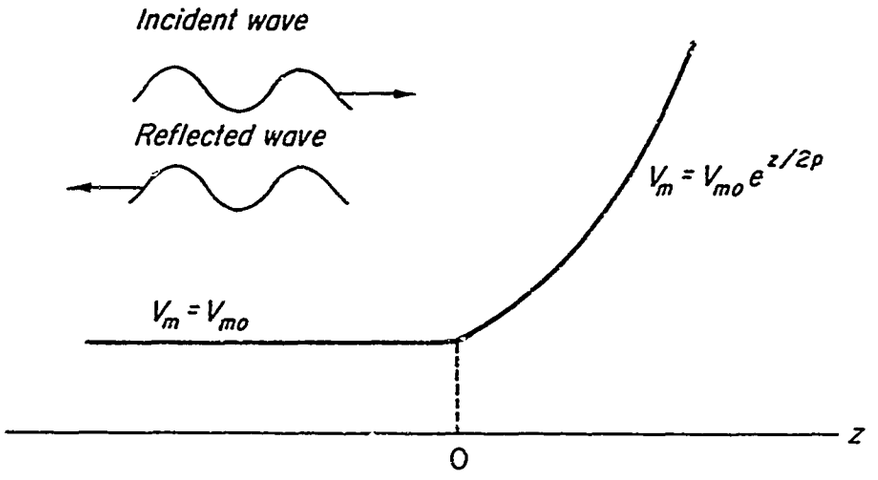

5554a

Fig. 3.16 Unlimited Exponential Barrier Problem

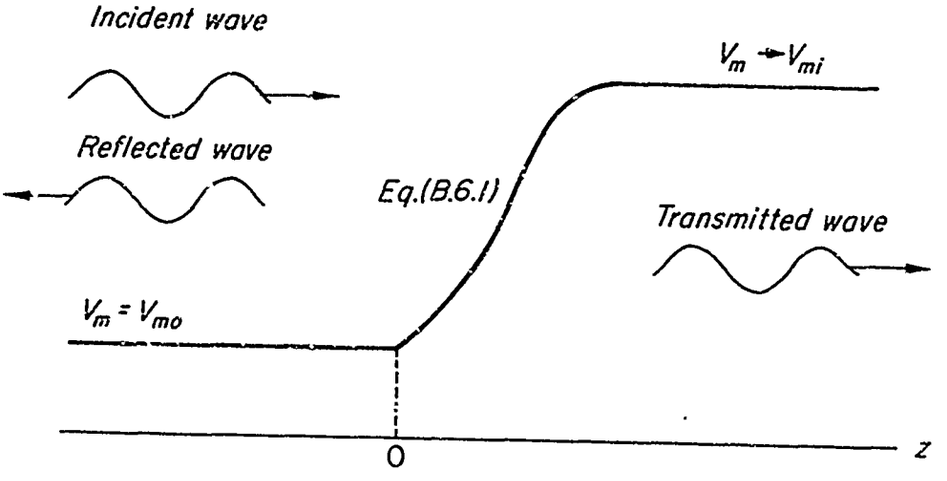

Fig. 3.17 Limited Exponential Barrier Problem

5554b

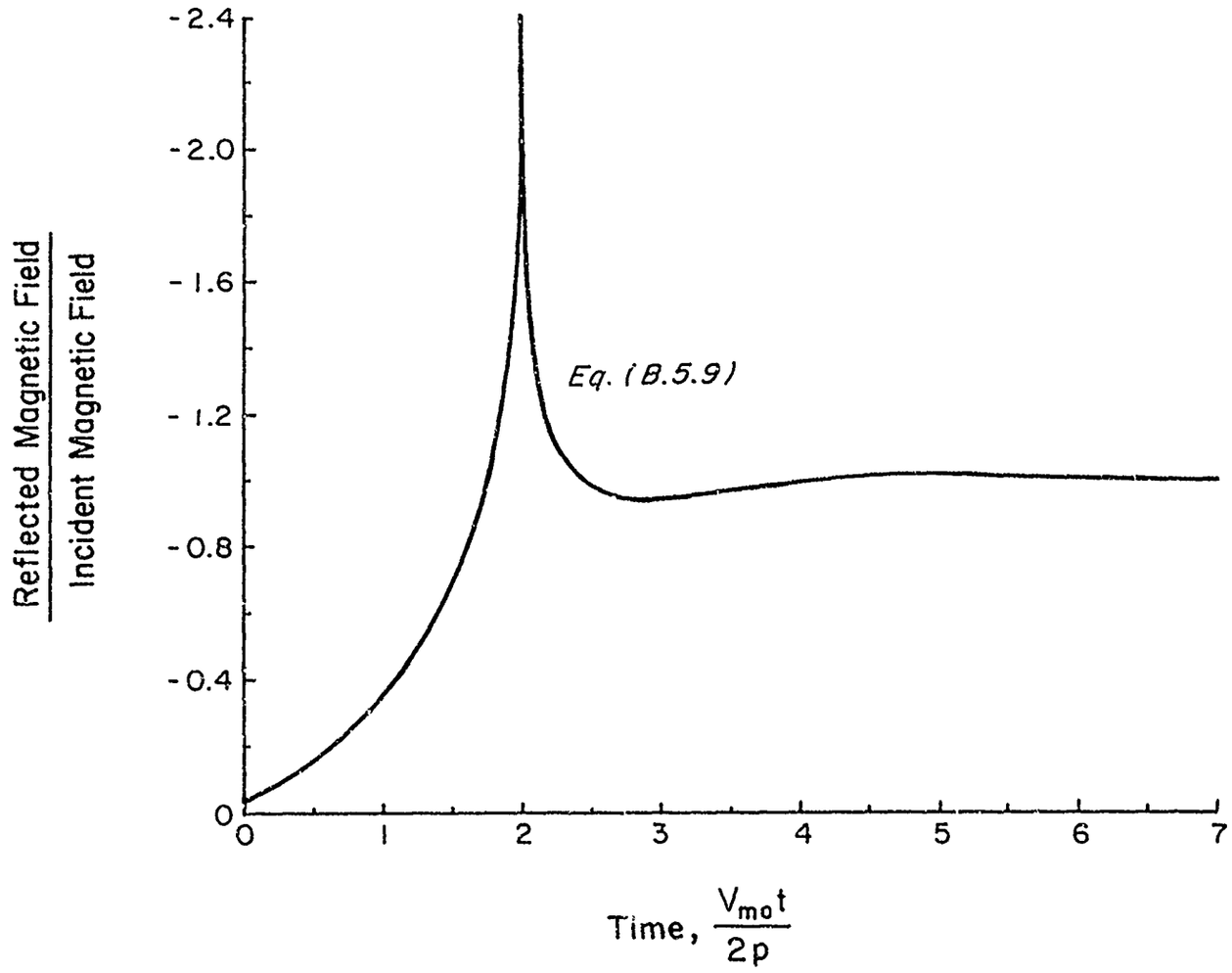

Figure 3.18 Reflected Wave Shape

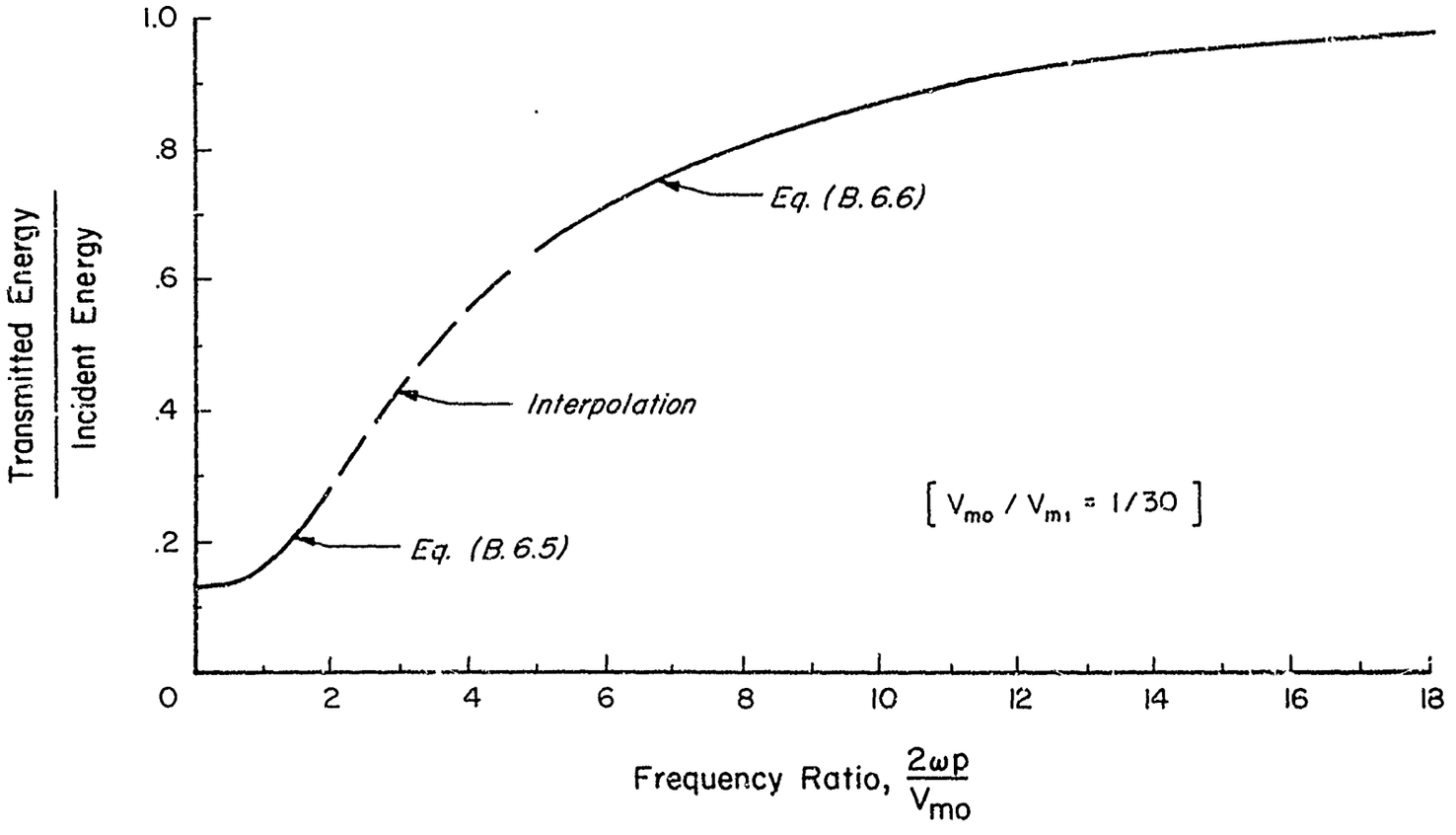

Figure 3.19 Energy Transmission Through an Exponential Barrier

3.7 OTHER PROBLEMS

In addition to the material specifically described above, Section B.8.1 of Appendix B presents some additional material relevant to the treatment of more complex one-dimensional cavity escape problems (Sec. B.8.1), plus some considerations of the simple problem of reflection and transmission of hydromagnetic waves at an abrupt barrier between two uniform plasma regions.

BLANK PAGE

SECTION IV

APPLICATION TO THE IONOSPHERE

This section offers some brief comments on the applicability of the results of the preceding sections to the propagation of ultra-low-frequency (ULF) waves in and below the ionosphere. Throughout this section we disregard the fact that our considerations in Section II were limited by the assumption of an isotropic conductivity law for the plasma regions concerned and are thus not exactly representative of the anistropic ionospheric plasma. This disregard is certainly justified for the essentially qualitative considerations given below; the reader need only recognize that the actual ionosphere will certainly demonstrate all of the types of phenomena characteristic of an isotropic plasma, plus additional complications characteristic of the anisotropic conductivity components.

Consider first the question of ULF wave propagation via the sub-ionosphere cavity, such as may be excited by lightning strokes or by the magnetic dipole produced by the detonation of a nuclear bomb. Two effects produced by a magnetic dipole suddenly appearing in or below the ionosphere have been shown in Sections II and III. First, a (hydromagnetic) wave moves downward from the dipole origin until it reaches the lower edge of the ionosphere and then immediately (at the speed of light) produces a world-wide magnetic disturbance, which, in turn, then relaxes or difuses upward into the ionosphere. This relaxation process has been considered in detail in Section 3.4 for a fairly realistic model of the nighttime ionosphere and has been shown to exhibit various resonant frequencies in the near 1 cps region. Also, the relaxation process for a step function magnetic flux excitation has been shown to consist of one dominant frequency below one cps, which persists for tens of seconds, plus higher frequency overtones which decay progressively more rapidly. For the daytime ionosphere, a similar but more complex response would be expected, added complexity being introduced by the Hall effect, which couples the Alfvén and modified Alfvén wave components in the E-layer.

It may be inferred from the above discussion, that the distant ULF effects of lightning strokes will also be subject to modification in the same manner as for nuclear bursts effects, the only basic differences for these two processes being in the frequency spectrum and geographic distribution and polarization of the primary exciting magnetic field traveling through the sub-ionosphere cavity. In the case of lightning, of course, only part of the wave energy occurs within the ULF range, to which the present discussion is limited.

Regarding wave propagation in the ionosphere above the dense (E layer) part of the ionosphere, it has been shown in Sections 2.4 and 2.5 that the field of a suddenly created magnetic dipole, when incident on an abrupt discontinuity in plasma density, can create a surface wave of strong intensity traveling along the interface. Since the upper ionosphere contains relatively strong density gradients at altitudes of about 400 kilometers and above, it may be expected that such a form of wave propagation will be important for the upper ionospheric travel of bomb-produced magnetic disturbances. It might also be noted that this surface-wave type of wave propagation differs from the purely radiation-type propagation associated with the duct theory of upper ionosphere wave propagation.

SECTION V

CONCLUDING REMARKS

This report has presented a series of solutions of one- and three-dimensional problems concerning electromagnetic and hydromagnetic wave propagation in various combinations of horizontally stratified plasma and vacuum regions, chosen to simulate significant characteristics of the ionosphere and sub-ionosphere cavity at ultra-low-frequencies (near 1 cps). It is believed that the results of these studies offer an increased understanding of propagation of electromagnetic and hydromagnetic waves produced by nuclear detonations and by distant lightning strokes. In particular, the frequency response and step-function response of the nighttime ionosphere to ultra-low-frequency waves has been clarified by a fairly realistic simulation of the ionosphere. The corresponding analysis for the daytime ionosphere would be considerably more difficult (because of the need to consider Hall effects), but could be performed in a similar manner, using methods outlined in this report.

BLANK PAGE

APPENDIX A

THREE-DIMENSIONAL ELECTROMAGNETIC FIELD PROBLEMS

A.1 INTRODUCTION

This part of this report is concerned with the calculation of the transient electromagnetic fields produced by magnetic dipoles in various types of horizontally stratified plasma and un-ionized media. It is assumed throughout that Maxwell's equations are applicable with an isotropic conductivity law and that the displacement current may be neglected in vacuum regions. This assumption of isotropic conductivity is, of course, not generally applicable to hydromagnetic wave propagation, which is our principal concern in this report. However, to a considerable extent, both qualitatively and quantitatively, the electromagnetic problems considered herein do offer some insight into the analogous hydromagnetic problems.

The following electromagnetic problems are considered, after presentation of basic equations in Section A.2. The magnetic field of a magnetic dipole in a uniform infinite plasma is considered in Section A.3. Sections A.4 and A.5, respectively, consider the electromagnetic fields produced by horizontal and vertical magnetic dipoles located in a semi-infinite plasma above a horizontal interface separating the plasma above from a semi-infinite vacuum region below. Section A.6 considers the electromagnetic fields produced by a horizontal magnetic dipole located in a semi-infinite plasma above a horizontal vacuum cavity, the lower edge of which is the surface of a perfect conductor.

For each of the above-mentioned problems, the analysis begins with a determination of the electromagnetic field for steady-state sinusoidal variations of the magnetic dipole moment. This is followed by evaluation of the transient magnetic fields produced by the sudden step-function creation of a magnetic dipole moment (see Appendix E). Numerical results are presented and discussed in Section II of the text.

A.2 BASIC EQUATIONS

A.2.1 Maxwell's Equations

The basic equations used in this Appendix are as follows. From Maxwell's equations in MKS units

$$\nabla \times \bar{B} = \mu \bar{J}_1 \tag{A.2.1}$$

$$\nabla \times \bar{E} = -\partial \bar{B} / \partial t \tag{A.2.2}$$

$$\bar{J}_1 = \bar{J} + c^{-2} \mu^{-1} \partial E / \partial t \tag{A.2.3}$$

where

$\bar{E}$	is the electric field vector
$\bar{B}$	is the magnetic field vector
μ	is the permeability in vacuum
t	is time
c	is the velocity of light in vacuum
$\bar{J}$	is the current density vector
$\bar{J}_1$	is the total current density vector, including the displacement current, which is, however, assumed zero in vacuum regions

We consider plasma regions with isotropic conductivity obeying an Ohm's law relationship for sinusoidal variations of the form

$$\bar{J}_1 = \sigma \bar{E} \quad ; \quad \left[\bar{E} \sim \exp (i\omega t) \right] \tag{A.2.4}$$

where

σ is the conductivity

Four types of media are considered, with σ defined as follows for each.

Perfect plasma:

$$\sigma = i\omega/(\mu V^2) \tag{A.2.5}$$

Complex plasma:

$$\sigma = \sigma_o + i\omega/(\mu V^2) = (\nu + i\omega)/(\mu V^2) \tag{A.2.6}$$

Ohmic plasma:

$$\sigma = \sigma_o \tag{A.2.7}$$

where

σ_o is the real component of the conductivity

V is the wave propagation speed for $\sigma_o = 0$

ν is a characteristic damping frequency, related to σ_o as

$$\nu = \sigma_o V^2 \mu \tag{A.2.8}$$

Vacuum

$$\sigma = 0 \tag{A.2.9}$$

The electric and magnetic fields for steady-state sinusoidal oscillations according to Equations (A.2.1) through (A.2.4) may be expressed in terms of a vector potential $\overline{F}$ as (Wait and Campbell 1953*)

$$\overline{B} = -\gamma^2 \overline{F} + \nabla \Phi \tag{A.2.10}$$

$$\overline{E} = -i\omega \nabla \times \overline{F} \tag{A.2.11}$$

$$\Phi = \nabla \cdot \overline{F} \tag{A.2.12}$$

$$\gamma = ik \tag{A.2.13}$$

$$k = \sqrt{-i\omega\mu\sigma} \tag{A.2.14}$$

---

* The F symbol used herein differs from Wait and Campbell's (1953) symbol by the factor $i\omega$.

where

$\bar{\varphi}$ is a scalar potential

k is the wave number

γ is the propagation constant

and where, for problems with symmetry with respect to the x = 0 plane of an XYZ-rectangular coordinate system (Wait and Campbell, 1953)

$$\left.\begin{aligned} F_x &= 0 \\ F_y, F_z &\sim \exp(i\omega t \pm u z)\, J_n(\lambda \rho) \cos n\theta \end{aligned}\right\} \qquad (A.2.15)$$

where

$$u = \sqrt{\lambda^2 - k^2} = \sqrt{\lambda^2 + \gamma^2} \qquad (A.2.16)$$

J_n is a Bessel function of the first kind

n is a constant

λ is a parameter

$$\rho = \sqrt{x^2 + y^2} \qquad (A.2.17)$$

$$\theta = \tan^{-1}(x/y) \qquad (A.2.18)$$

For each problem considered here, the exciting disturbance is taken as a horizontal or vertical magnetic dipole, which is characterized in a uniform plasma by the vector potential (Wait and Campbell 1953)

$$F = C \exp(-\gamma r)/r \qquad (A.2.19)$$

$$C = \mu m_o/(4\pi) \qquad (A.2.20)$$

m_o is the dipole moment

r is the distance between the dipole and any point (x, y, z)

where F is a horizontal vector (F_y) for a horizontal dipole and a vertical vector (F_z) for a vertical dipole.

A.1.2 Boundary Conditions

Boundary conditions to be satisfied at the boundary between plasma and plasma-vacuum regions are continuity of the horizontal electric and magnetic fields, or in terms of the vector potential, for a horizontal plane boundary, the following quantities must be continuous across the boundary (Wait and Campbell, 1953):

$$F_z,\ \Phi,\ \gamma^2 F_y,\ \partial F_y/\partial z \quad \text{continuous} \tag{A.2.21}$$

At the horizontal surface of a perfect conductor, the boundary condition to be satisfied is the vanishing of the horizontal electric field, or in terms of the vector potential

$$F_z = \partial F_y/\partial z = 0 \tag{A.2.22}$$

A.3 MAGNETIC DIPOLE IN A UNIFORM PLASMA

A.3.1 Frequency Response

This section considers the electromagnetic field of a magnetic dipole in a uniform plasma. The dipole is assumed to be located at the origin of an XYZ-axis system (Fig. A.1) with the dipole axis parallel to the Y-axis. The electromagnetic field for this problem for sinusoidal oscillations may be expressed in terms of a vector potential having only a y-component as (e.g., Wait and Campbell, 1953)

$$F_y = C \exp(-\gamma r)/r \tag{A.3.1}$$

where

$$r = \sqrt{x^2 + y^2 + z^2} \tag{A.3.2}$$

$$\gamma = ik \tag{A.3.3}$$

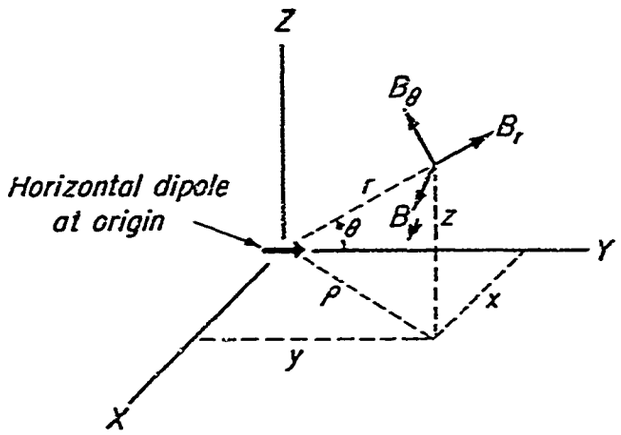

Fig. A. 1 Horizontal Dipole Problem Geometry

The magnetic field components then follow from Equations (A.2.10) and (A.2.12) as

$$B_r = 2C(1 + \gamma r)\exp(-\gamma r)\cos\theta / r^3 \qquad (A.3.4)$$

$$B_\theta = C\left[1 + \gamma r + (\gamma r)^2\right]\exp(-\gamma r)\sin\theta / r^3 \qquad (A.3.5)$$

$$B_\psi = 0 \qquad (A.3.6)$$

where r, θ, ψ are spherical polar coordinates with respect to the dipole axis (Fig. A.1). These three equations, taken with Equations (A.2.13) and (A.2.5) through (A.2.7) of Section A.2, give the magnetic disturbance or frequency response in a plasma resulting from a steady-state sinusoidal variation of magnetic dipole moment.

A.3.2 Step-Function Response

It is now desired to obtain the transient response of the plasma to a step function dipole input. This may be done conveniently by replacing ω by $-is$ in the preceding equations, where s is considered to be the transformed variable of the Laplace transform (Churchill, 1944), by then dividing the field expressions by s, and then inverting the resulting Laplace transforms.

Complex plasma:

For the general case of a complex plasma, the step function response corresponding to Equations (A.3.4) and (A.3.5) may be obtained with the aid of items 1 and 2 in Table E.1 of Appendix E as

$$B_r(t) = 2(C/r^3)\left[\left[\delta(\tau - 1) + a^2\tau\, I_1^*(a\sqrt{\tau^2 - 1}) + a I_0(a\sqrt{\tau^2 - 1})\right]\exp(-a\tau) + \exp(-a) + a^2 A_1(\tau)\right] S(\tau - 1)\cos\theta \qquad (A.3.7)$$

$$B_\theta(t) = (C/r^3)\Big\{\Big[\delta_1(\tau - 1) + (1 + a + \tfrac{1}{2}a^2)\,\delta(\tau - 1)\Big]\exp(-a)$$

$$+\Big[\Big\{a^2(\tau + a - 2\tau/(\tau^2 - 1))\,I_1^*(a\sqrt{\tau^2-1}) + a\,(1 + a\tau/(\tau^2 - 1))I_o(a\sqrt{\tau^2 - 1})\Big\}\exp(-a\tau)$$

$$+ \exp(-a) + a^2 A_1(\tau)\Big]S(\tau - 1)\Big\}\sin\theta \qquad \text{(A.3.8)}$$

$$A_1(\tau) = \int_o^\tau I_1^*(a\sqrt{\tau^2 - 1})\exp(-a\tau)\,d\tau \qquad \text{(A.3.9)}$$

$$I_1^*(a\sqrt{\tau^2 - 1}) = I_1(a\sqrt{\tau^2 - 1})\,S(\tau - 1)/(a\sqrt{\tau^2 - 1}) \qquad \text{(A.3.10)}$$

$$\tau = Vt/r \qquad \text{(A.3.11)}$$

$$a = \tfrac{1}{2}\,r\,\nu/V = \tfrac{1}{2}\mu\,\sigma_o\,r\,V \qquad \text{(A.3.12)}$$

Perfect plasma:

For the case of a perfect plasma ($\nu = 0$), the magnetic field is given by the simpler equations

$$B_r(t) = 2(C/r^3)\Big[S(\tau - 1) + \delta(\tau - 1)\Big]\cos\theta \qquad \text{(A.3.13)}$$

$$B_\theta(t) = (C/r^3)\Big[S(\tau - 1) + \delta(\tau - 1) + \delta_1(\tau - 1)\Big]\sin\theta \qquad \text{(A.3.14)}$$

Ohmic plasma:

For the case of an ohmic plasma

$$B_r(t) = (2C/r^3)\Big[\operatorname{erfc} x_1 + x_1\,\operatorname{erf}' x_1\Big] \qquad \text{(A.3.15)}$$

$$B_\theta(t) = (C/r^3)\Big[\operatorname{erfc} x_1 + x_1(1 + 2x_1^2)\operatorname{erf}' x_1\Big] \qquad \text{(A.3.16)}$$

where

$$x_1 = \frac{1}{2}\, r \sqrt{\mu \sigma_o / t} = \frac{1}{2}(r/V)\sqrt{\nu/t} \qquad \text{(A.3.17)}$$

$$\text{erf}' x_1 = (2/\sqrt{\pi}) \exp(-x_1^2) \qquad \text{(A.3.18)}$$

Transient magnetic field variations according to Equations (A.3.7) through (A.3.18) are presented and discussed in Section 3.2 of Section III.

A.4 HORIZONTAL MAGNETIC DIPOLE IN A SEMI-INFINITE PLASMA

A.4.1 Frequency Response

This section considers the electromagnetic fields produced by a horizontal magnetic dipole located above a horizontal interface separating a plasma (above) from a vacuum (Fig. A.2). This problem has been analyzed by Wait and Campbell (1953) for sinusoidal variations of the dipole strength, whose results for the magnetic field may be stated in the form

$$\overline{B} = \nabla \Phi - \gamma^2 \overline{F} \qquad \text{(A.4.1)}$$

where, for the plasma region ($z > 0$)

$$\left.\begin{aligned} F_x &= 0 \\ F_y &= C\left[P(|z-h|,\rho) - P(z+h,\rho)\right] \\ F_z &= -2C\gamma^{-2}\left[(\partial^3/\partial y\,\partial z^2)\,N(z+h,\rho) + (\partial^2/\partial y\,\partial z)\,P(z+h,\rho)\right] \\ \Phi &= C(\partial/\partial y)\Big[P(|z-h|,\rho) - P(z+h,\rho) \\ &\quad - 2\gamma^2(\partial^2/\partial z^2)\left[P(z+h,\rho) + (\partial/\partial z)\,N(z+h,\rho)\right]\Big] \end{aligned}\right\} \text{(A.4.2)}$$

and where the P and N functions are defined by Equations (C.5) and (C.7) of Appendix C.

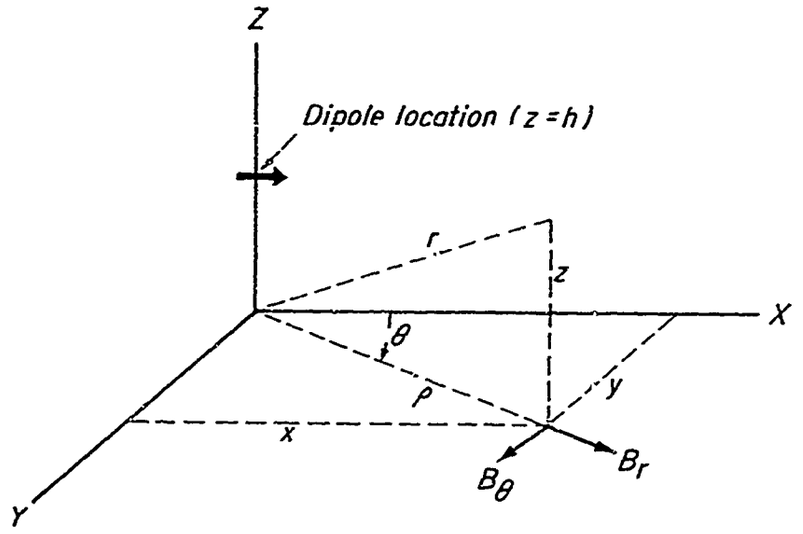

5563 a

Fig. A. 2 Horizontal Dipole in a Semi-infinite Plasma

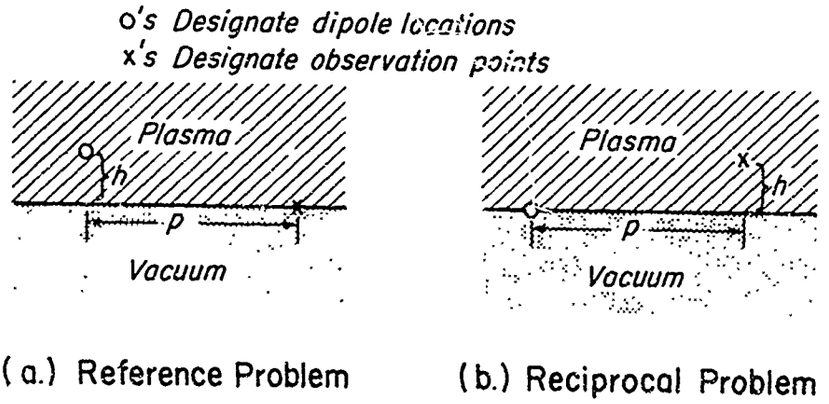

5563 b

Fig. A. 2 Two Equivalent Problems

It may be noted from the form of Equations (A.4.1) and(A.4.2) that the following reciprocity law, illustrated in Figure A.3, is valid in the plasma. Specifically if z has the same numerical value as h and either h or z is zero the magnetic fields for these two cases are identical. That is, the magnetic field at the plasma-vacuum interface created by a dipole at the altitude h (Fig. A.3a) is the same as the magnetic field created at the altitude h by a dipole at the interface (Fig. A.3b).

The rest of this section is restricted to the special case where the dipole is at the inferface between the plasma and the vacuum (h = 0). For this case the horizontal magnetic field components at the interface are obtained by reduction of Equations (A.4.2) and (A.4.3) as

$$\left.\begin{aligned} B_\rho &= 2C(\cos\theta/\rho^3)\left[2 - 12/f^2 + (f + 5 + 12/f + 12/f^2)\exp(-f)\right] \\ B_\theta &= C(\sin\theta/\rho^3)\left[2 - 6/f^2 + (2 + 6/f + 6/f^2)\exp(-f)\right] \end{aligned}\right\} \quad (A.4.3)$$

where

$$f = \gamma\rho = ik\rho \quad (A.4.4)$$

and where B_ρ and B_θ are the radial and tangential components of the magnetic field in polar coordinates in the plane where z = 0 (Fig. A.4.1). These equations, taken with (A.2.5) through (A.2.8) give the magnetic field frequency response resulting from a steady-state sinusoidal variation of magnetic dipole moment.

A.4.2 Step-Function Response

It is next desired to obtain the transient magnetic disturbance in the plasma resulting from a step function dipole input. This transient response function for perfect and ohmic plasmas may be obtained from Equation (A.4.3) with the aid of Churchill's (1944) Appendices II and III as

$$\begin{aligned} B_\rho &= 2CB_\rho^* \cos\vartheta/\rho^3 \\ B_\theta &= CB_\theta^* \sin\theta/\rho^3 \end{aligned} \quad (A.4.5)$$

where B_ρ^* and B_θ^* are normalized values of the magnetic field components (unity at $t \to \infty$) which are defined below

Perfect plasma ($\nu = \sigma_o = 0$)

$$\left.\begin{aligned} B_\rho^* &= 2 - 6\tau^2 + (6\tau^2 - 1)\, S(\tau - 1) + \delta(\tau - 1) \\ B_\theta^* &= 2 - 3\tau^2 + (3\tau^2 - 1)\, S(\tau - 1) \\ \tau &= Vt/\rho \end{aligned}\right\} \qquad (A.4.6)$$

Ohmic plasma:

$$\left.\begin{aligned} B_\rho^* &= 2 - 12\,\tau_1 \operatorname{erf}\left(\tfrac{1}{2}/\sqrt{\tau_1}\right) - \operatorname{erfc}\left(\tfrac{1}{2}/\sqrt{\tau_1}\right) \\ &\quad + \left(12\sqrt{\tau_1/\pi} + 1/\sqrt{\pi\,\tau_1}\right) \exp\left(-\tfrac{1}{4}/\tau_1\right) \\ B_\theta^* &= 2 - 6\,\tau_1 \operatorname{erf}\left(\tfrac{1}{2}/\sqrt{\tau_1}\right) - \operatorname{erfc}\left(\tfrac{1}{2}/\sqrt{\tau_1}\right) + 6\sqrt{\tau_1/\pi}\, \exp\left(-\tfrac{1}{4}/\tau_1\right) \end{aligned}\right\} \qquad (A.4.7)$$

where

$$\tau_1 = t/(\mu\sigma_o r^2) \qquad (A.4.8)$$

Magnetic field variations according to Equations (A.4.6) and (A.4.7) are presented and discussed in Section 2.3 of Section II .

A.5 VERTICAL MAGNETIC DIPOLE IN A SEMI-INFINITE PLASMA

A.5.1 Frequency Response

This section considers the electromagnetic fields produced by a vertical magnetic dipole located above a horizontal interface separating a plasma (above) from a vacuum (see Fig. A.4). This is the same problem treated in Section A.4, except for the orientation of the dipole axis. This problem has been treated previously by various authors (e.g., Wait, 1951; Bhattacharyya, 1959, 1963), who have established basic mathematical approaches to the problem and have dealt in detail with special cases.

The electric and magnetic fields for this problem may be expressed in terms of a single magnetic potential F as (Bhattacharyya, 1963)

$$\left.\begin{aligned} B_z &= GF \\ B_\rho &= \partial^2 F/\partial\rho\,\partial z \\ E_\theta &= i\omega\partial F/\partial\rho \\ E_\rho &= E_z = B_\theta = 0 \end{aligned}\right\} \qquad (A.5.1)$$

where G represents the operator

$$G = -\rho^{-1}(\partial/\partial\rho)\rho\,\partial/\partial\rho \qquad (A.5.2)$$

and where

$$\rho = \sqrt{x^2 + y^2} \qquad (A.5.3)$$

θ is the azimuthal angle of the radius vector

and where the subscripts z, ρ, θ designate the corresponding components of the electromagnetic field in cylindrical coordinates (Fig. A.4).

The magnetic vector potential F has been obtained in an integral form by Bhattacharyya (1963), whose Equations (6) and (7) for the upper half-space (when conduction and displacement currents are neglected in the lower half-space) may be reduced to the explicit form

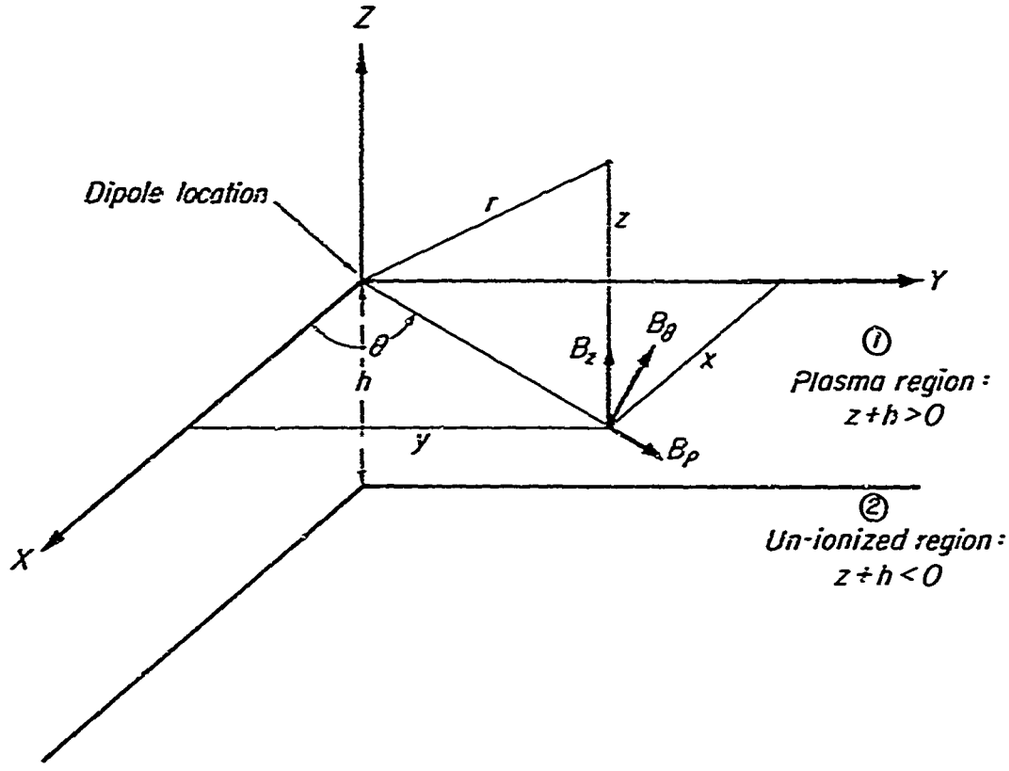

Fig. A. 4 Vertical Dipole in a Semi-infinite Plasma

$$F_{z1} = C\Big[P(|z|, \rho) + P(z_1, \rho) + (2/\gamma^2) G\Big[P(z_1, \rho) + \partial N(z_1, \rho) / \partial z_1 \Big]\Big] \qquad \text{for } z + h > 0 \qquad \text{(A.5.4)}$$

where

$$\left.\begin{aligned} P(z_1, \rho) &= \exp(-\gamma r_1)/r_1 \\ N(z_1, \rho) &= I_o\Big[\tfrac{1}{2}\gamma (r_1 - z_1)\Big] K_o\Big[\tfrac{1}{2}\gamma (r_1 + z_1)\Big] \\ r_1 &= \sqrt{\rho^2 + z_1^2} \end{aligned}\right\} \qquad \text{(A.5.5)}$$

$$z_1 = z + 2h \qquad \text{(A.5.6)}$$

Hereafter we restrict our attention to the special case where the dipole is at the interface between the two media ($h = 0$), and for this case, after considerable reduction, Equations (A.5.1) through (A.5.6) lead to the following expressions for the three non-zero components of the electromagnetic field at the boundary between the two media ($z = 0$).

$$\left.\begin{aligned} B_z(i\omega) &= B_{zs}\, B_z^*(i\omega) \\ B_\rho(i\omega) &= B_{zs}\, B_\rho^*(i\omega) \\ E_\theta(i\omega) &= B_{zs}\, E_\theta^*(i\omega) \end{aligned}\right\} \qquad \text{(A.5.7)}$$

where

$$B_{zs} = -C/\rho^3 = -\mu m_o/(4\pi\rho^3) \qquad \text{(A.5.8)}$$

$$B_z^*(i\omega) = 18/(\gamma^2\rho^2) - \left[18/(\gamma^2\rho^2) + 18/(\gamma\rho) + 8 + 2\gamma\rho\right] \exp(-\gamma\rho) \qquad (A.5.9)$$

$$B_\rho^*(i\omega) = -2\rho^3 (\partial/\partial\rho)\rho^{-1}(\partial/\partial\rho)\left[I_1(\tfrac{1}{2}\gamma\rho)K_1(\tfrac{1}{2}\gamma\rho)\right] \qquad (A.5.10)$$

$$E_\theta^*(i\omega) = 2i\omega\rho\left(3/(\gamma\rho)^2 - \left[1 + 3/(\gamma\rho) + 3/(\gamma\rho)^2\right]\exp(-\gamma\rho)\right) \qquad (A.5.11)$$

The above expressions have been normalized in terms of the vertical magnetic field for a static dipole (B_{zs}), the normalized variables being designated by asterisks. (Eqs. (A.5.9) and (A.5.11) were previously obtained by Wait (1951) and, in a more general form, by Bhattacharyya (1959).)

A.5.2 Step Function Response

It is next desired to obtain the transient electromagnetic disturbances produced by a step-function dipole input for a perfect plasma. These response functions may be obtained from Equations (A.5.9) through (A.5.11) with the aid of item 15 in Table E.1 of Appendix E, together with elementary Laplace transforms (Churchill, 1944), as

$$B_z^*(\tau) = 9\tau^2 - (9\tau^2 - 1)\,S(\tau - 1) - 2\,\delta(\tau - 1)$$

$$B_\rho^*(\tau) = 2\tau\left[Q_{-\frac{1}{2}}(2\tau^2 - 1) - (8\tau^2 - 7)Q_{\frac{1}{2}}(2\tau^2 - 1)\right]\Big/\left[\pi\left|\tau^2 - 1\right|\right] \qquad (A.5.12)$$

$$E_\theta^*(\tau) = 2V\left[3\tau - \delta(\tau - 1) - 3\tau S(\tau - 1)\right]$$

where

$$\tau = Vt/\rho \qquad (A.5.13)$$

and where the Q's are Legendre functions of the second kind, which may be expressed in terms of tabulated elliptic integrals by the relationships given by Abramowitz et.al.* (1964). and Erdelyi, et. al. (1953, I).

Magnetic field variations according to Equations (A.5.12) are presented and discussed in Section 2.4 of Section II .

---

* Equations 8.3.10 and 8.3.12 of this reference appear incorrect and were not used.

A.6 HORIZONTAL MAGNETIC DIPOLE ABOVE A VACUUM CAVITY

A.6.1 Frequency Response

This section considers the three-dimensional problem where a horizontal magnetic dipole is placed in a plasma above a horizontal vacuum cavity, the lower edge of which is the surface of a perfect conductor (Fig. A.5).

The x, y, z-components of the vector potential $\overline{F}$ for this problem for sinusoidal oscillations may be written by a straightforward generalization of Wait's (1953) equations as

$$\left.\begin{aligned} F_x &= 0 \\ F_{yp} &= C \int_0^\infty \left[\exp(-u|z-h|) + f_p \exp(-uz)\right] (\lambda/u)\, J_o(\lambda\rho)\, d\lambda \\ F_{yv} &= C \int_0^\infty \left[f_{v+} \exp(+\lambda z) + f_{v-} \exp(-\lambda z)\right] J_o(\lambda\rho)\, d\lambda \\ F_{zp} &= C \int_0^\infty g_p \exp(-uz)\, \lambda^2 J_1(\lambda\rho)\, d\lambda \cos\theta \\ F_{zv} &= C \int_0^\infty \left[g_{v+} \exp(+\lambda z) + g_{v-} \exp(-\lambda z)\right] \lambda^2 J_1(\lambda\rho)\, d\lambda \cos\theta \end{aligned}\right\} \quad (A.6.1)$$

where

$$\left.\begin{aligned} u &= \sqrt{\lambda^2 - k^2} = \sqrt{\lambda^2 + \gamma^2} \\ \gamma &= ik \end{aligned}\right\} \quad (A.6.2)$$

The f's and g's are functions of λ to be determined, the dipole axis is parallel to the Y-axis, and

v is a subscript designating the vacuum region

p is a subscript designating the plasma region

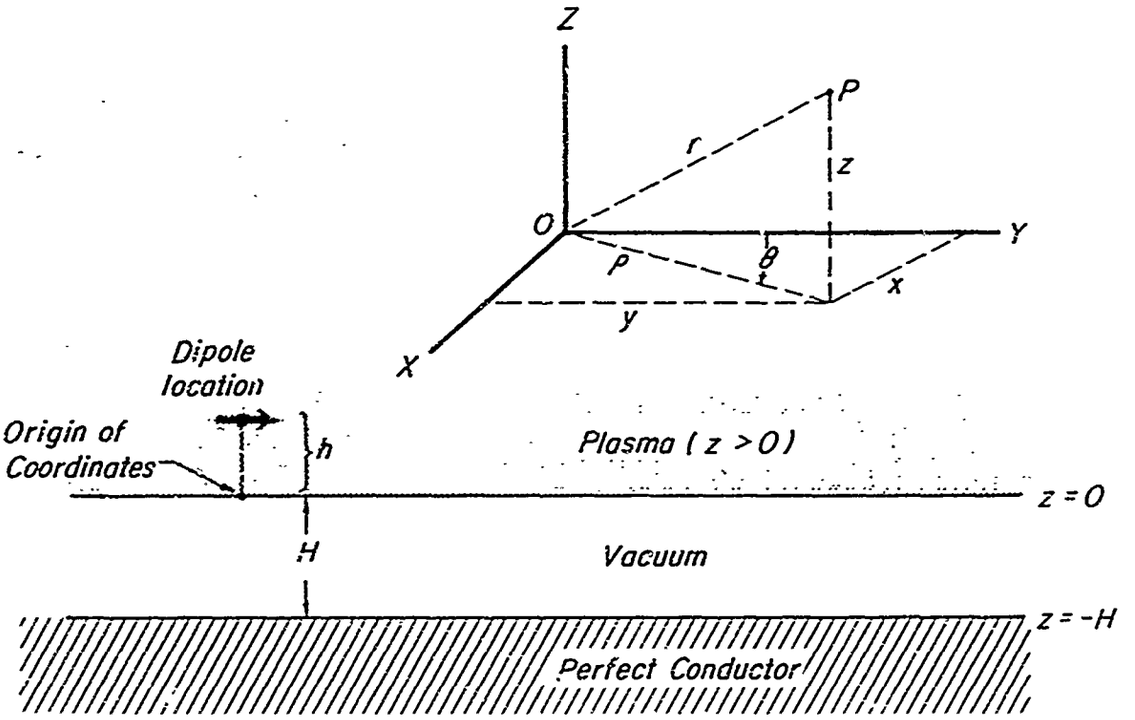

Fig. A. 5 Horizontal Dipole Above a Vacuum Cavity

r is the distance from the dipole to a point P (Fig. A.6.1)

ρ is the horizontal projection of P

θ is the angle between the Y-axis and the horizontal projection of the line OP (Fig. A.5)

Through application of the boundary conditions of continuity of the electric and magnetic fields at $z = 0$ and vanishing of the horizontal electric field at $z = -H$, six simultaneous equations are obtained for the unknown functions $f_{v\pm}$, $g_{v\pm}$, f_p and g_p. Substitution of the resulting values of these functions into Equation (A.6.1) yields the following expressions for the vector potential and its divergence Φ at $z = 0$.

$$\left.\begin{aligned} F_{yp} &= C \int_0^\infty \left[\exp(-u|z-h|) - \exp(-u(z+h))\right] (\lambda/u)\, J_0(\lambda\rho)\, d\lambda \\ F_{yv} &= 2C \int_0^\infty \exp(-uh) \left[\cosh(\lambda(z+H))/\sinh \lambda H\right] J_0(\lambda\rho)\, d\lambda \\ F_{zp} &= 2C \int_0^\infty \left[\exp(-u(z+h))/(\lambda + u \tanh \lambda H)\right] \lambda\, J_1(\lambda\rho)\, d\lambda \cos\theta \\ F_{zv} &= 2C \int_0^\infty \left[\exp(-uh) \sinh(\lambda(z+H))/\left[(\lambda + u \tanh \lambda H) \sinh \lambda H\right]\right] \lambda\, J_1(\lambda\rho)\, d\lambda \cos\theta \end{aligned}\right\} \quad (A.6.3)$$

$$\Phi = \nabla \cdot \bar{F}_p \Big|_{z=0} = 2CV \cos\theta \quad (A.6.4)$$

where

$$V = (\partial/\partial\rho) \int_0^\infty v\, J_0(\lambda\rho)\, d\lambda \quad (A.6.5)$$

$$v = \left[u/(\lambda + u \tanh \lambda H)\right] \exp(-uh) \quad (A.6.6)$$

It is now desired to determine the horizontal magnetic fieldin the vacuum cavity. This will be done first by considering the magnetic field in the plasma at the lower edge of the plasma region ($z = 0^+$), which is given in polar coordinates in the plane $z = 0$ by the expressions

$$B_\rho = \partial\Phi/\partial\rho \tag{A.6.7}$$

$$B_\theta = \rho^{-1}\partial\Phi/\partial\theta \tag{A.6.8}$$

where Φ, as given by (A.6.4), is the potential of the horizontal magnetic field. By combining Equations (A.6.4) through (A.6.8) and performing the indicated differentiations with respect to ρ and θ, the following expressions are obtained for B_ρ and B_θ

$$B_\rho = 2C\rho^{-3}\cos\theta\,[T_1 - T_0] \tag{A.6.9}$$

$$B_\theta = 2C\rho^{-3}\sin\theta\,[T_1] \tag{A.6.10}$$

where

$$T_0 = \int_0^\infty F\,\lambda\rho\,J_0(\lambda\rho)\,d\,(\lambda\rho) \tag{A.6.11}$$

$$T_1 = \int_0^\infty F\,J_1\,(\lambda\rho)\,d\,(\lambda\rho) \tag{A.6.12}$$

$$F = \lambda\rho v \tag{A.6.13}$$

In order to evaluate the integrals T_0 and T_1, the subsequent analysis is restricted to the study of conditions far from the dipole in the sense that $\rho >> H$ and $\rho >> h$. For these conditions the function F behaves as follows (see Eqs. (A.6.6) and (A.6.13)).

$$F \approx [\gamma\rho/(1+\gamma H)]\exp(-\gamma h)\begin{cases}\lambda h << 1\\ \lambda H << 1\\ \lambda\rho \leq L\end{cases} \tag{A.6.14}$$

$$\left.\begin{aligned} F &\approx \rho\sqrt{\lambda^2 + \gamma^2} \\ &\approx \rho\sqrt{2k(\lambda - k)} \end{aligned}\right\} \quad ; \lambda \approx k \qquad \text{(A. 6. 15)}$$

where L is some large number ($L >> 1$). For values of λ not covered by the above expressions, $\lambda\rho v$ is a slowly varying function in the sense that $f'(x)/f(x) << 1$.

With the aid of the above observations, the integral T_1 (Eq. A. 6. 12) may be approximately integrated as follows

$$T_1 \approx \int_0^L [\gamma\rho/(1 + \gamma H)] \exp(-\gamma h) J_1(\lambda\rho)\, d\lambda + \int_L^\infty F J_1^*(\lambda\rho)\, d(\lambda\rho) \qquad \text{(A. 6. 16)}$$

where $J_1^*(\lambda\rho)$ is an asymptotic expression for $J_1(\lambda\rho)$ for large arguments (see Eq. (D. 18) of Appendix D).

The first term on the right hand side of Equation (A. 6. 16) is easily integrated, the second term may be integrated approximately by Equation (D. 20)* of Appendix D. The result of these integrations is

$$T_1 \approx -[\gamma\rho/(1 + \gamma H)] \exp(-\gamma h) [J_0(L) - 1] + [\gamma\rho/(1 + \gamma H)] \exp(-\gamma h) [J_0^*(L) + (2L)^{-1} J_1^*(L)] + \exp(-\gamma\rho) \qquad \text{(A. 6. 17)}$$

where Equation (A. 6. 14) was used to evaluate the function F at $\lambda\rho = L$. The first and third terms in Equation (A. 6. 17) cancel,** since L is large, so that

* The integration procedure used here to evaluate T_1 and T_0 requires that $k\rho$ or $\gamma\rho >> 1$; modifications of results obtained here to include the case of smaller $k\rho$ are discussed subsequently.

** Their sum is a term of order $L^{-\frac{1}{2}}$.

$J_0(L) \approx J_0^*(L)$; the fourth term is negligible compared to the second term. Hence Equation (A. 6.17) reduces to the form

$$T_1 \approx [\gamma\rho/(1+\gamma H)] \exp(-\gamma h) + \exp(-\gamma\rho) \qquad \text{(A. 6.18)}$$

Similarly T_0 is found to be given by the expression

$$T_0 \approx [\gamma\rho/(1+\gamma H)] \exp(-\gamma h) [L J_1(L) - 0]$$

$$- [\gamma\rho/(1+\gamma H)] \exp(-\gamma h) [L J_1^*(L) + \tfrac{1}{2} J_0^*(L)]$$

$$- \gamma\rho \exp(-\gamma\rho) \qquad \text{(A. 6.19)}$$

The first and third terms in Equation (A. 6.19) cancel* since L is large and $J_1(L) \approx J_1^*(L)$. The fourth term is of order $L^{-\frac{1}{2}}$, which is negligible compared to the first term in the T_1 expression, which appears beside T_0 in the only equation in which T_0 is used (Eq. A. 6. 9). Hence, Equation (A. 6.19) reduces to the form

$$T_0 \approx -\gamma\rho \exp(-\gamma\rho) \qquad \text{(A. 6.20)}$$

The expressions derived above for T_0 and T_1 are valid for all large values of the parameter $k\rho$ but not for smaller values. (The used expressions (D.14) and (D.15) from Appendix D require that the parameter A be a slowly varying function near $x = x_m$, which is true here only for large $k\rho$.) Consequently, another set of expressions must be derived for T_0 and T_1 for smaller values of $k\rho$. For this purpose, it is convenient to approximate Equation (A. 6. 6) by the expression

$$v \doteq [u/\lambda] \exp(-uh) \qquad \text{(A. 6. 21)}$$

---

* Their sum is a term of order $L^{-\frac{1}{2}}$

which is valid for all small values of λH ($H << \rho$) up to some value of $\lambda\rho = L$ where L is a large number. For larger values of $\lambda\rho$, the integrals T_0 and T_1 (Eqs. (A.6.11) and (A.6.12)) do not depend on the intermediate shape of the integrand function F (see Appendix D), hence Equation (A.6.21) can be used to evaluate Equations (A.6.11) and (A.6.12) for the entire range of λ (for $\gamma\rho \leq L$; $\gamma H << 1$). The result is (noting Eqs. (C.5), (C.6), and (C.9) through (C.11) of Appendix C).

$$T_0 = \rho^3 \int_0^\infty \lambda u \exp(-uh) J_0(\lambda\rho)\, d\lambda$$

$$= \rho^3 \partial^2/\partial h^2 \int (\lambda/u) \exp(-uh) J_0(\lambda\rho)\, d\lambda$$

$$= \rho^3 \partial^2 P(h,\rho)/\partial h^2 \qquad \text{(A.6.22)}$$

$$T_1 = \rho^2 \int_0^\infty u \exp(-uh) J_1(\lambda\rho)\, d\lambda$$

$$= \rho^2 \partial^2/\partial h^2 \int_0^\infty u^{-1} \exp(-uh) J_1(\lambda\rho)\, d\lambda$$

$$= \rho^2 \partial^2 Q(h,\rho)/\partial h^2 \qquad \text{(A.6.23)}$$

Evaluation of the derivatives of P and Q and neglect of higher order terms ($h/\rho << 1$) gives the results

$$T_0 \approx -(1 + \gamma\rho - \gamma^2 h^2) \exp(-\gamma\rho) \qquad \text{(A.6.24)}$$

$$T_1 \approx \gamma\rho \exp(-\gamma h) + (1 - \gamma h^2/\rho) \exp(-\gamma\rho) \qquad \text{(A.6.25)}$$

We now have two sets of expressions for T_0 and T_1, one set valid for large $k\rho$ (Eqs. (A.6.18) and (A.6.20)) and one valid for $k\rho \lesssim L$, $kH << 1$ and

$kh << 1$ where L is a large number (Eqs. (A.6.24) and A.6.25)). Furthermore the range of validity of the expressions overlaps, hence the following solutions valid for the entire range of λ may be obtained by inspection of these two sets of equations

$$T_0 \approx - (1 - \gamma\rho) \exp(-\gamma\rho) \qquad \text{(A.6.26)}$$

$$T_1 \approx [\gamma\rho/(1 + \gamma H)] \exp(-\gamma h) + \exp(-\gamma\rho) \qquad \text{(A.6.27)}$$

which are seen to satisfy Equations (A.6.18) and (A.6.20) for large $\gamma\rho$ and Equations (A.6.24) and (A.6.25) for kh and kH small (kρ not necessarily small).

The horizontal magnetic field components at the upper edge of the vacuum cavity then follow from Equations (A.6.9), (A.6.10) (A.6.26), and (A.6.27) as

$$\left.\begin{aligned} B_\theta &= 2\,C\,(\sin\theta/\rho^3)\left[\gamma\rho \exp(-\gamma h)/(1 + \gamma H) + g \exp(-\gamma\rho)\right] \\ B_\rho &= 4\,C\,(\cos\theta/\rho^3)\left[\tfrac{1}{2}\gamma\rho \exp(-\gamma h)/(1 + \gamma H)\right. \\ &\quad \left. + (1 + \tfrac{1}{2}\gamma\rho)\, g \exp(-\gamma\rho)\right] \end{aligned}\right\} \qquad \text{(A.6.28a)}$$

where

$$g = 1 \qquad (\text{for } z = 0) \qquad \text{(A.6.28b)}$$

In a similar manner, the magnetic field components may be evaluated at the surface of the perfect conductor ($z = - H$), the only essential change in the derivation being that the potential of the horizontal magnetic field is given by expressions like Equations (A.6.4) and A.6.5) with v replaced by $v/\cosh kh = v/\cos\gamma h$. The resulting expressions for the horizontal magnetic field components are found to satisfy Equations (A.6.28) provided that g is defined as

$$g = \sec\gamma H \qquad (\text{for } z = - H) \qquad \text{(A.6.28c)}$$

A.6.2 Step-Function Response

The transient response of the vacuum cavity to a step function dipole input may be obtained by applying items 1, 2, 8, 13 and 14 of Table E.1 to Equation (A.6.28) and is given by the following equations for the three types of plasma considered.

$$\left.\begin{aligned} B_\theta &= 2\,C\,(\sin\theta/\rho^3)\left[(\rho/H)\,B_1 + B_2\right] \\ B_\rho &= 4\,C\,(\cos\theta/\rho^3)\left[\tfrac{1}{2}(\rho/H)B_1 + B_2 + B_3\right] \end{aligned}\right\} \qquad (A.6.29)$$

Perfect plasma:

$$B_1 = \exp\left[-\,(Vt - h)/H\right] S(Vt - h) \qquad (A.6.30)$$

For $z = 0$:

$$B_2 = S\,(Vt - \rho) \qquad (A.6.31)$$

$$B_3 = \delta\,(Vt/\rho - 1) \qquad (A.6.32)$$

For $z = -H$:

$$B_2 = \tfrac{1}{2} + \pi^{-1}\,\mathrm{sgn}\,(Vt - \rho)\,\tan^{-1}\left[\sinh\left|\tfrac{1}{2}\pi\,(Vt - \rho)/H\right|\right] \qquad (A.6.33)$$

$$B_3 = \tfrac{1}{4}\,(\rho/H)/\cosh\left|\tfrac{\pi}{2}\,(Vt - \rho)/H\right| \qquad (A.6.34)$$

Complex plasma:

$$B_1 = \exp\,(-\,\tfrac{1}{2}h\nu/V)\,S\,(Vt - h)\;;\quad Vt - h < 0^+ \qquad (A.6.35)$$

Ohmic plasma:

$$B_1 = \exp\,(h/H + \tau_1)\,\mathrm{erfc}\left[\sqrt{\tau_1} + \tfrac{1}{2}(h/H)/\sqrt{\tau_1}\right] \qquad (A.6.36)$$

$$B_2 = \mathrm{erfc}\,(\sqrt{\tau_2^{-1}}) \qquad (\text{for } z = 0) \qquad (A.6.37)$$

$$B_3 = \tfrac{1}{2}\,\mathrm{erf}'\,(\sqrt{\tau_2^{-1}})/\sqrt{\tau_2} \qquad (\text{for } z = 0) \qquad (A.6.38)$$

$$\tau_1 = t/(\mu \sigma_o H^2) \qquad \text{(A.6.29)}$$

$$\tau_2 = t/(\tfrac{1}{4}\mu \sigma_o \rho^2) \qquad \text{(A.6.40)}$$

Magnetic field variations according to the above equations are presented and discussed in Section 2.5 of Section II .

APPENDIX B

ONE-DIMENSIONAL HYDROMAGNETIC WAVE PROBLEMS

B.1 INTRODUCTION

This appendix is concerned with the analysis of four one-dimensional problems of hydromagnetic wave propagation, which are related to the electromagnetic phenomena produced by a high altitude nuclear detonation. The following problems are considered, using the basic assumptions and equations given in Section B.2.

Section B.3 considers the problem where a magnetic disturbance is suddenly applied inside a vacuum cavity, located between a perfect conductor and a semi-infinite hydromagnetic plasma. The decay of this disturbance in the cavity and its propagation into the plasma are examined.

Section B.4 considers the problem where a hydromagnetic wave, descending through a semi-infinite plasma, encounters a horizontal vacuum cavity, the lower edge of which is bounded by a perfect conductor. The growth of the magnetic field in the cavity and the strength of the wave reflected back into the plasma are examined.

Sections B.5 and B.6 consider two similar problems where a hydromagnetic wave, traveling in a uniform plasma, suddenly encounters a region of exponentially increasing Alfvén speed. For the problem in Section B.5, the Alfvén speed is assumed to increase indefinitely with increasing altitude, but in Section B.6 is assumed to have a finite upper limit. Reflection and transmission coefficients are calculated for these problems.

Section B.7 considers the reflection and transmission coefficients for a steady-state sinusoidal wave crossing an abrupt boundary between two different plasma regions.

Section B.8 considers the problem where a magnetic disturbance is suddenly or sinusoidally applied inside a horizontal vacuum cavity, located above a perfect conductor and below various combinations of horizontally stratified plasma regions simulating the lower ionosphere. The decay of the magnetic field in the cavity and the cavity frequency response are examined.

B.2 BASIC EQUATIONS

The basic equations used are as follows. From Maxwell's equations, with the displacement current being neglected:

$$\nabla \times E = - \partial \overline{B} / \partial t \qquad (B.2.1)$$

$$\nabla \times B = \mu \overline{J} \qquad (B.2.2)$$

The following different types of media are considered, with the indicated relationships between the electric and current fields.

Vacuum region

$$\overline{J} = 0 \qquad (B.2.3)$$

Simple conductor (hereafter called ohmic plasma)

$$\overline{J} = \sigma \overline{E} \qquad (B.2.4)$$

Perfect hydromagnetic plasma

$$\overline{E} = - \overline{v} \times \overline{B}_o \qquad (B.2.5)$$

$$\rho \partial \overline{v} / \partial t = \overline{J} \times \overline{B}_o \qquad (B.2.6)$$

where

$\overline{v}$ is the plasma velocity

B_o is a constant ambient magnetic field vector

Complex hydromagnetic plasma

$$\overline{E} = - \overline{v} \times \overline{B}_o \qquad (B.2.7)$$

$$\rho \partial \overline{v} / \partial t + \rho \nu \overline{v} = \overline{J} \times \overline{B}_o \qquad (B.2.8)$$

where

ν is a collision frequency

The above current-electric-field relationships are standard relationships except possibly for the last set. These particular relationships, for a complex hydromagnetic plasma are applicable, for example, for hydromagnetic

wave propagation in a weakly ionized plasma without substantial Hall effects; in particular for the F-layer of the ionosphere, if ν is taken equal to the frequency of collisions of positive ions with neutral particles.

Hall-effect plasma (weakly ionized gas)

$$\overline{J} = \sigma_1 \overline{E} - \sigma_2 \overline{E} \times \overline{b}_o - (\sigma_o - \sigma_1)(\overline{E} \cdot \overline{b}_o)\, \overline{b}_o \qquad \text{(B.2.9)}$$

where

$$\sigma_o = \infty \qquad \text{(B.2.10)}$$

$$b_o = \overline{B}_o / |B_o| \qquad \text{(B.2.11)}$$

σ_o is the parallel conductivity

σ_1 is the Pedersen conductivity

σ_2 is the Hall conductivity

and where σ_1 and σ_2 are considered to be real constants. These equations and assumptions are appropriate, for example, to the lower E-layer of the ionosphere, above about 90 km, for frequencies considerably lower than the ion collision frequency.

One-dimensional condition

This appendix is restructed to the treatment of one-dimensional problems ($\partial/\partial x = \partial/\partial y = 0$), for which case the preceding equations take the following simplified forms, when expressed in an X, Y, Z rectangular coordinate system. Equations referring to the modified Alfvén mode of wave propagation are placed below on the left hand side of the page, those for the Alfvén mode on the right hand side, and common or miscellaneous relationships in the center. It is also assumed here, without loss of generality, that the constant ambient magnetic field vector ($\overline{B}_o$) lies in the YZ-plane ($B_{ox} = 0$).

Maxwell's equations

Modified Alfven Mode		Alfven Mode	
$\partial B_y/\partial t = -\partial E_x/\partial z$	$\partial B_z/\partial t = 0$	$\partial B_x/\partial t = +\partial E_y/\partial z$	(B.2.12)
$\mu J_x = -\partial B_y/\partial z$	$J_z = 0$	$\mu J_y = +\partial B_x/\partial z$	(B.2.13)

Complex hydromagnetic plasma

$E_x = -v_y B_{oz} + v_z B_{oy}$	$E_y = +v_x B_{oz}$; $E_z = -v_x B_{oy}$	(B.2.14)
$\rho(\partial v_y/\partial t + \nu v_y) = -J_x B_{oz}$	$\rho(\partial v_x/\partial t + \nu v_x) = +J_y B_{oz}$	(B.2.15)
$\rho(\partial v_z/\partial t + \nu v_z) = +J_x B_{oy}$		

(For a perfect hydromagnetic plasma set $\nu = 0$ in the above equations.)

Ohmic plasma

$J_x = \sigma E_x$	$J_y = \sigma E_y$	(B.2.16)

Hall-effect plasma

$$J_x = \sigma_1 E_x + \sigma_2 E_r$$

$$J_r = -\sigma_2 E_x + \sigma_1 E_r$$

$$J_z = 0 \qquad \text{(B.2.17)}$$

$$E_y = -E_r \cos\theta$$

$$E_z = E_r \sin\theta$$

where

$$J_r = -J_y \cos\theta \qquad \text{(B.2.18)}$$

θ is the angular deviation of the ambient magnetic field vector ($\overline{B}_o$) from the vertical Z-axis toward the Y-axis.

E_r is the resultant electric field in the YZ-plane.

Differential equations

The differential equations for $\overline{B}$ and $\overline{E}$ obtained from the above relationships for a complex or perfect plasma are

$$\left.\begin{aligned} \partial^2\overline{E}/\partial t^2 + \nu\,\partial\overline{E}/\partial t &= V_m^2\,\partial^2\overline{E}/\partial z^2 \\ \partial^2\overline{B}/\partial t^2 + \nu\,\partial^2\overline{B}/\partial t &= V_m^2\,\partial^2\overline{B}/\partial z^2 \end{aligned}\right\} \text{(complex plasma)} \qquad \text{(B.2.19)}$$

where

Modified Alfvén mode	Alfvén mode
$V_m = \sqrt{B_o^2/(\mu\rho)}$	$V_m = \sqrt{B_{oz}^2/(\mu\rho)}$

(B.2.20)

and $\nu = 0$ for a perfect plasma. Also, for vacuum regions

$$\partial\overline{B}/\partial z = 0 \text{ (vacuum)} \qquad \text{(B.2.21)}$$

and for a simple ohmic plasma

$$\left.\begin{aligned} \partial^2\overline{B}/\partial z^2 &= \mu\sigma\,\partial\overline{B}/\partial t \\ \partial^2\overline{E}/\partial z^2 &= \mu\sigma\,\partial\overline{E}/\partial t \end{aligned}\right\} \text{ohmic plasma} \qquad \text{(B.2.22)}$$

For a Hall-effect plasma, the differential equations resulting from the coupled Equations (B.2.12), (B.2.13), (B.2.17), and (B.2.18) may be conveniently expressed in terms of two separated mode equations (designated by ± superscripts) as follows.

$$\left.\begin{aligned} \partial^2 E^{\pm}/\partial z^2 &= \mu\sigma^{\pm}\,\partial E^{\pm}/\partial t \\ \partial B^{\pm}/\partial t &= \partial E^{\pm}/\partial z \end{aligned}\right\} \qquad \text{(B.2.23)}$$

where

$$\left.\begin{aligned} B^{\pm} &= B_x + b^{\pm} B_y \\ E^{\pm} &= E_y - b^{\pm} E_x \end{aligned}\right\} \qquad \text{(B.2.24)}$$

$$\left.\begin{aligned} \sigma^{\pm} &= \sigma_1/\cos^2\theta + \sigma_2\, b^{\pm}/\cos\theta \\ b^{\pm} &= \beta/(-1 \pm \sqrt{1-\beta^2}) \\ \beta &= 2(\sigma_2/\sigma_1)\cos\theta/\sin^2\theta \end{aligned}\right\} \qquad \text{(B.2.25)}$$

and where the inverse relationships to those of Equation (B.2.24) are

$$\left.\begin{aligned} B_x &= (b^+ B^- - b^- B^+)/(b^+ - b^-) \\ B_y &= (B^+ - B^-)/(b^+ - b^-) \\ E_x &= -(E^+ - E^-)/(b^+ - b^-) \\ E_y &= (b^+ E^- - b^- E^+)/(b^+ - b^-) \end{aligned}\right\} \qquad \text{(B.2.26)}$$

Sinusoidal wave motion

For sinusoidal wave motions in uniform plasma regions, solutions of Equations (B.2.19), (B.2.22), and (B.2.23) take the form

$$B,\ E \sim \exp i(\omega t \pm k z) = \exp(i\omega t \pm \gamma z) \qquad \text{(B.2.27)}$$

where

k is the wave number

γ is the wave propagation constant (ik)

Substitution of Equation (B.2.27) into Equations (B.2.19), (B.2.22), and (B.2.23) gives k and γ as

$$\gamma = ik = \begin{cases} \sqrt{(i\omega)^2 + (i\omega)\nu} / V_m & \text{complex plasma} \quad (B.2.28) \\ i\omega / V_m & \text{perfect plasma} \quad (B.2.29) \\ \sqrt{i\omega\mu\sigma} & \text{ohmic plasma} \quad (B.2.30) \\ \sqrt{i\omega\mu\sigma^{\pm}} & \text{Hall-effect plasma} \quad (B.2.31) \end{cases}$$

B.3 ESCAPE OF A MAGNETIC PULSE FROM A VACUUM CAVITY

B.3.1 Derivation of Equations

This section considers the escape of a finite magnetic pulse, suddenly applied to a vacuum cavity, which is bounded below by a perfect conductor and above by a plasma medium (Fig. B.1).

The initial conditions of this problem are

$$\left.\begin{aligned} & B = E = 0 \;\; ; \;\; t \leq 0 \;\; ; \;\; z > 0 \\ & B(z) = B_{vo} = \Phi_o / H \;\; ; \;\; -H < z < 0 \;\; ; \;\; t = 0 \end{aligned}\right\} \quad (B.3.1)$$

where

$$\Phi_o = \int_{-H}^{o} B(z,0)\, dz = B_{vo} H \quad (B.3.2)$$

Φ_o is the initial magnetic flux in the vacuum cavity

B_{vo} is the initial (uniform) magnetic field in the cavity

H is the height of the cavity

z is distance above the upper edge of the cavity

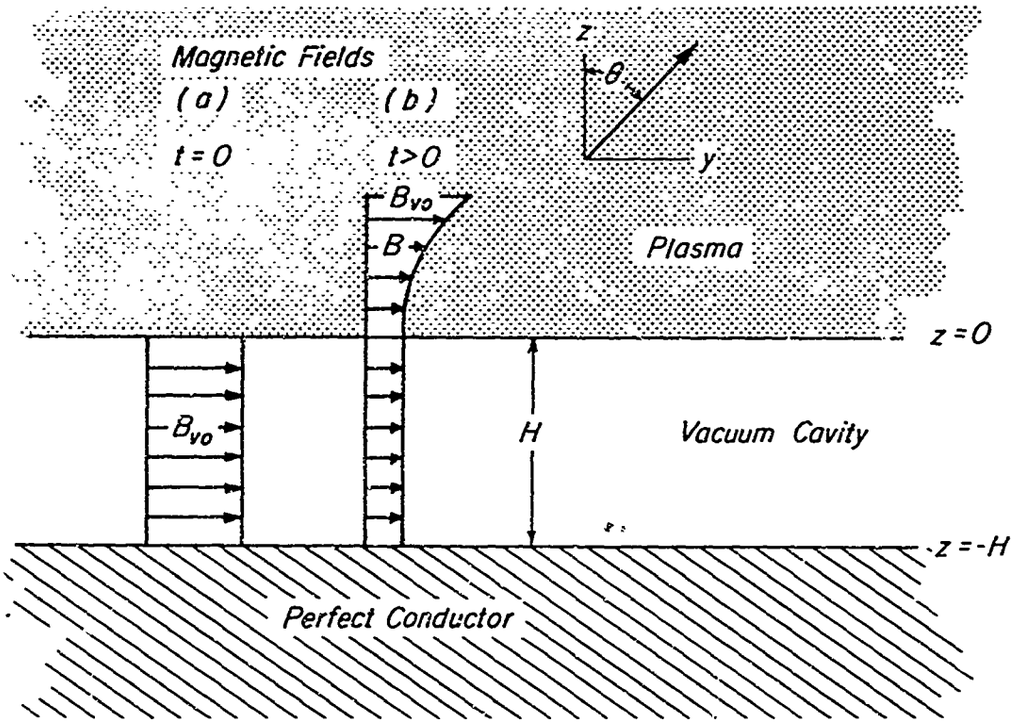

Fig. B.1 Escape of a Magnetic Field from a Vacuum Cavity into a Semi-Infinite Plasma

5547 a

The boundary conditions to be satisfied for $t > 0$ are continuity of B and E at the boundary at $z = 0$, vanishing of the electric field at the surface of the perfect conductor ($z = -H$), and vanishing of the field at infinity ($z = +\infty$).

This problem may be conveniently solved by taking the Laplace transforms of the appropriate differential equations with respect to time and satisfying the boundary conditions for the transformed variables.

B.3.2 Complex Hydromagnetic Plasma

Considering first the case of a complex hydromagnetic plasma, the Laplace transform of the differential Equation (B.2.19) is

$$s^2 E^*(z,s) + \nu s E^*(z,s) = V_m^2 \partial^2 E^*(z,s)/\partial z^2 \quad ; z > 0 \qquad (B.3.3)$$

where the component subscripts given in Section B.2 are omitted here, asterisks are used to designate Laplace transforms with respect to t, and s is the transformed variable of the Laplace transform. The solution of this equation which vanishes at positive infinity is of the form

$$E^*(z,s) = A(s) \exp\left[-\sqrt{s^2 + \nu s}\ (z/V_m)\right] \quad ; \quad z > 0 \qquad (B.3.4)$$

where A(s) is to be determined. The corresponding expression for the magnetic field is (using Eq. (B.2.12))

$$B^*(z,s) = \pm A(s) \left[\sqrt{s^2 + \nu s}\ /(s V_m)\right] \exp\left[-\sqrt{s^2 + \nu s}\ (z/V_m)\right]; \quad z > 0 \qquad (B.3.5)$$

where upper signs apply to the modified Alfvén mode and lower signs to the Alfvén mode.

From Equations (B.2.12) and (B.2.21), with the electric field vanishing at $z = -H$, the Laplace transform of the electric field expression for the vacuum cavity takes the form

$$E^{*}(z,s) = \mp (z + H)\left[s B_v^{*}(s) - B_{vo} \right] \quad ; \quad -H < z < 0 \qquad (B.3.6)$$

where $B_v(t)$ is the magnetic field in the cavity (independent of z).

The unknown functions $A(s)$ and $B_v^{*}(s)$ are determined by the requirement of continuity of E and B at $z = 0$ as

$$A(s) = \pm V_m H B_{vo} / (V_m + H\sqrt{s^2 + \nu s}) \qquad (B.3.7)$$

$$B_v^{*}(s) = (B_{vo}/s)\left[H\sqrt{s^2 + \nu s} / (V_m + H\sqrt{s^2 + \nu s}) \right] \qquad (B.3.8)$$

These Laplace transforms may be placed in a convenient form for inversion by rationalizing their denominators, dividing remaining irrational terms by $\sqrt{s^2 + \nu s}$, and applying partial fraction expansions to rational polynomials in the denominators. For example, Equation (B.3.8) may be rewritten in the form

$$B_v^{*}(s)/B_{vo} = s^{-1} + (s^{-1} - a\sqrt{(as + 2b)/as}) \left[(as + b - \sqrt{b^2 + 1})^{-1} - (as + b + \sqrt{b^2 + 1})^{-1} \right] / (2\sqrt{b^2 + 1}) \qquad (B.3.9)$$

where

$$a = H/V_m$$
$$b = \tfrac{1}{2}\, \nu H/V_m \qquad (B.3.10)$$

Inversion of the above Laplace transforms may be accomplished with the aid of standard elementary Laplace transform tables (Churchill, 1944) and Erdelyi's (1954, I) transform 5.3 (27). The resulting expression for the magnetic field in the cavity is

$$B(t)/B_{vo} = \exp(-bt/a)\left[\exp(\beta t/a)/(\beta - b) + \exp(-\beta t/a)/(\beta + b) + 2\sinh(\beta t/a)\, I_o(-bt/a) - I_+ - I_- \right] / (2\beta) \qquad (B.3.11)$$

where

$$I_{\pm} = (\beta \pm b) \int_{o}^{t/a} \exp(\mp \beta \tau)\, I_o(-b\tau)\, d\tau \qquad \text{(B.3.12)}$$

$$\beta = \sqrt{1 + b^2} \qquad \text{(B.3.13)}$$

and $\underline{a}$ and $\underline{b}$ are given by Equation (B.3.10).

B.3.3 Perfect Hydromagnetic Plasma

For a perfect hydromagnetic plasma, the Laplace transform of the magnetic field is simply

$$B^{*}(z, s) = \left[B_{vo} H/(V_m + Hs)\right] \exp(-sz/V_m) \quad ; \; z \geq 0 \qquad \text{(B.3.14)}$$

the inverse transform of which is (Churchill, 1944)

$$B(z, t) = B_{vo} \exp\left[-(\tau - z/H)\right] S(\tau - z/H); \qquad \text{(B.3.15)}$$

where

$$\tau = V_m t/H \qquad \text{(B.3.16)}$$

and where the magnetic field in the cavity is given by (B.3.15) with $z = 0$.

B.3.4 Ohmic Plasma

For a simple ohmic plasma, the Laplace transform of the magnetic field expression is easily found to be

$$B^{*}(z, s) = B_{vo} T \exp\left[-\sqrt{sT}\,(z/H)\right] \Big/ \left[\sqrt{sT}\,(1 + \sqrt{sT})\right] \quad ; \; z \geq 0 \qquad \text{(B.3.17)}$$

where

$$T = \mu \sigma H^2 \qquad \text{(B.3.18)}$$

and the inverse of this is (Churchill, 1944)

$$B(z,t) = B_{vo}\exp(\tau_1 + z/H)\ \mathrm{erfc}\left[\sqrt{\tau_1} + \tfrac{1}{2}(z/H)/\sqrt{\tau_1}\right];\ z \geq 0 \qquad (B.3.19)$$

where

$$\tau_1 = t/T \qquad (B.3.20)$$

The magnetic field in the cavity is obtained from Equation (B.3.19) with z = 0 as

$$B_v(t) = B_{vo}w(i\sqrt{t/T}) \qquad (B.3.21)$$

where

$$w(x) = \exp(-x^2)\ \mathrm{erfc}(-ix) \qquad (B.3.22)$$

and where w(x) is a tabulated function (e.g., Abramowitz, et al, 1964).

B.3.5 Hall-Effect Plasma

For the case of a Hall-effect plasma, the Laplace transforms of the differential equations (B.2.23) with respect to time, for the plasma region, in terms of the variables $E^{\pm}$ (see Eq. (B.2.24)), are

$$\partial^2 E^{\pm}(z,s)/\partial z^2 = \mu\sigma^{\pm} s\, E^{\pm}(z,s) \quad ;\ z > 0 \qquad (B.3.23)$$

The solutions of these equations which vanish at positive infinity are of the form

$$E^{\pm *}(z,s) = A^{\pm}(s)\exp(-\sqrt{\mu\sigma^{\pm} s}\, z)\ ;\ z > 0 \qquad (B.3.24)$$

where the A's are to be determined. The corresponding expressions for the magnetic field are (using Eq. (B.2.12))

$$B^{\pm *}(z,s) = -\left[A^{\pm}(s)\sqrt{\mu\sigma^{\pm}/s}\right]\exp(-\sqrt{\mu\sigma^{\pm} s}\, z)\ ;\ z > 0 \qquad (B.3.25)$$

The corresponding expressions for the electric field in the vacuum cavity follow from Equation (B.3.6) as

$$\left.\begin{aligned} E_x^*(z,s) &= -(z+H)\left[s\,B_{yv}^*(s) - B_{yvo}\right] \\ E_y^*(z,s) &= +(z+H)\left[s\,B_{xv}^*(s) - B_{xvo}\right] \end{aligned}\right\} \quad -H < z < 0 \qquad \text{(B.3.26)}$$

where

B_{xvo}, B_{yvo} are the initial XY magnetic field components in the vacuum cavity

or in terms of $E^{\pm}$ (see Eq. (B.2.24))

$$E^{\pm *}(z,s) = (z+H)\left[s\,B_v^{\pm *}(s) - B_{vo}^{\pm}\right] \qquad \text{(B.3.27)}$$

where

$$B_{vo}^{\pm} = B_{xo} + b^{\pm} B_{yo} \qquad \text{(B.3.28)}$$

The unknown functions $A^{\pm}(s)$ and $B_v^{\pm *}(s)$ are determined by the requirement of continuity of $E^{\pm}$ and $B^{\pm}$ at $z = 0$ (using Eqs. (B.3.24), (B.3.25), and (B.3.27)) as

$$B_v^{\pm *}(s) = B^{\pm *}(0,s) = H\,B_{vo}^{\pm} \Big/ \left[H\,s + \sqrt{s/\mu\sigma^{\pm}}\right] \qquad \text{(B.3.29)}$$

$$A^{\pm}(s) = -B_v^{\pm *}(s)\sqrt{s/\mu\sigma^{\pm}} \qquad \text{(B.3.30)}$$

The Laplace transform of the magnetic field in the plasma then follows from Equations (B.3.25), (B.3.29), and (B.3.30) as

$$B^{\pm *}(z,s) = B_{vo}^{\pm}\,T_{\pm} \exp\left[-\sqrt{s\,T_{\pm}}\,(z/H)\right] \Big/ \sqrt{s\,T_{\pm}}\left(1 + \sqrt{s\,T_{\pm}}\right) \qquad \text{(B.3.31)}$$

where

$$T_{\pm} = \mu\sigma^{\pm} H^2 \qquad \text{(B.3.32)}$$

The magnetic field in the plasma is obtained by inverting Equation (B.3.31), the result being the same as Equation (B.3.19), with ± subscripts or superscripts applied to B and T. For the magnetic field in the cavity (z = 0), the result is (see Eq. (B.3.21))

$$B_v^{\pm}(t) = B_{vo}^{\pm}\, w\left(i\sqrt{t/T_{\pm}}\right) \tag{B.3.33}$$

or in terms of B_x and B_y (see Eqs. (B.3.25), (B.2.26), and (B.3.28)).

$$\left.\begin{aligned} B_x(t) &= C_{11}\, w_+ + C_{12}\, w_- \\ B_y(t) &= C_{21}\, w_+ + C_{22}\, w_- \end{aligned}\right\} \tag{B.3.34}$$

where

$$\left.\begin{aligned} C_{11} &= -\,c^-(B_{xo} + b^+ B_{yo}) \\ C_{12} &= c^+(B_{xo} + b^- B_{yo}) \\ C_{21} &= (B_{xo} + b^+ B_{yo})/(b^+ - b^-) \\ C_{22} &= -\,(B_{xo} + b^- B_{yo})/(b^+ - b^-) \\ c^{\pm} &= b^{\pm}/(b^+ - b^-) \\ w_{\pm} &= w\left(i\sqrt{t/T_{\pm}}\right) \end{aligned}\right\}$$

B.4 DESCENT OF A HYDROMAGNETIC WAVE INTO A VACUUM CAVITY

B.4.1 Derivation of Equations

This section considers the descent of a hydromagnetic wave front from a perfect hydromagnetic plasma into a vacuum cavity bounded at its lower edge by a perfectly conducting plane (Fig. B.2).

The initial conditions for this problem are

$$B = E = 0 \; ; \; t < 0 \; ; \; z < 0 \tag{B.4.1}$$

$$\left.\begin{aligned} B(z) &= B_i(z) \\ E(z) &= 0 \end{aligned}\right\} \; t = 0 \; ; \; z > 0 \tag{B.4.2}$$

The boundary conditions and differential equations are the same as in the preceding section. The solution to this problem may be considered to consist of three parts: an incident wave of amplitude B_i, the disturbance in the vacuum cavity of amplitude B_v, and a reflected wave of amplitude B_r, whose respective amplitudes may be conveniently evaluated by considering the conservation of magnetic flux flowing into the cavity. The net inflowing flux is $V_m(B_i - B_r)$ which must be equal to the rate of increase of flux in the cavity $H\partial B_v/\partial t$, or

$$H\partial B_v/\partial t = V_m(B_i - B_r) \tag{B.4.3}$$

Also, there must be continuity of the magnetic field at the upper boundary of the cavity, or

$$B_v = B_i + B_r \tag{B.4.4}$$

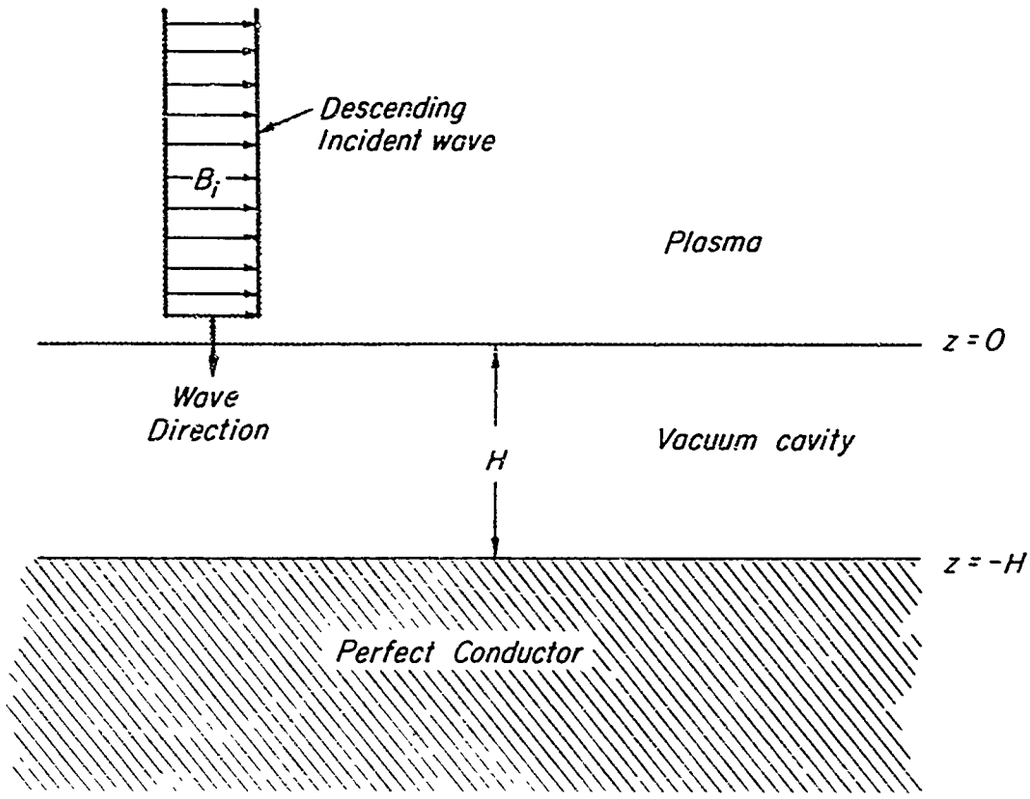

Fig. B. 2 Descent of a Hydromagnetic Wave into a Vacuum Cavity

By combining Equations (B.4.3) and(B.4.4) to eliminate B_r, the following differential equation for B_v is obtained

$$(H/V_m)dB_v/dt + B_v = 2B_i \tag{B.4.5}$$

which has the solution for constant B_i that

$$B_v = 2B_i\left[1 - \exp(-V_m t/H)\right] \tag{B.4.6}$$

The intensity of the reflected magnetic field at the boundary at $z = 0$ follows from (B.4.4) and (B.4.6) as

$$B_r = B_i\left[1 - 2\exp(-V_m t/H)\right] \quad ; \quad z = 0 \tag{B.4.7}$$

The amplitude of the reflected wave anywhere in the fluid obviously differs from (B.4.7) only by a time lag factor $\Delta t = z/V_m$, or

$$\left.\begin{array}{l} B_r(z,t) = B_i\left[1 - 2\exp(-(V_m t - z)/H)\right] S(V_m t - z) \\ \qquad\qquad \text{for } z > 0 \end{array}\right\} \tag{B.4.8}$$

For an incident wave front of arbitrary structure where $B_i(z)$ is not constant, the magnetic field in the cavity follows from Duhamel's integral and Equation (B.4.6) as

$$B_v = 2\exp(-\tau)\int_0^{\tau} B_i(\tau)\exp(+\tau)\,d\tau \tag{B.4.9}$$

where

$$\tau = V_m t/H$$

and

$$B_i(\tau) = B_i(V_m t/H) \text{ for } z = 0$$

Also of interest is the case of a steady state sinusoidal descending wave. For this case the magnetic field of the descending wave (at $z = 0$) can be represented as

$$B_i(t) = B_{im} \exp(i\omega t) ; \quad z = 0 \qquad \text{(B.4.10)}$$

where

B_{im} is the amplitude of the wave.

The corresponding expressions for the magnetic field in the cavity and the amplitude of the reflected wave (at $z = 0$) are found to be of the form

$$B_v/B_i = 2/(1 + i\omega H/V_m) \qquad \text{(B.4.11)}$$

$$B_r/B_i = (1 - i\omega H/V_m)/(1 + i\omega H/V_m) \qquad \text{(B.4.12)}$$

B.5 REFLECTION FROM AN UNLIMITED EXPONENTIAL BARRIER

B.5.1 Frequency Response

This section considers the problem where a hydromagnetic wave traveling in a uniform perfect plasma (with phase speed V_{mo}) suddenly encounters a plasma barrier region of exponentially increasing phase speed

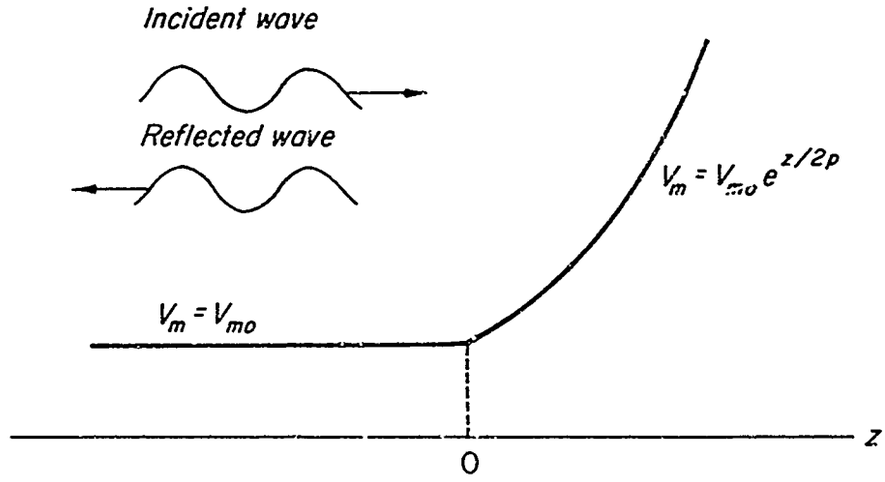

Fig. B. 3 Unlimited Exponential Barrier Problem

(at z = 0 in Fig. B. 3). For this situation, the hydromagnetic wave is totally reflected. For sinusoidal steady state waves, the appropriate differential equations are

$$\partial^2 E/\partial^2 z + (\omega^2 / V_m^2)E = 0 \qquad \text{(B.5.1)}$$

$$\omega B = \pm i \partial E/\partial z \qquad \text{(B.5.2)}$$

where

$$V_m = \begin{cases} V_{mo} & ; z < 0 \\ V_{mo} \exp(z/2p) & ; z > 0 \end{cases} \qquad \text{(B.5.3)}$$

V_{mo} is the initial phase speed

p is a scale distance

where (B.5.1) and (B.5.2) were obtained by setting $\nu = 0$ and $\partial/\partial t = i\omega$ in (B.2.19) and (B.2.12), component subscripts being omitted here, and where the upper sign in (B.5.2) refers to the modified Alfvén wave mode and the lower one to the Alfvén mode. The reflection coefficient for the magnetic field of incident waves moving to the right in Figure B.3 may be conveniently obtained with the aid of Smiley's (1964, II) Equation (3.25), and with $\nu_1 = 0$ and written in a different form, as

$$B_r/B_i = - \exp(- 2i\alpha) \tag{B.5.5}$$

where

$$\alpha = \tan^{-1} \left[J_1(\xi)/J_o(\xi) \right] \tag{B.5.6}$$

$$\xi = 2\omega p/V_{mo} \tag{B.5.7}$$

B.5.2 Step-Function Response

It is next desired to obtain the wave form of the reflected wave which is produced by the incidence of a step function (shock) wave upon the exponential barrier.

It is first convenient to replace the exact expression (B.5.5) by a more tractable approximate expression. We choose the approximation

$$- B_r/B_i = \begin{cases} \exp(- i\xi) & ; \ \xi < \frac{1}{2}\pi \\ \exp\left[- i(2\xi - \frac{1}{2}\pi) \right] & ; \ \xi > \frac{1}{2}\pi \end{cases} \tag{B.5.8}$$

which is compared with the exact expression (B.5.5) in Figure B.4. The corresponding step-function response may be obtained by applying Equations (E.3) and (E.7) of Appendix E, to (B.5.8) or, more conveniently, by setting $\epsilon = 0$ in Equation (B.6.8) of Section B.6.2 as

$$- B_r = \frac{1}{2} + \pi^{-1} \mathrm{Si}\left[\frac{\pi}{2}(\tau - 1)\right] - \pi^{-1} \mathrm{Ci}\left[\frac{\pi}{2}\left|\tau - 2\right|\right] \qquad \text{(B.5.9)}$$

where

$$B_i = S(\tau)$$

$$\tau = \frac{1}{2} V_{mo} t/p \qquad \text{(B.5.11)}$$

The time history shape of the reflected wave, according to Equation (B.5.9). is shown in Figure 3.18 of Section III. It is seen that the reflected wave intensity is small at first, then builds up to a peak (which is infinite) in the time $4p/V_{mo}$, and then rapidly decreases to a final reflection coefficient of minus unity.

B.6 REFLECTION AND TRANSMISSION AT A LIMITED EXPONENTIAL BARRIER

B.6.1 Frequency Response

This section considers the problem where a hydromagnetic wave traveling in a uniform perfect plasma (with phase speed V_{mo}) suddenly encounters a plasma barrier region where the phase speed increases exponentially at first and then asympototically approaches a constant large phase speed V_{m1} (Fig. 3.9). This is the same problem as that of Section B.5, except that the phase speed here is finite at $z = \infty$, but was infinite in Section B.6.

For this problem the phase speed is represented as

$$V_m^{-2} = \begin{cases} V_{mo}^{-2} & ; \ z < 0 \\ (V_{mo}^{-2} - V_{m_1}^{-2}) \exp(-z/p) + V_{m1}^{-2} & ; \ z > 0 \end{cases} \qquad \text{(B.6.1)}$$

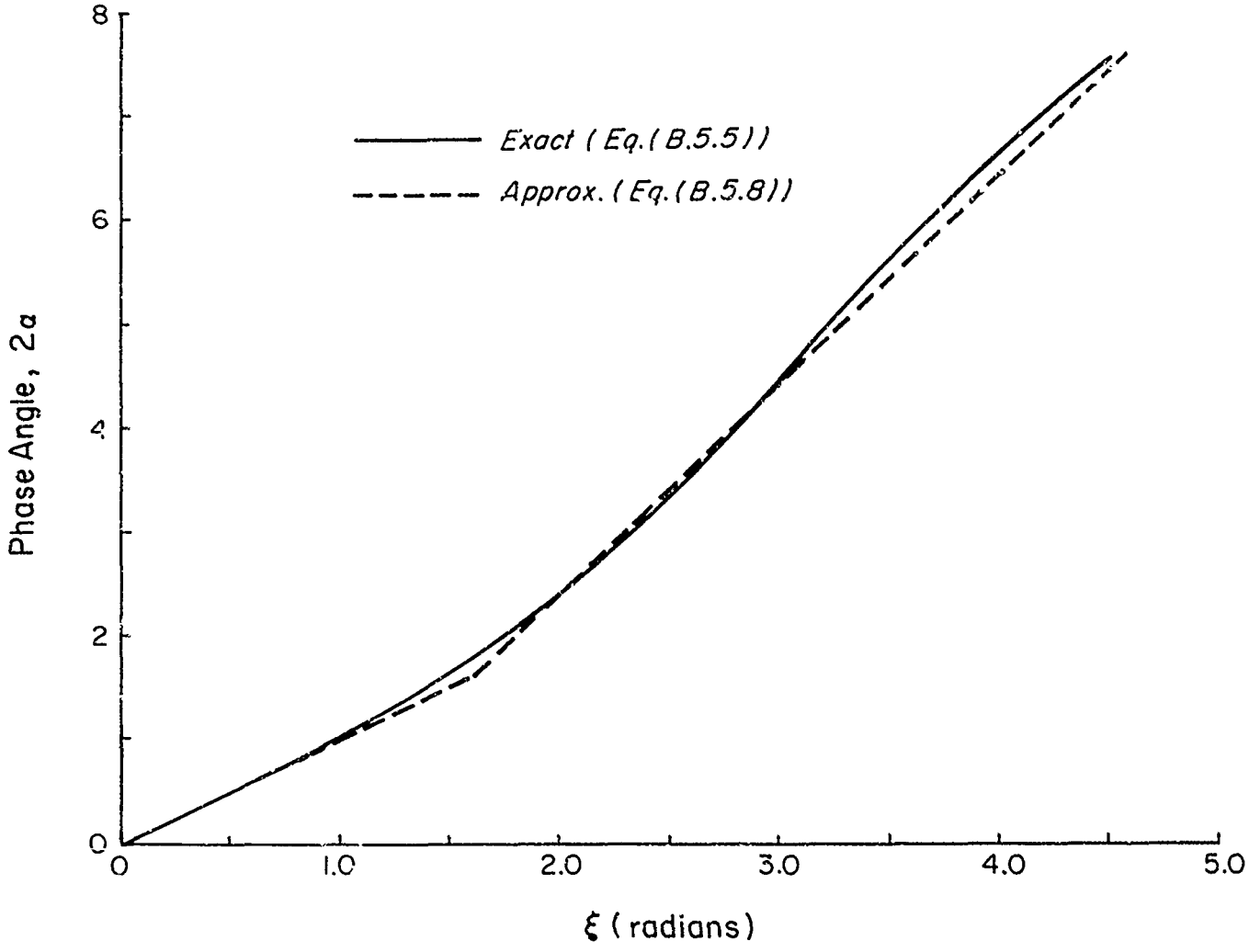

Fig. B. 4 Comparison of Exact and Approximate Expressions

where

V_{mo} is the initial phase speed

V_{m1} is the final phase speed

p is a scale distance

The differential equations (B.5.1) and (B.5.2) remain applicable. The reflection coefficient for the magnetic field of incident waves moving to the right in Figure 3.17 may be conveniently obtained with the aid of Smiley's (1964, II) Equation (3.25) as

$$B_r/B_i = - \exp\left[+2i\cot^{-1}\left(\sqrt{1 + \nu_I^2/\xi^2}\; J_{i\nu_I}(\xi)/J'_{i\nu_I}(\xi)\right)\right] \qquad (B.6.2)$$

where

$$\begin{aligned} \nu_I &= 2\omega p/V_{m1} \\ \xi &= 2\omega p/V_{mo} \end{aligned} \qquad (B.6.3)$$

B_i is the amplitude of the incident magnetic field

B_r is the amplitude of the reflected magnetic field

We shall consider only the special case of small V_{mo}/V_{m1} (therefore, small ν_I/ξ), for which case Equation (B.6.2) reduces to the form

$$-B_r/B_i = \begin{cases} \exp(-2i\alpha) & ; \xi < N \\ \exp\left[-i(2\xi - \frac{1}{2}\pi) - \pi|\nu_I|\right] & ; \xi > N \end{cases} \qquad (B.6.4a)$$

where N is any large number ($>>1$) chosen such that $NV_{mo}/V_{m1} = N\nu_I/\xi$ is a small number ($<<1$), and α is given by Equation (B.5.6). Equation (B.6.4) may be obtained from (B.6.2) through examination and application of the series expansions of Erdélyi (1953, II) for Bessel functions with small and large arguments, while noting the implied restriction here that $\nu_I/\xi << 1$ (since $V_{mo}/V_{m1} << 1$).

Another convenient approximation for Equation (B.6.2) for small ν_I / ξ is the expression

$$-B_r/B_i = \exp(-2i\alpha - \pi|\nu_I|) \qquad \text{(B.6.4b)}$$

Also of interest is the energy content of the transmitted wave, which may be obtained from Smiley's (1964, II) Equations (3.24) and (3.28) as

$$S_t/S_i = \left[4(\sinh \pi\nu_I)/(\pi\sqrt{\xi^2 + \nu_I^2})\right] / \left| J_{i\nu_I}(\xi) - i\xi J'_{i\nu_I}(\xi)/\sqrt{\xi^2 + \nu_I^2} \right|^2 \qquad \text{(B.6.5)}$$

where

S_i is the incident energy flux

S_t is the transmitted energy flux

$J_{i\nu_I}(\xi)$ is a Bessel function of the first kind of imaginary order and real variable

For $\nu_I/\xi \to 0$ and ξ large, S_t/S_i may be evaluated more simply from Equation (B.6.4), using the equation $S_t/S_i = 1 - \left| B_r/B_i \right|^2$, as

$$S_t/S_i = 1 - \exp(-2\pi\nu_I) \quad \text{for } \xi \text{ large} \qquad \text{(B.6.6.a)}$$

For ν_I/ξ and ξ small, another equation may be obtained through use and simplification of Smiley's (1964, II) Equation (3.71) as

$$S_t/S_i = 4(\nu_I/\xi)(1 + \tfrac{1}{2}\xi^2)/[1 + \xi^2/4 + 2(\nu_I/\xi)(1 + \tfrac{1}{2}\xi^2)]; \ \xi \lesssim 1 \qquad \text{(B.6.6b)}$$

Equation (B.6.5) is plotted in Figure 3.19 of Section III for a ratio of V_{mo}/V_{m1} equal to 1/30.

B.6.2 Step-Function Response

It is next desired to obtain the wave form of the reflected wave which is produced by the incidence of a step function (shock) wave upon the exponential barrier. As in Section B.5.2, it is convenient here to first replace the

expression (B.6.4) by a more tractable approximate expression, which we choose as

$$-B_r/B_i = \begin{cases} \exp(-i\xi) & ; \ \xi < \frac{1}{2}\pi \\ \exp\left[-i(2\xi - \frac{1}{2}\pi) - \pi\nu_I\right] & ; \ \xi > \frac{1}{2}\pi \end{cases} \qquad (B.6.7)$$

This expression is analogous to Equation (B.5.8) and is as accurate (for $\nu_I/\xi << 1$) as is implied by the comparison of the exact and approximate expressions in Figure B.4.

The step-function reflected wave response corresponding to (B.6.7) may be obtained by applying Papoulis' (1962) Equation 6-21 to the upper term in Equation (B.6.7) and by applying Equations (E.3) and (E.7) of Appendix E to the lower term in Equation (B.6.7). The resulting equation for the reflected wave response is

$$-B_r = \tfrac{1}{2} + \pi^{-1}\mathrm{Si}\left[\tfrac{\pi}{2}(\tau - 1)\right] + \pi^{-1}R\left\{E_1\left[\tfrac{\pi}{2}(i(\tau - 2) - \epsilon)\right]\right\} \qquad (B.6.8)$$

where

$$B_i = S(\tau)$$

$$\tau = Vt/2p$$

$$E_1(z) = \int_z^\infty \left[\exp(-z)/z\right]dz \qquad (B.6.9)$$

$$\epsilon = V_{mo}/V_{m_1}$$

$$\mathrm{Si}(x) = \int_o^x (\sin x/x)dx$$

$E_1(z)$ is the exponential integral according to the convention of Abramowitz et al. (1964)

It may also be noted that since ϵ has been assumed to be small for the present problem, the exponential integral in Equation (B.6.9) can usually be replaced by the corresponding expression for $\epsilon = 0$, which is (Abramowitz et al., 1964)

$$R\left\{E_1\left[\tfrac{1}{2}\,\pi\, i(\tau - 2)\right]\right\} = -\,Ci\left[\tfrac{1}{2}\,\pi\,\left|\tau - 2\right|\right] \qquad (B.6.10)$$

where

$$Ci(x) = -\int_x^\infty (\cos x/x)\,dx$$

This will give a good approximation except where $|\tau - 2| \lesssim \epsilon$, near which point ϵ is important.

The time history of the reflected magnetic field, according to Equation (B.6.8), is essentially the same as is given by the curve in Figure 3.18 of Section III for $V_{m1} = \infty$, except that the narrow infinite peak is reduced to a finite value. For example, for $V_{mo}/V_{m1} = 1/30$, the peak would be reduced from $-\infty$ to the value -1.7.

B.7 REFLECTION AND TRANSMISSION AT AN ABRUPT BARRIER

This section considers the reflection and transmission of hydromagnetic waves at an abrupt boundary between two uniform plasma regions of different phase speeds V_{mi} and V_{mt} (Fig. B.5).

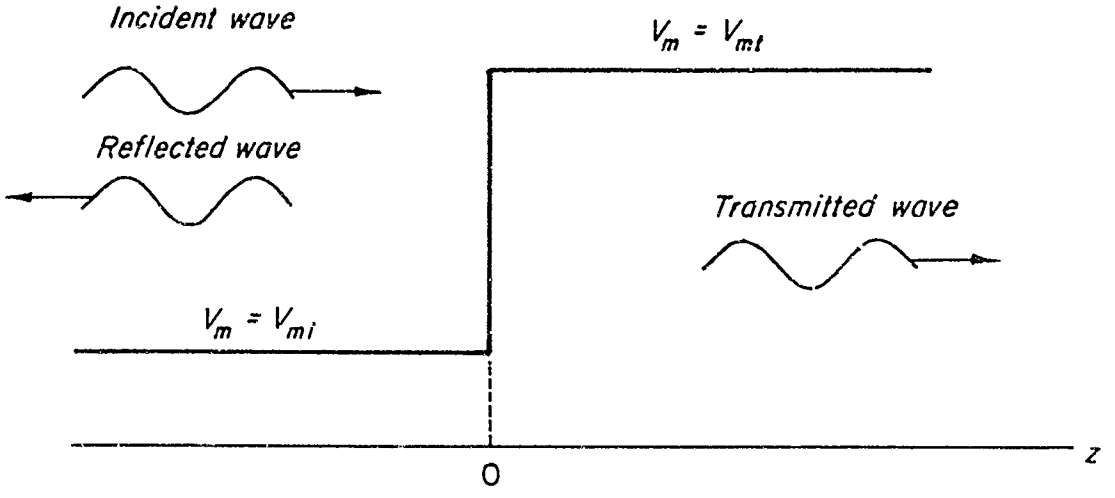

Fig. B.5 Abrupt Barrier Problem

For sinusoidal steady state waves, the magnetic fields for this problem may be represented in the form

$$B = \begin{cases} B_i \exp(-ik_i z) + B_r \exp(+ik_i z) & ; z \leq 0 \\ B_t \exp(-ik_t z) & ; z \geq 0 \end{cases} \tag{B.7.1}$$

where B_i, B_r, B_t are the amplitudes of the incident, reflected and transmitted waves, respectively, where a common time factor exp (iωt) has been omitted and where

k_i is the incident wave number

k_t is the transmitted wave number

and where the wave numbers are related to the corresponding phase speeds or conductivities by Equations (B.2.28) through (B.2.30). Component subscripts for the two possible wave modes are omitted in this section (see Section B.2).

The electric field equations corresponding to Equations (B.7.1) follow from Equation (B.2.12) as

$$E = \begin{cases} E_i \exp(-ik_i z) + E_r (+ik_i z) & ; z \leq 0 \\ E_t \exp(-ik_t z) & ; z \geq 0 \end{cases} \tag{B.7.2}$$

where

$$\left.\begin{aligned} E_i &= \pm(\omega / k_i) B_i \\ E_r &= \mp(\omega / k_i) B_r \\ E_t &= \pm(\omega / k_t) B_r \end{aligned}\right\} \tag{B.7.3}$$

and where the upper signs refer to the modified Alfvén mode and lower signs to the Alfvén mode.

Application of the boundary conditions of continuity of the electric and magnetic fields at the boundary at z = 0 to Equations (B.7.1) and (B.7.2) gives the equations

$$\left.\begin{aligned} E_i + E_r &= E_t \\ B_i + B_r &= B_t \end{aligned}\right\} \qquad \text{(B.7.4)}$$

and combination of these equations with Equation (B.7.3) gives the following reflection and transmission coefficients

$$\left.\begin{aligned} E_r/B_i &= -E_r/E_i = (k_t - k_i)\ /\ (k_t + k_i) \\ B_t/B_i &= 2\,k_t/(k_t + k_i) \\ E_t/E_i &= 2\,k_i/(k_t + k_i) \end{aligned}\right\} \qquad \text{(B.7.5)}$$

For the special case where a wave moves into a much denser medium (with a much lower phase speed), $k_t \gg k_i$ and Equations (B.7.5) reduce to the form

$$\left.\begin{aligned} B_r/B_i &= -E_r/E_i = 1 - 2\epsilon_1 \\ B_t/B_i &= 2\,(1 - \epsilon_1) \\ E_t/E_i &= 2\epsilon_1 \\ \epsilon_1 &= k_i/k_t \ll 1 \end{aligned}\right\} \qquad \text{(B.7.6)}$$

For the special case where a wave moves into a much more rarefied region, $k_t \ll k_i$ and Equation (B.7.5) reduce to the form

$$\left.\begin{aligned} B_r/B_i &= -E_r/E_i = -(1 - 2\epsilon_2) \approx -1 \\ B_t/B_i &= 2\epsilon_2 \\ E_t/E_i &= 2\,(1 - \epsilon_2 \\ \epsilon_2 &= k_t/k_i \ll 1 \end{aligned}\right\} \qquad \text{(B.7.7)}$$

B.8 ESCAPE OF A MAGNETIC PULSE FROM A VACUUM CAVITY II

This section considers the escape of a finite magnetic pulse, suddenly applied to a vacuum cavity, which is bounded below by a perfect conductor and above by a finite uniform plasma region (Region II in Fig. B.6), which is in turn bounded above by another region or set of regions (Region III and IV in Fig. B.6) of various properties. This problem is a generalization of the problem in Section B.3 and most of the equations derived in that section apply here also with minor modifications. Also considered here is the frequency response of the vacuum cavity for a sinusoidal application of magnetic flux.

B.8.1 Basic Equations

Equations (E.3.1) through (B.3.3 and (B.3.6) apply to the present problem for regions I and II without modification. Equations (B.3.4) and (B.3.5) must be modified to include the presence of a reflected wave moving downward in region II, and may be generalized as

$$E^*(z,s) = A(s)\,[\exp(-\gamma z) - R(s)\exp(+\gamma z)] \qquad (B.8.1)$$

$$B^*(z,s) = \pm A(s)\,(\gamma/s)\,[\exp(-\gamma z) + R(s)\exp(+\gamma z)] \qquad (B.8.2)$$

where

$$\gamma = \gamma(s) = \sqrt{s^2 + \nu s}\ /V_m \qquad (B.8.3)$$

and where R(s) is a reflection coefficient which may be defined by the requirement that R(iω) is the ratio of the reflected magnetic field to the incident magnetic field produced by a steady-state sinusoidal wave moving upward in the plasma region II, as measured just above the lower edge of the plasma region II (at $z = 0^+$).

The overall reflection coefficient R may be expressed in terms of reflection, transmission and attenuation factors for the regions and boundaries between regions in Figure B.6 as follows. (It is convenient here to think in terms of sinusoidal steady-state wave motion with coefficients being functions of iω instead of Laplace transform functions of s.) Reflection and transmission coefficients at the various boundaries in Figure B.6 are defined as indicated by the various arrow clusters as

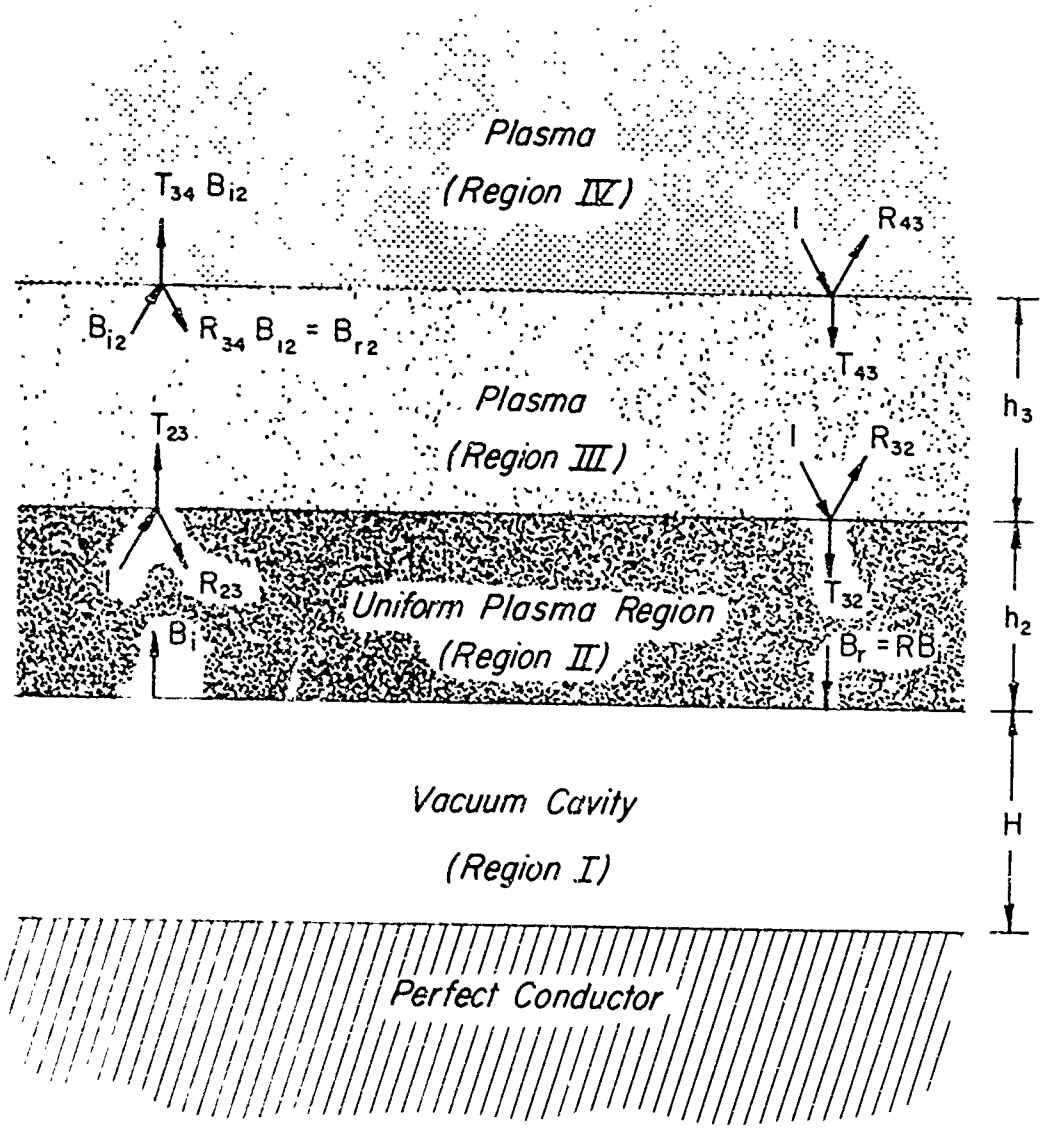

Fig. B.6 Multiple Layer Problem

$R_{jr}(i\tau)$ is the reflection coefficient for a wave crossing the boundary from region j to region r

$T_{jr}(i\tau)$ is the transmission coefficient for a wave crossing the boundary from region j to region r

$\eta_j(i\tau)$ is the attenuation experienced by a wave traversing the region j, which may be expressed in the forms

$$\eta_j(i\tau) = \exp\left[-i k_j(i\tau) h_j\right] = \exp\left[-\gamma_j(i\tau) h_j\right] \qquad (B.8.4)$$

$k_j(i\tau)$ is the wave number in region j

$$\gamma(i\tau) = i k(i\tau) \qquad (B.8.5)$$

h_j is the height of the j'th region

If the region III is semi-infinite (no region IV) the overall reflection coefficient R may be expressed simply as

$$R = R_{23}\,\eta_2^2 \qquad \text{(no region IV)} \qquad (B.8.6)$$

If the region IV is present, a more complicated expression results as a consequence of multiple reflections in the region III. Referring to the arrow groups in Figure B.6, continuity of the descending magnetic field at the lower edge of region II (at $z = 0^+$) gives the relationship

$$(B_i\,\eta_2\,R_{23} + B_{r2}\,\eta_3\,T_{32})\,\eta_2 = RB_i \qquad (B.8.7)$$

and for the region III, continuity of the ascending magnetic field at the upper edge of the region requires

$$(B_i\,\eta_2\,T_{23} + B_{r2}\,\eta_3\,R_{32})\,\eta_3 = B_{i2} \qquad (B.8.8)$$

where

$$B_{r2} = B_{i2}\,R_{34} \qquad (B.8.9)$$

B_i, B_r designate the magnetic fields of the ascending and descending waves, respectively, at $z = 0^+$

B_{i_2}, B_{r_2} designate the magnetic fields of the descending and ascending waves, respectively, at the upper edge of the region III

Solution of Equations (B.8.6) through (B.8.8) for the overall reflection factor R gives the result

$$R = \eta_2^2 \left[R_{23} + \eta_3^2 \, T_{23} \, T_{32} \, R_{34} \, / \, (1 - \eta_3^2 \, R_{32} \, R_{34}) \right] \qquad (B.8.10)$$

Returning now to the Laplace transforms of the differential Equations (B.8.6), (B.8.1) and (B.8.2), the unknown functions A(s) and $B_v^*(s)$ are determined by the requirement of continuity of E and B at z = 0, which gives the relationships

$$A(s) \left[1 - R(s) \right] = \mp H \left[s \, B_v^*(s) - B_{vo} \right] \qquad (B.8.11)$$

$$\pm A(s) \, (\gamma/s) \left[1 + R(s) \right] = B_v^*(s) \qquad (B.8.12)$$

where upper signs refer to the modified Alfvén mode and lower signs to the Alfvén mode. The solution of these equations for $B_v^*(s)$ is

$$B_v^*(s) = B_{vo} \left[1 + P(s) \right]^{-1} / s \qquad (B.8.13)$$

where

$$P(s) = \left[(1 - R)/(1 + R) \right] / (\gamma H)$$

$$= \left[\gamma H \tanh \delta \right]^{-1} \qquad (B.8.14)$$

$$\delta = -\tfrac{1}{2} \ln (-R)$$

The inverse Laplace transform of Equation (B.8.12) gives the cavity response to a step function flux input. Also of interest is the frequency response $H(i\omega)$ of the cavity to a steady-state flux input, which is obtained by multiplying Equation (B.8.13) by s and replacing s by $i\omega$, or

$$H(i\omega) = 1/[1 + P(i\omega)] \qquad (B.8.15)$$

where this expression has been normalized by setting $B_{v0} = 1$. The corresponding characteristic or resonant frequencies occur at the poles of $H(i\omega)$, where

$$P(i\omega_n) = -1 \qquad \text{(resonant condition)} \qquad (B.8.16)$$

where

ω_n is a characteristic frequency

B.8.2 Case I

The simplest case of interest here is the case where the plasma region above the vacuum cavity is semi-infinite (regions III and IV in Figure B.6 are absent). This is the same problem considered in Section B.3. For a plasma without Hall effects present, the frequency response function of the cavity for this case follows from Equations (B.8.14) and (B.8.15), with $R = 0$, as

$$\begin{aligned} H(i\omega) &= \gamma H/(1 + \gamma H) \\ &= i k H/ (1 + i k H) \end{aligned} \qquad (B.8.17)$$

where γ and k are considered functions of $i\omega$. The corresponding step function response is given by Equations (B.3.11), (B.3.15) and (B.3.19) for complex, perfect and ohmic plasma regions, respectively.

Hall-effect plasma

For the case of a Hall-effect plasma, the step-function response is given by Equation (B.3.34). The frequency response function is a four-component tensor $H_{ij}(i\omega)$, whose form may be inferred by inspection of Equations (B.3.31) and (B.3.34) to be as follows

$$\left.\begin{aligned} H_{xx}(i\omega) &= C_{11}\, A_+ \\ H_{xy}(i\omega) &= C_{12}\, A_- \\ H_{yx}(i\omega) &= C_{21}\, A_+ \\ H_{yy}(i\omega) &= C_{22}\, A_- \end{aligned}\right\} \qquad \text{(B.8.18)}$$

where

$$A_\pm = \sqrt{i\omega T_\pm}\ /\ (1 + \sqrt{i\omega T_\pm}\ ) \qquad \text{(B.8.19)}$$

$H_{ij}(i\omega)$ is the frequency response in the i-direction due to a unit flux applied in the j-direction

and where the C_{ij}'s and T_{ij} are defined in Section B.3.5.

B.8.3 Case II

The next case to be considered is that case where the region II in Figure B.6 is bounded above by a semi-infinite uniform plasma region III of much lower density than region II. In this case the reflection coefficient R is given by Equation (B.8.6) with $R_{23} \approx -1$ from Equation (B.7.7) of Section B.7, or

$$R(s) = -\eta_2^2 = -\exp\left[-2h_2\,\gamma(s)\right] \qquad \text{(B.8.20)}$$

The corresponding frequency response function is (using Eqs. (B.8.14), (B.8.15) and (B.8.16)):

$$\begin{aligned} H(i\omega) &= (1 + [\gamma H \tanh(\gamma h_2)]^{-1})^{-1} \\ &= (1 - [k H \tan k h_2]^{-1})^{-1} \end{aligned} \qquad \text{(B.8.21)}$$

and the corresponding Laplace transform of the step function response is

$$sB_v^*(s) = (1 + [\gamma H \tanh(\gamma h_2)]^{-1})^{-1} \qquad \text{(B.8.22)}$$

In order to invert the last expression, it is convenient to first expand the right hand side of Equation (B.8.22) in an infinite partial fraction series (e.g., Churchill, 1944), which leads to the result

$$B_v^*(s) = [1 + 2\sum_n C_n \xi_n^2 / [(\xi^2 - \xi_n^2)s] \qquad \text{(B.8.23)}$$

where

$$\xi = k h_2 = -i\gamma h_2 \qquad \text{(B.8.24)}$$

$$a = H/h_2 \qquad \text{(B.8.25)}$$

$$C_n = a/[1 + a + a^2 \xi_n^2] \qquad \text{(B.8.26)}$$

and where the ξ_n's are the n positive roots of the equation:

$$a \xi_n \tan \xi_n = 1 \qquad \text{(B.8.27)}$$

B.8.3.1 Complex Plasma

For the case of a complex plasma, Equation (B.8.3) applies and Equation (B.8.23) takes the form

$$B_v^*(s) = [1 - 2 \sum_n C_n \zeta_n^2 / (s^2 + \nu s + \zeta_n^2)]/s \qquad \text{(B.8.28)}$$

where

$$\zeta_n = \xi_n V_m / h_2 \qquad \text{(B.8.29)}$$

This equation may be inverted with the aid of Erdelyi's (1954, p. 230) transform (9), to give the cavity step function response as

$$B_v(t) = 1 - 2\Sigma\, C_n\left(1 - \exp\left(-\tfrac{1}{2}\nu t\right)\left[\cos \omega_n t + \tfrac{1}{2}(\nu/\omega_n) \sin \omega_n t\right]\right) \quad \text{(B.8.30a)}$$

$$= 2\Sigma\, C_n \exp\left(-\tfrac{1}{2}\nu t\right)\left[\cos \omega_n t + \tfrac{1}{2}(\nu/\omega_n) \sin \omega_n t\right] \quad \text{(B.8.30b)}$$

where

$$\omega_n = \sqrt{\zeta_n^2 - (\nu/2)^2} \quad \text{(B.8.31)}$$

B.8.3.2 Perfect Plasma

For the case of a perfect plasma, Equations (B.8.30) and (B.8.31) apply with $\nu = 0$.

B.8.3.3 Ohmic Plasma

For the case of a simple ohmic plasma, Equation (B.2.30) applies (s replacing iω), and Equation (B.8.23) takes the form

$$\left.\begin{aligned} B_v^*(s) &= [1 - 2\Sigma\, C_n \eta_n/(s + \eta_n)]/s \\ \text{where} \\ \eta_n &= \xi_n^2/(\mu\sigma h_2^2) \end{aligned}\right\} \quad \text{(B.8.32)}$$

and the inverse transform of this equation is

$$B_v(t) = W(a,\ t/T) \quad \text{(B.8.33)}$$

where

$$T = \mu\sigma H^2 \quad \text{(B.8.34)}$$

$$W(a,\tau) = 1 - 2\sum_n C_n[1 - \exp(-a^2\xi_n^2\tau)] \quad \text{(B.8.35)}$$

$$= 2\sum_n C_n \exp(-a^2\xi_n^2\tau)$$

and the ξ_n's are the positive roots of Equation (B.8.27)

B.8.3.4 Hall-Effect Plasma

For the case of a Hall-effect plasma, the step function response function may be directly inferred by comparing Equations (B.3.21), (B.3.34) and (B.8.33), with the result that the lower case w's in Equation (B.3.34) are replaced by upper case W's to give

$$\left.\begin{aligned} B_x(t) &= C_{11}\, W(a,\ t/T_+) + C_{12}\, W(a,\ t/T_-) \\ B_y(t) &= C_{21}\, W(a,\ t/T_+) + C_{22}\, W(a,\ t/T_-) \end{aligned}\right\} \qquad \text{(B.8.36)}$$

The corresponding frequency response function is a four component tensor of the form

$$\left.\begin{aligned} H_{xx}(i\omega) &= C_{11}\, A_+ \\ H_{xy}(i\omega) &= C_{12}\, A_- \\ H_{yx}(i\omega) &= C_{21}\, A_+ \\ H_{yy}(i\omega) &= C_{22}\, A_- \end{aligned}\right\} \qquad \text{(B.8.37)}$$

where

$$A_\pm = \left(1 + \left[\sqrt{i\omega T_\pm}\ \tanh\left(\sqrt{i\omega T_\pm}/a\right)\right]^{-1}\right)^{-1} \qquad \text{(B.8.38)}$$

B.8.4 Case III

The next case to be considered is that case where the region II in Figure B.6 is a uniform perfect plasma, bounded above by a semi-infinite region III, where the phase speed at first increases exponentially with increasing altitude and then approaches a constant large phase speed at high altitudes. (No region IV is assumed present.) The specific assumed phase speed variation is given by Equation (B.6.1), referenced to the lower edge of Region III. The phase speed in the uppermost part of region III (V_{m_1}) is assumed much larger than that in the uniform plasma region II (V_{m_0}).

The corresponding overall reflection factor R for this problem is given by Equation (B.8.6) with R_{23} given approximately by Equation (B.6.4b), or

$$R = - \eta_2^2 \exp \left[- 2i\alpha - \pi \left| \nu_I \right| \right] \tag{B.8.39}$$

where

$$\eta_2 = \exp \left(- ik_2 h_2 \right) \tag{B.8.40}$$

$$k_2 = \omega / V_{mo} = - i\gamma_2 \tag{B.8.41}$$

$$\alpha = \tan^{-1} \left[J_1(\xi) / J_0(\xi) \right] \tag{B.5.6}$$

$$\left.\begin{aligned} \xi &= 2\omega p / V_{mo} \\ \nu_I &= 2\omega p / V_{m1} \end{aligned}\right\} \tag{B.6.3}$$

V_{mo} is the phase speed at the lower edge of region III and in region II

V_{m1} is the phase speed in the uppermost part of region IV

$2p$ is the scale height for the exponential phase speed variation in region III.

In a more convenient form, Equation (B.8.39) may be expressed as

$$R = - \exp \left(-2i\alpha - 2ib\xi \right) \tag{B.8.42}$$

where

$$b = \tfrac{1}{2}(h_2 / p \mp i\pi\epsilon) \; ; \; \omega \gtrless 0 \tag{B.8.43}$$

$$\epsilon = V_{mo} / V_{m1} \ll 1 \tag{B.8.44}$$

and the corresponding parameter β (see Eq. (B.8.14)) is

$$\beta = i(\alpha + b\xi) \tag{B.8.45}$$

The characteristic frequencies for this system are given by Equations (B.8.14), (B.8.16) and (B.8.41) as

$$ik_2 H \tanh \beta + 1 = 0$$

or

$$k_2 H \tan (\alpha + b\xi) = 1 \tag{B.8.46}$$

or

$$a\xi \tan (\alpha + b\xi) = 1 \tag{B.8.47}$$

where

$$a = \tfrac{1}{2} H/p \tag{B.8.48}$$

The roots of Equation (B.8.47) occur in pairs, each related by the equation

$$\xi_- = -\bar{\xi}_+ \tag{B.8.49}$$

where

$\xi_\pm$ are the two values of ξ for each pair

$\bar{\xi}$ is the complex conjugate of ξ

The frequency response function for this system is given through Equations (B.6.3), (B.8.14), (B.8.15), (B.8.42) and (B.8.45) as

$$H(i\omega) = \left[1 + \frac{1}{\gamma_2 H \tanh \beta}\right]^{-1}$$

$$= 1 + \frac{1}{a\xi \tan (\alpha + b\xi) - 1} \tag{B.8.50}$$

It is now convenient to expand the right hand side of Equation (B.8.50) in an infinite partial fraction series (e.g., Churchill, 1944), which gives the result

$$H(i\omega) = 1 + \sum_n A_n/(\xi - \xi_n) \tag{B.8.51}$$

where

$$A_n = a\xi_n/[a + g_n(1 + a^2\xi_n^2)] \tag{B.8.52}$$

$$\left.\begin{aligned} g_n &= b + d\alpha/d\xi \text{ for } \xi = \xi_n \\ &= b + 1 - J_0(\xi_n)\, J_1(\xi_n)/[\xi_n (J_0^2(\xi_n) + J_1^2(\xi_n))] \end{aligned}\right\} \tag{B.8.53}$$

and where the ξ_n's are the roots of Equation (B.8.47). This series may be simplified by considering the symmetry of this problem (e.g., see Eq. (B.8.49)) as

$$H(i\omega) = 1 + \sum_n A_n/(\xi - \xi_n) - \Sigma \bar{A}_n/(\xi + \bar{\xi}_n) \tag{B.8.54}$$

and where the summation here is only for the (nearly) real and positive roots of Equation (B.8.47).

Finally, the step function response may be conveniently obtained by replacing $H(i\omega)$ in Equation (B.8.54) by $sB^*(s)$, and ω by $-is$, and by inverting the resulting function $B^*(s)$, considered as a Laplace transform. The resulting step function response is

$$B_v(t) = 1 - 2R(\Sigma\, C_{n1}\,[1 - \exp(i\omega_n t)]) \tag{B.8.55a}$$

$$= 2R\Sigma C_{n1} \exp(i\omega_n t) \tag{B.8.55b}$$

where

$$C_m = A_n/\xi_n = a/[a + g_n(1 + a^2\xi_n^2)] \qquad \text{(B.8.56)}$$

$$w_n = \tfrac{1}{2}\xi_n V_{m\infty}/p \qquad \text{(B.8.57)}$$

R( ) designates the real part of ( )

BLANK PAGE

APPENDIX C

VARIOUS INTEGRALS

The following integrals, not listed in elementary tables of integrals, were of interest for the present studies

$$\int \sqrt{x} \cos x \, dx = + \sqrt{x} \sin x - \sqrt{\pi/2}\, S^{*} (\sqrt{2x/\pi}) \tag{C.1}$$

$$\int \sqrt{x} \sin x \, dx = - \sqrt{x} \cos x + \sqrt{\pi/2}\, C^{*}(\sqrt{2x/\pi}\ ) \tag{C.2}$$

where $S^{*}(x)$ and $C^{*}(x)$ are the Fresnel integrals:

$$C^{*}(x) = \int_{o}^{x} \cos (\pi x^2/2)\, dx \tag{C.3}$$

$$S^{*}(x) = \int_{o}^{x} \sin (\pi x^2/2)\, dx \tag{C.4}$$

The following two integrals were obtained by Foster (Wait and Campbell, 195[illegible]

$$P\left[g,\rho\right] = \int_{o}^{\infty} \exp (-u\, g)\, J_{o} (\lambda\rho)\, u^{-1} \lambda \, d\lambda \tag{C.5}$$

$$= \exp (- \gamma \sqrt{g^2 + \rho^2}\ ) / \sqrt{g^2 + \rho^2} \tag{C.6}$$

$$N\left[g,\rho\right] = \int_{o}^{\infty} \exp (-u\, g)\, J_{o} (\lambda\rho)\, u^{-i}\, d\lambda \tag{C.7}$$

$$= I_{o}\left[\tfrac{1}{2}\, \gamma(\sqrt{g^2 + \rho^2} - g)\right] K_{o}\left[\tfrac{1}{2}\, \gamma(\sqrt{g^2 + \rho^2} + g)\right] \tag{C.8}$$

where

$$u = \sqrt{\lambda^2 + \gamma^2} \tag{C.9}$$

From Erdelyi (1954, II, 8.4 (10))

$$Q[g, \rho] = \int_0^\infty \exp(-u\, g)\, J_1(\lambda \rho)\, u^{-1}\, d\lambda \qquad \text{(C. 10)}$$

$$= \left[\exp(-\gamma g) - \exp\left(-\gamma \sqrt{g^2 + \rho^2}\right)\right] / (\gamma \rho) \qquad \text{(C. 11)}$$

APPENDIX D

EVALUATION OF INTEGRALS

This appendix considers the evaluation of integrals of the form

$$y = \int_a^b f(x)\, g_n(x)\, dx \tag{D.1}$$

where

$$\left.\begin{aligned} g_1(x) &= \sin x \\ g_2(x) &= \cos x \end{aligned}\right\} \tag{D.2}$$

where $f(x)$ is primarily a slowly varying function in the sense that $f'(x)$ is relatively constant between adjacent zeros of $g_n(x)$. In addition, effects of step changes in $f(x)$ and variations of the form $f(x) = \sqrt{x}$ are considered.

Considering $g_1(x)$ first, evaluation of Equation (D.1) over any range of x where $f'(x)$ is constant gives

$$y_1 = \int_a^b \left[f(a) + f'(x)(x - a)\right] \sin x\, dx \tag{D.3}$$

and using Pierce and Foster's (1956) Equation 345

$$y_1 = \left(\left[-f(a) + a\, f'(x)\right] \cos x + f'(x) \sin x - f'(x)\, x \cos x\right)\Big|_a^b$$

or, in a more convenient form

$$y_1 = \left[- f(x) \cos x + f'(x) \sin x\right]\Big|_a^b \quad ; f'(x) = \text{constant} \tag{D.4}$$

It is now assumed that $f(x)$ can be represented adequately in the range $a < x < b$ by a series of straight line segments with slope changes at the zeros of $\sin x$, as indicated by the solid line in the sketch below. (That is,

it is assumed that the integral $\int_a^b f(x)\,dx$ can be evaluated adequately

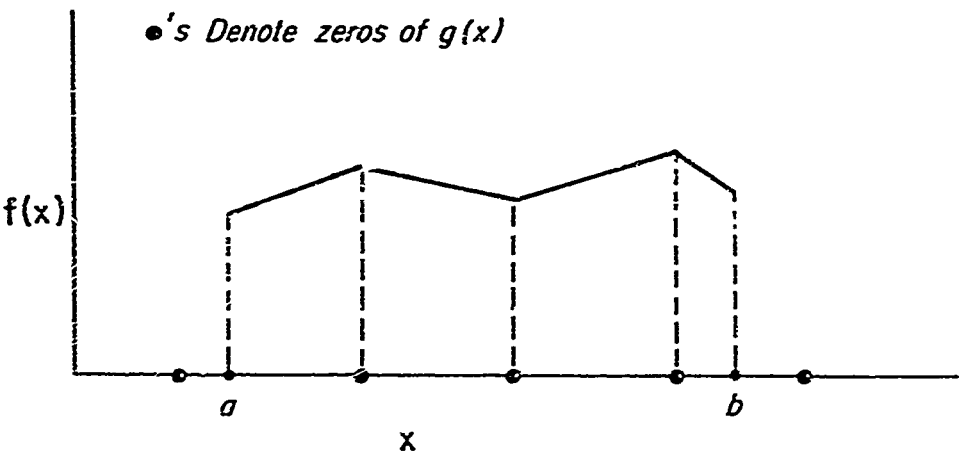

by the trapezoidal rule with intervals equal to the half-period of $g_n(x)$.) It then follows through progressive application of (D.4) to each segment in the sketch that

$$y_1 = \left[- f(x) \cos x + f'(x) \sin x \right] \Bigg|_a^b \qquad \text{(D.5)}$$

which is the same form as (D.4), but without the restriction that $f'(x)$ be constant over the entire interval $a < x < b$.

The corresponding expressions for y_2 may be obtained similarly through use of Pierce and Foster's (1956) Equation 349 as

$$y_2 = \left[f(x) \sin x + f'(x) \cos x \right] \Bigg|_a^b \qquad \text{(D.6)}$$

If the function $f(x)$ contains discontinuities in slope which do not occur at the zeros of $\sin x$ or $\cos x$, it is evident from inspection of Equations (D.4) through (D.6) that there are then additional contributions Δy_1 and Δy_2 to the integrals y_1 and y_2 of the form

$$\Delta y_1 = - \sum_n \delta f'(x_n) \sin x_n \qquad \text{(D.7)}$$

$$\Delta y_2 = - \sum_n \delta f'(x_n) \cos x_n \qquad \text{(D.8)}$$

where

x_n is the value of x at the n'th discontinuity in $f'(x)$

$\delta f'(x_n)$ is the increase (jump) in $f'(x_n)$ at x_n with increasing x

An additional generalization may be obtained as follows for the case where f(x) behaves as required above except near a point x_m where it behaves as

$$f_1(x) = A\sqrt{x - x_m} \quad ; x \to x_m \tag{D.9}$$

where A is a slowly varying function of x and $f'_1(x)$ is seen to be infinite at $x = x_m$. The effect of this infinity of $f'(x)$ on the integral (D.5) may be obtained by integrating (D.1) between the limits $x_1 = x_m - \delta_1$ and $x_2 = x_m + \delta_2$, where δ_1 and δ_2 are large constants and A is considered constant. With the aid of Equations (C.1) and (C.2) of Appendix C, this integral is obtained as

$$\int_{x_1}^{x_2} A\sqrt{x - x_m}\,\sin x\,dx = -f_1(x)\cos x\Big|_{x_1}^{x_2}$$

$$+\sqrt{\pi/2}\;A\left[\cos x_m\, C^*\left(\sqrt{2(x - x_m)/\pi}\right) - \sin x_m S^*\left(\sqrt{2(x - x_m)/\pi}\right)\right]\Big|_{x_1}^{x_2} \tag{D.10}$$

The Fresnel integrals C^* and S^* may be evaluated from the first two terms in their asymptotic series expansion for large real arguments (Martz, 1964, Eq. (11)) as

$$\left.\begin{aligned} C^*(x) &= \tfrac{1}{2} + \sin\left(\tfrac{1}{2}\pi x^2\right)/(\pi x) \\ S^*(x) &= \tfrac{1}{2} - \cos\left(\tfrac{1}{2}\pi x^2\right)/(\pi x) \end{aligned}\right\} \quad x >> 1 \text{ and real} \tag{D.11}$$

and for imaginary arguments by the relationships (Abramowitz, et. al., 1964)

$$\left.\begin{aligned} C^*(ix) &= iC^*(x) \\ S^*(ix) &= -iS^*(x) \end{aligned}\right\} \tag{D.12}$$

Application of Equations (D. 11) and D. 12) to (D. 10) gives the result

$$\int_{x_1}^{x_2} f_1(x) \sin x \, dx = \left[- f_1(x) \cos x + f_1'(x) \sin x \right] \Big|_{x_1}^{x_2}$$

$$+ \tfrac{1}{2}\sqrt{\pi} \; A \exp \left[- i(x_m + \pi/4) \right] \qquad \text{(D. 13)}$$

Now, by comparison of Equations (D. 13) and (D. 5), it is seen that the contribution of the infinite derivative of $f_1(x)$ at x_m to the integral y_1 is

$$\Delta y_1 = \tfrac{1}{2}\sqrt{\pi} \; A \exp \left[- i(x_m + \pi/4) \right] \qquad \text{(D. 14)}$$

and by a similar procedure for y_2

$$\Delta y_2 = - \tfrac{1}{2} \pi \, A \exp \left[- i(x_m - \pi/4) \right] \qquad \text{(D. 15)}$$

We are particularly interested in the application of the above equations to integrals of the form

$$y = \int_{x_1}^{\infty} f(x) \, J_n^*(x) \, dx \qquad \text{(D. 16)}$$

where the J_n^*'s are the following first terms in the asymptotic expressions for Bessel functions of the first kind of orders zero and one with large arguments (Dwight, 1947)

$$J_o^*(x) = (\sin x + \cos x)/\sqrt{\pi x} \quad ; \quad x >> 1 \qquad \text{(D. 17)}$$

$$J_1^*(x) = (\sin x - \cos x)/\sqrt{\pi x} \quad ; \quad x >> 1 \qquad \text{(D. 18)}$$

It is assumed that the function f(x) is everywhere slowly varying, except near x_m, where it varies according to Equation (D. 9), and that f(x) vanishes exponentially at infinity. It then follows from Equations (D. 5), (D. 6), (D. 14), (D. 15), (D. 17) and (D. 18) that the integrals (D. 16) have the values

$$\int_{x_1}^{\infty} f(x)\, J_o^{*}(x)\, dx = -\, f(x_1) J_1^{*}(x_1)$$

$$-\sqrt{x_1}\left(d/dx\,[\,f(x)/\sqrt{x}\,]\right)\Big|_{x = x_1} J_o^{*}(x_1) - i\sqrt{\pi/2}\; A^{*} \exp(-ix_m) \qquad \text{(D.19)}$$

$$\int_{x_1}^{\infty} f(x)\, J_1^{*}(x)\, dx = f(x_1) J_o^{*}(x_1)$$

$$-\sqrt{x_1}\left(d/dx\,[\,f(x)/\sqrt{x}\,]\right)\Big|_{x = x_1} J_1^{*}(x_2) + \sqrt{\pi/2}\; A^{*} \exp(-ix_m) \qquad \text{(D.20)}$$

where

$$A^{*} = \left[f(x)/\sqrt{\pi x(x - x_m)}\right]\Big|_{x = x_m} \qquad \text{(D.21)}$$

BLANK PAGE

APPENDIX E

FREQUENCY-TIME TRANSFORMS

This appendix is concerned with the development and tabulation of the impulse-response and step-function-response of linear systems characterized by various frequency response functions. The following conventional definitions are used.

If a steady-state sinusoidal input of the form $\exp(i\omega t)$ is applied to a linear system, the output will be of the form $H(i\omega)\exp(i\omega t)$ where $H(i\omega)$ is called the complex frequency response or system function or transfer function of the linear system.

The corresponding response $h(t)$ of a linear system to a unit impulsive input $\delta(t)$ is given by the following equivalent Fourier transform equations (Papoulis, 1962)

$$h(t) = (2\pi)^{-1} \int_{-\infty}^{\infty} H(i\omega) \exp(i\omega t)\, d\omega \qquad \text{(E. 1)}$$

$$= \pi^{-1} \int_{0}^{\infty} \left[R(\omega) \cos \omega t - X(\omega) \sin \omega t \right] d\omega \qquad \text{(E. 2)}$$

$$= \pi^{-1} \mathrm{Re} \left[\int_{0}^{\infty} H(i\omega) \exp(i\omega t)\, d\omega \right] \qquad \text{(E. 3)}$$

where

$R(\omega)$ is the real part of $H(i\omega)$

$X(\omega)$ is the imaginary part of $H(i\omega)$

$\mathrm{Re}[x]$ designates the real part of $[x]$

$h(t)$ is the response to a unit impulse $\delta(t)$ where $h(t)$ is assumed to be a real function

and for the simpler case of causal linear systems (Papoulis, 1962), where the response $h(t)$ is zero for negative time,* the following simpler equations apply

$$h(t) = (2/\pi) \int_0^\infty R(\omega) \cos \omega t \, d\omega \qquad \text{(E. 4)}$$

$$= - (2/\pi) \int_0^\infty X(\omega) \sin \omega t \, d\omega \qquad \text{(E. 5)}$$

$$= L^{-1} \left[H(s) \right] \qquad \text{(E. 6)}$$

where $L^{-1}[f(s)]$ is the inverse Laplace transform of $f(s)$, subject to the restriction that $f(s)$ is analytical in the right half of the complex s-plane where the real part of s is positive.

The response of a linear system $A(t)$ to a unit step function $S(t)$ is in general given by

$$A(t) = \int_{-\infty}^{t} h(t) \, dt \qquad \text{(E. 7)}$$

where

$A(t)$ is the response to a unit step function $S(t)$

and, for the case of causal systems, by(Papoulis, 1962)

$$A(t) = (2/\pi) \int_0^\infty \left[R(\omega)/\omega \right] \sin \omega t \, d\omega \qquad \text{(E. 8)}$$

$$= R(0) + (2/\pi) \int_0^\infty \left[X(\omega)/\omega \right] \cos \omega t \, d\omega \qquad \text{(E. 9)}$$

$$= L^{-1} \left[H(s)/s \right] \qquad \text{(E. 10)}$$

* While real physical systems are, of course, all causal (i.e., output does not precede input), the approximations involved in deriving some equations in this report result in a few non-causal expressions.

Table E.1 presents expressions for h(t) and A(t) computed according to the above equations for a variety of frequency response functions of interest in other parts of this report. The remainder of this section consists of a partial listing of the integral transforms used to determine each listed function.

Item 1.1: Inverse Laplace Transform; Churchill (1944), Appendix II (14); Erdelyi et al. (1954, I), 5.6 (35); Papoulis (1962), Eq. (3-4).

Item 1.2: Papoulis (1962), Eq. (3-4).

Item 1.3: Inverse Laplace transform; Churchill (1944), Appendix III (82, 83).

Item 2.1a: Inverse Laplace transform; Churchill (1944), Appendix II(14); Erdelyi, et. al. (1954, I), 5.6 (36) and (37).

Item 2.1b: Differentiation of 2.1a with respect to c.

Item 3.2: Inverse Laplace transform; Churchill, Appendix III (8, 12).

Item 3.3: Inverse Laplace transform; Churchill, Appendices II (14)and III (37, 43).

Item 5: Papoulis (1962), Eq. (3-3).

Items 6 and 7: Papoulis (1962), Eq. (3-32).

Item 8.1: h(t) determined by convolution of Items 1 and 4.

Item 8.2: Inverse Laplace transform; Churchill (1944), Appendices II (12, 13) and III (8).

Item 8.3: Inverse Laplace transform; Churchill (1944), Appendices II (14) and III (87).

Item 9: Equations (E.3) and (E.7); Grobner and Hofreiter (1958), p. 128 (67a).

Item 11: Equations (E.3) and (E.7); Grobner and Hofreiter (1958), p. 127 (66b).

Item 13: Equations (E.3) and (E.7); Erdelyi et al. (1954, I), 1.9 (1); Dwight (1947), 679.10.

Item 15: Take imaginary part of expression; apply Equation (E.5), using Erdelyi et al (1954, I), 2.12 (27).

Table E. 1

TABLE OF TRANSFORMS

[$s = i\omega a$; $\tau = t/a$; $g = bc$; $x = b\tau$; $\xi = bc$]

Item	$H(i\omega)$	$h(t)$	$A(t)$
—	$H(s, a, b, \cdots)$	$h(t, a, b, \cdots)$	$A(t, a, b, \cdots)$
1	$\exp(-c\gamma)$	$h_1(t)$	$A_1(t)$
1.1	$\gamma = \sqrt{s^2 + 2bs}$	$[(b^2c/a)\, I_1^*(b\tau, bc) + \delta(t - ac)]\exp(-b\tau)$	$U(b\tau, bc)$
1.2	$\gamma = s$	$\delta(t - ac)$	$S(t - ac)$
1.3	$\gamma = \sqrt{s}$	$\frac{1}{2} c\sqrt{a/\pi t^3}\exp(-ac^2/4t)$	$\operatorname{erfc}(\frac{1}{2} c/\sqrt{\tau})$
2*	$\gamma^n \exp(-c\gamma)$	$(-1)^n(\partial^n/\partial c^n)\, h_1(t)$	$(-1)^n(\partial^n/\partial c^n)\, A_1(t)$
3	$(1 + d\gamma)^{-1}$	$h_3(t, a, b, d)$	$A_3(t)$
3.1	—	$h_{3,1}(t = 0^+) = 0$	$A_{3,1}(t = 0^+) = 0$
3.2	—	$\exp(-t/ad)/ad$	$1 - \exp(-\tau/d)$
3.3	—	$\left[1/\sqrt{\pi\tau/d^2} - \exp(\tau/d^2)\operatorname{erfc}(\sqrt{\tau/d^2})\right]/ad^2$	$1 - \exp(\tau/d^2)\operatorname{erfc}(\sqrt{\tau/d^2})$
4	$\gamma/(1 + d\gamma)$	$\left[\delta(t) - h_3(t)\right]/d$	$\left[1 - A_3(t)\right]/d$
5	1	$\delta(t)$	$S(t)$
6	s	$a\,\delta_1(t)$	$a\,\delta(t)$
7	s^n	$a^n\delta_n(t)$	$a^n\delta_{n-1}(t)$
8	$\gamma\exp(-c\gamma)/(1 + d\gamma)$	—	—
8.1	—	—	$A_{8,1}(0 < t < ac + \epsilon) = \exp(-bc)\, S(t - ac)/d$; $\epsilon \to 0$
8.2	—	—	$\exp\left[-(\tau - c)/d\right] S(\tau - c)/d$
8.3	—	—	$\left[\exp(c/d + \tau/d^2)\operatorname{erfc}(\sqrt{\tau/d^2} + \frac{1}{2}(c/d)/\sqrt{\tau/d^2})\right]/d$
9	$\exp(-s)/\left[1 - (ds)^2\right]$	$\frac{1}{2}\exp(-\lvert\tau - 1\rvert/d)/(ad)$	$S(\tau - 1) - \frac{1}{2}\operatorname{sgn}(\tau - 1)\exp(-\lvert\tau - 1\rvert/d)$
10	$s\exp(-s)/\left[1 - (ds)^2\right]$	$-\frac{1}{2}\operatorname{sgn}(\tau - 1)\exp(-\lvert\tau - 1\rvert/d)/(ad^2)$	$\frac{1}{2}\exp(-\lvert\tau - 1\rvert/d)/d$
11	$s^2\exp(-s)/\left[1 - (ds)^2\right]$	$\left[h_9(t) - \delta(t - a)\right]/d^2$	$-\frac{1}{2}\operatorname{sgn}(\tau - 1)\exp(-\lvert\tau - 1\rvert/d)/d^2$
12	$s^n\exp(-s)/\left[1 - (ds)^2\right]$	$\left[h_{n-2}(t) - a^{n-2}\delta_{n-2}(t - a)\right]/d^2$	$\left[A_{n-2}(t) - a^{n-2}\delta_{n-3}(t - a)\right]/d^2$
13	$\exp(-cs)/\cos bs$	$\left[2ab\cosh\lvert\frac{1}{2}\pi(\tau - c)/b\rvert\right]^{-1}$	$\frac{1}{2} + \pi^{-1}\tan^{-1}(\sinh[\frac{1}{2}\pi(\tau - c)/b])$
14	$s\exp(-cs)/\cos bs$	—	$\left[2b\cosh\lvert\frac{1}{2}\pi(\tau - c)/b\rvert\right]^{-1}$
15	$I_1(s)K_1(s)$	$\pm(\pi a)^{-1}Q_{\frac{1}{2}}(\frac{1}{2}\tau^2 - 1)$; $\tau \gtrless 2$	—

*See also 2.1a and 2.1b on next page

Table E.1 (Cont)

Table of Transforms

Item	H (iω)	A (t)
2.1a	$\gamma \exp(-c\gamma)$	$c^{-1} f \exp(-x)\left[\delta(x-f) + I_o(\sqrt{x^2-f^2})\, S(x-f) + x I_1^*(\sqrt{x^2-f^2})\right]$
2.1b	$\gamma^2 \exp(-c\gamma)$	$c^{-2} f^2 \exp(-x)\left[\delta_1(x-f) + (1+\frac{1}{2}f)\,\delta(x-f)\right.$ $\left. + (fx/(x^2-f^2))\, I_o(\sqrt{x^2-f^2})\, S(x-f) + f(1-2x/(x^2-f^2))\, I_1^*(\sqrt{x^2-f^2})\right]$

$$I_1^*(x,f) = I_1(\sqrt{x^2-f^2})\, S(x-f)/\sqrt{x^2-f^2} \qquad \text{(E.11)}$$

$$U(x,f) = \exp(-f)\, S(x-f) + f \int_o^x I_1^*(x,f) \exp(-x)\, dx \qquad \text{(E.12)}$$

The step function S(t), the delta or impulse function $\delta(t)$ or $\delta_o(t)$, and the n'th derivative of the delta function $\delta_n(t)$ are defined as (Papoulis, 1962)

$$S(t) = \begin{cases} 0 & ; t < 0 \\ 1 & ; t > 0 \end{cases} \qquad \text{(E.13)}$$

$$\delta(t) \equiv \delta_o(t) = dS(t)/dt \qquad \text{(E.14)}$$

$$\delta_n(t) = d^n\delta/dt^n \qquad \text{(E.15)}$$

$$\int_{-\infty}^{\infty} \delta_n(t - t_o)\, f(t)\, dt = (-1)^n (d^n/dt^n)\, f(t_o) \qquad \text{(E.16)}$$

BLANK PAGE

REFERENCES

1. Abramowitz, M., et.al., 1964: Handbook of Mathematical Functions, Supt. of Documents, U.S. Govt. Printing Office, Washington, D.C.

2. Bhattacharyya, B.K., 1959: "Electromagnetic Fields of a Transient Magnetic Dipole on the Earth's Surface," Geophysics, Vol. 24, No. 1, pp. 89-108.

3. Bhattacharyya, B.K., 1963: "Electromagnetic Fields of a Vertical Magnetic Dipole Placed Above the Earth's Surface," Geophysics, Vol. 28, No. 3, pp. 408-425.

4. Churchill, R.V., 1944: Modern Operational Mathematics in Engineering, McGraw-Hill Book Co., New York.

5. Dwight, H.B., 1947: Tables of Integrals and Other Mathematical Data, Revised Edition, the Macmillan Company, New York

6. Erdelyi, A., et.al., 1953: Higher Transcendental Functions, 3 Vols., McGraw-Hill Book Co., New York.

7. Erdelyi, A., et.al., 1954: Tables of Integral Transforms, 2 Vols., McGraw-Hill Book Col, New York.

8. Grobner, W., and N. Hofreiter, 1958: Integraltafel, Zweiter Teil, Bestimmte Integral, Springer-Verlag, Wein.

9. Martz, C.W., 1964: Tables of the Complex Fresnel Integral, NASA SP-3010.

10. Papoulis, A., 1962: The Fourier Integral and Its Applications, McGraw-Hill Book Co., New York.

11. Pierce, B.O., and R.M. Foster, 1956: A Short Table of Integrals, Fourth Edition, Ginn and Company, New York.

12. Smiley, R.F., 1964: Transmission of Vertically Incident Plane Hydromagnetic Waves Through a Horizontally Stratified Collision-Free Plasma, Final Report, Vol. II, Contract No. DA-36-039-SC-89177, USAEL Ft. Monmouth, New Jersey, Doc. No. ARA-T-9197-14, Allied Research Associates, Inc. (AD 461699; NAS N65-23748).

13. Wait, J.R., 1951: "The Magnetic Dipole Over the Horizontally Stratified Earth," Canadian Jour. Phys., Vol. 29, pp. 577-592.

14. Wait, J.R., and L.L. Campbell, 1953: "The Fields of an Oscillating Magnetic Dipole in a Semi-Infinite Conducting Medium," Jour. Geophys. Res., Vol. 58, No. 2, pp. 167-178.

BIBLIOGRAPHY

This bibliography consists of four sections related to various aspects of the problem of hydromagnetic and electromagnetic wave propagation through and below the ionosphere.

Section A presents a bibliography of reports pertaining to natural ULF (near 1 cps) magnetotelluric phenomena (see also Section B).

Section B presents a bibliography of reports relating to ULF effects of lightning, plus a few comprehensive books and bibliographies covering a broader frequency range of lightning effects.

Section C covers reports concerning the reflection and refraction of plane hydromagnetic waves at plane interfaces between different media, including transformations between hydromagnetic, electromagnetic, and sound waves.

Section D is a bibliography of reports dealing with ULF wave propagation in the ionosphere, with particular reference to the penetration of hydromagnetic waves through the ionosphere from above. Also included are reports dealing with the resonant modes and frequencies associated with hydromagnetic wave propagation through the ionosphere.

The reports listed in this bibliography consist of the majority of the reports on the above-described subjects which were encountered in the course of research under Contracts No. DA-36-039-SC-89177 and DA-28-043-AMC-01241(E).

A. NATURAL ULF MAGNETOTELLURIC PHENOMENA

1. Anonymous, 1964: Report of the Geomagnetic and Geoelectric Observations, 1961-62, Kakioka Magnetic Observatory, Kakioka, Japan. (NASA N64-23904).

2. Anonymous, 1964: Report of the Geomagnetic and Geoelectric Observations, 1963 (Rapid Variations), Kakioka Magnetic Observatory, Kakioka, Japan, (NASA N65-10669).

3. Anonymous, 1964: Symposium on Ultra Low Frequency Electromagnetic Fields (from 30 c/s to 0.001 c/s), August 17-20, 1964, NBS Report 8815. (See also: Radio Science, Vol. 69D, No. 8, August 1965).

4. Anonymous, 1965: Study of the Origin of Micropulsations in Certain Frequency Bands, McGill University, Annual Report - Grant No. DA 49-092-ARO-G46, July 15, 1964 - July 15, 1965. (AD 622760).

5. Balser, M., and C.A. Wagner, 1960: "Observations of Earth-Ionosphere Cavity Resonances," Nature, Vol. 188, No. 4751, pp. 638-641.

6. Balser, M., and C.A. Wagner, 1962: "Diurnal Power Variations of the Earth-Ionosphere Cavity Modes and Their Relationship to Worldwide Thunderstorm Activity," Jour of Geophys. Res., Vol. 67, No. 2, pp. 619-625.

7. Benioff, H., 1960: "Observations of Geomagnetic Fluctuations in the Period Range 0.3 to 120 Seconds," Jour. of Geophs. Res., Vol. 65, No. 5, pp. 1413-1422.

8. Berthold, W.K., A.K. Harris, and H.J. Hope, 1960: "Correlated Micropulsations at Magnetic Sudden Commencements," Jour. of Geophys. Res., Vol. 65, No. 2, pp. 613-618.

9. Bleil, D. F. (ed.), 1964: Natural Electromagnetic Phenomena Below 30 kc/s, Phenum Press, New York.

10. Bomke, H. A., 1962: "The Relation of Magnetic Micropulsations to Electric-Current and Space-Charge Systems in the Lower Ionosphere," Jour. of Geophys. Res., Vol. 67, No. 1, pp. 177-181.

11. Bostick, F. X., Jr., and H. W. Smith, 1962: "Investigation of Large-Scale Inhomogeneities in the Earth by the Magnetotelluric Method," Proc. IRE, Vol. 50, No. 11, pp. 2339-2346.

12. Campbell, W. H., 1959: "Studies of Magnetic Field Micropulsations with Periods of 5 to 30 Seconds," Jour. of Geophys. Res., Vol. 64, No. 11, pp. 1819-1826.

13. Campbell, W. H., 1960: "Natural Electromagnetic Energy Below the ELF Range," Jour. Res. NBS - Sec. D - Radio. Prop., Vol. 64D, No. 4, pp. 409-411.

14. Campbell, W. H., 1961: "Magnetic Field Micropulsations and Electron Bremsstrahlung," Jour. of Geophys. Res., Vol. 66, No. 10, pp. 3599-3600.

15. Campbell, W. H., 1963: "Natural Electromagnetic Field Fluctuations in the 3.0- to 0.02-cps Range," Proc. IEEE, Vol. 15, pp. 1337-1342.

16. Campbell, W. H., 1964: A Review of Seven Studies of Geomagnetic Pulsations Associated with Auroral Zone Disturbance Phenomena, Paper presented at the Symposium on Ultra Low Frequency Electromagnetic Fields, Boulder, Colo., Aug. 17-20, 1964.

17. Campbell, W. H., 1964: "A Study of Geomagnetic Effects Associated with Auroral Zone Electron Precipitation Observed by Balloons," Jour. of Geomag. Geoelec., Vol. 16, No. 1, pp. 41-61. (IAA A65-18696).

18. Campbell, W.H., and H. Leinbach, 1961: "Ionospheric Absorption at Times of Auroral and Magnetic Pulsations," Jour. of Geophs. Res., Vol. 66, No. 1, pp. 25-34.

19. Campbell, W.H., and S. Matsushita, 1962" "Auroral Zone Geomagnetic Micropulsations with Periods of 5 to 30 Seconds," Jour. of Geophys. Res., Vol. 67, No. 2, pp. 555-573.

20. Campbell, W.H., and E.C. Stiltner, 1965: "Some Characteristics of Geomagnetic Pulsations Near 1 c/s," Radio Science, Vol 69D, No. 8, pp. 1117-1132.

21. Duffus, H.J., et.al., 1962: "Spatial Variations in Geomagnetic Micropulsations," Can. Jour. Phys., Vol. 40, pp. 1133-1152.

22. Duncan, R.A., 1961: "Some Studies of Geomagnetic Micropulsations," Jour. of Geophys. Res., Vol. 66, No. 7, pp. 2087-2094.

23. Fraser, B.J., P.W. McNabb, and C.D. Ellyett, 1963: Geomagnetic Micropulsations at Christchurch, New Zealand, Final Report, Research Grant NONR(G) - 00027-62, ONR. (NASA N64-17634).

24. Fraser, B.J., and C.D. Ellyett, 1964: Observations in New Zealand of Geomagnetic Micropulsations in the 0.008-2.0 c/s Band, Final Report, Research Grant NONR(G)- 00020-63, ONR. (AD 607359).

25. Green, A.W., Jr., B.H. List, and J.F.P. Zengel, 1962: "The Theory, Measurement, and Applications of Very-Low-Frequency Magnetotelluric Variations," Proc. IRE, Vol. 50 , No. 11, pp. 2347-2363.

26. Heacock, R.R., and V.P. Hessler, 1965: "Pearl-Type Micropulsations Associated with Magnetic Storm Sudden Commencements," Jour. of Geophys. Res., Vol. 70, No. 5, pp. 1103-1111.

27. Hodder, D.T., et.al., 1963: A Study of High Altitude Nuclear Blast Data, Rep. No. 2, Contract No. DA 36-039-AMC-00079(E), USASRDL, Ft. Monmouth, New Jersey, North American Aviation Rep. No. SID 63-656.

28. Hodder, D.T., et.al., 1965: A Study of High Altitude Nuclear Blast Data, Rep. No. 3, Contract No. DA 36-039-AMC-03729(E), USAEL, Ft. Monmouth, New Jersey, North American Aviation Rep. No. SID 64-143. (AD 458343).

29. Jacobs, J.A., and E.J. Jolley, 1962: "Geomagnetic Micropulsations with Periods 0.3-3 Sec. (Pearls)," Nature, Vol. 194, No. 4829, pp. 641-643.

30. Kalashnikov, A.G., and V.A. Troitskaya (ed.), 1961: Short Period Pulsations of the Earth's Electromagnetic Field, NASA TT-F-104, 1965.

31. Kalinin, D. (ed.), 1959: Magnetic and Ionospheric Disturbances, NASA TT-F-49, 1961.

32. Keefe, T.J., C. Polk, and H.L. Koenig, 1965: Results of Simultaneous ELF Measurements at Brannenburg [Germany] and Kingston, R.I., AFCRL-65-200(1). (AD 614012).

33. Komack, R.L., 1964: Analysis of Magnetotelluric Micropulsations at Widely Separated Stations, AFCRL-64-10. (AD 432046).

34. Komack, R.L., et.al., 1964: "Simultaneous Measurements and Spectral Analysis of Micropulsation Activity," Nature, Vol. 201, No. 4918, pp. 460-462, and Vol. 204, No. 4958, pp. 534-537.

35. Konig, H., 1959: "Atmospherics geringster Frequenzen," (Atmospherics of Very Low Frequency), Zeitschrift fur angewandte Physik, Vol. 11, No. 7; pp. 264-274. (Eng. transl.: Am. Met. Soc. T-G-229; AD 453050).

36. Lokken, J.E., J.A. Shand, and C.S. Wright, 1962: "A Note on the Classification of Geomagnetic Signals Below 30 Cycles per Second," Can. Jour. Phys., Vol. 40, pp. 1000-1009.

37. Lokken, J.E., J.A. Shand, and C.S. Wright, 1963: "Some Characteristics of Electromagnetic Background Signals in the Vicinity of One Cycle Per Second," Jour. of Geophs. Res., Vol. 68, No. 3, pp. 789-794.

38. Maple, E., 1959a: "Geomagnetic Oscillations at Middle Latitudes, Part I. The Observational Data," Jour. of Geophys. Res., Vol. 64, No. 10, 11. 1395-1404.

39. Maple, E., 1959b: "Geomagnetic Oscillations at Middle Latitudes, Part II. Sources of the Oscillations," Jour. of Geophys. Res., Vol. 64, No. 10, pp. 1405-1409.

40. Orange, A.S., and F.X. Bostick, 1965: "Magnetotelluric Micropulsations at Widely Separated Stations," Jour. of Geophys. Res., Vol. 70, No. 6, pp. 1407-1413.

41. Poeverlein, H., 1959: Low and Very Low Frequency Propagation, AFCRC-TR-60-106. (AD 237296).

42. Pope, J.H., 1964: "An Explanation for the Apparent Polarization of Some Geomagnetic Micropulsations (Pearls)," Jour. of Geophys Res., Vol. 69, No. 3, pp. 399-405.

43. Santirocco, R.A., and D.G. Parker, 1963a: Geomagnetic Noise 0.005 to 5 cps in Bermuda, Report GD 1463-50, General Dynamics/Electronics-Rochester. (AD 426711).

44. Santirocco, R.A., and D.G. Parker, 1963b: "The Polarization and Power Spectrums of Pc Micropulsations in Bermuda," Jour of Geophys. Res., Vol. 68, No. 19, pp. 5545-5558.

45. Schlich, R., 1963: "Micropulsations de Periods Comprises Entre 0.5 et 6s Observées dans les Regions de Hautes et Moyennes Latitudes," Ann. Geophys., Vol. 19, No. 4, pp. 347-355.

46. Shand, J.A., 1965: A Review of PNL Observations of the Schuman-ELF Natural Electromagnetic Background, Pac. Nav. Lab. TM 65-6. (AD 474889).

47. Shostak, A., and E.H. Huriburt, 1963: "Electromagnetic Phenomena in the Audio and Sub-Audio Frequency Ranges," Naval Research Reviews, Vol. 16, No. 12, pp. 1-6.

48. Smith, H.W., 1962: Report of Co-operative Geomagnetic Measurement Program of the Pacific Naval Laboratory, the University of British Columbia, the University of Alberta, the University of Texas, EERL, Rep 128, Univ. of Texas. (AD 277429).

49. Smith, H.W., 1963: A Survey of Geomagnetic Micropulsation Research Conducted in Connection with the Co-operative Geomagnetic Micropulsation Measurement Program, EERL Rep. 130, Univ. of Texas. (AD 419864; NASA N63-21464).

50. Smith, H.W., 1964: "Some Observations of Type Pc1 Geomagnetic Micropulsations," Jour. of Geophys. Res., Vol. 69, No. 9, pp. 1875-1881.

51. Smith, H.W., L.D. Provazek, and F.X. Bostick, Jr., 1961: "Directional Properties and Phase Relations of the Magnetotelluric Fields at Austin, Texas," Jour. of Geophys. Res., Vol. 66, No. 3, pp. 879-888.

52. Tepley, L.R., 1961: "Observations of Hydromagnetic Emissions," Jour. of Geophys. Res., Vol. 66, No. 6, pp. 1651-1658.

53. Tepley, L., and K.D. Amundsen, 1965: "Observations of Continuous Sub-ELF Emissions in the Frequency Range 0.2 to 1.0 Cycles Per Second," Jour. of Geophys. Res., Vol. 70, No. 1, pp. 234-239.

54. Tepley, L.R., and R.C. Wentworth, 1962a: Structure and Attenuation of Hydromagnetic Emissions, 2 Vols., Sci. Rep. 1, Contract AF 19(604)-5906, Lockheed Missiles and Space Company. (AD 274486, and AD 274485; AFCRL 62-32).

55. Tepley, L.R., and R.C. Wentworth, 1962b: "Hydromagnetic Emissions, X-Ray Bursts, and Electron Bunches, 1. Experimental Results," Jour. of Geophys. Res., Vol. 67, No. 9, pp. 3317-3333.

56. Tepley, L., R.C. Wentworth, and K.D. Amundsen, 1963: Sub ELF Geomagnetic Fluctuations, Vol. I, Frequency-Time Characteristics of Hydromagnetic Emissions, Final Rep., Vol. I, Contract AF 19(628)-462, Lockheed Missiles and Space Co., (AD 437332).

57. Tepley, L.R., R.C. Wentworth, and K.D. Amundsen, 1964: Further Investigations of Storm-Time Sub ELF Emissions, Tech. Rep., Contract NOnr-4454(00), for Geophysics Branch, Earth Sciences Div., ONR, Lockheed Missiles and Space Co.

58. Troitskaya, V., 1957: "Earth-Current Installations at the Stations of the U.S.S.R.," IGY Annals, Vol. IV, Pt. IV, pp. 322-329.

59. Troitskaya, V.A., 1961: "Pulsation of the Earth's Electromagnetic Field with Periods of 1 to 15 Seconds and Their Connection with Phenomena in the High Atmosphere," Jour. of Geophys. Res., Vol. 66, No. 1, pp. 5-18.

60. Vladimirov, N.P., and S.M. Krylov, 1964: "Characteristics of Micropulsations of the Natural Electromagnetic Field," Izv. Geophys. Ser., USSR, No. 6, pp. 872-882. (Eng. Trans.: IAA A65-10035).

61. Vozoff, K., R.M. Ellis, and G.D. Garland, 1962: "Composition of Pearls," Nature, Vol. 194, No. 4828, pp. 539-541.

62. Vozoff, K., and R.M. Ellis, 1963: "Further Analysis of Pearls," Geofisica Pura e Applicata, Vol. 55, No. 2, pp. 101-109.

63. Wentworth, R.C., 1963: Sub ELF Geomagnetic Fluctuations, Vol. II, Statistical Studies of Hydromagnetic Emissions, Final Rep., Vol. II, Contract AF 19(628)-462, Lockheed Missiles and Space Co. (AD 437330).

64. Yanagihara, K., 1963: "Geomagnetic Micropulsations with Periods from 0.03 to 10 Seconds in the Auroral Zones with Special Reference to Conjugate-Point Studies," Jour. of Geophys. Res., Vol. 68, No. 11, pp. 3383-3397.

B. ULTRA-LOW-FREQUENCY LIGHTNING EFFECTS

1. Baker, R., and E. Kiss, 1963: "Annotated Bibliography on the Physics of the Lightning Flash," Met. and Geoastro. Abstracts, Vol. 14, No. 9, pp. 2923-2988.

2. Byers, H.R., 1953: Thunderstorm Electricity, Univ. of Chicago Press, Chicago.

3. Chalmers, J.A., 1957: Atmospheric Electricity, Pergamon Press, New York.

4. Coroniti, S.C. (ed), 1963: Problems of Atmospheric and Space Research, Elsevier Publ. Co., New York.

5. Fischer, W.H., 1965: "The Radio Noise Spectrum from ELF to EHF," Jour. Atm. Terr. Phys., Vol. 27, pp. 475-480.

6. Handbook of Geophysics, Revised Edition, 1960, the Macmillan Co., New York.

7. Kasemir, H.W., 1962: Analysis of the Electrostatic Field of a Lightning Stroke, USAELRDL TR 2321. (AD 296395).

8. Kitagawa, N., M. Brooke, and E.J. Workman, 1962: "Continuing Currents in Cloud-to-Ground Lightning Discharges," Jour. Geophys. Res., Vol. 67, No. 2, pp. 637-647.

9. Norinder, H., 1963: Magnetic Field Variations in Vicinity of Lightning Discharges, Univ. of Uppsala, Final Scientific Report, Contract AF 61(052)-171. (AFCRL-64-78; AD 434772).

10. Pierce, E.T., 1955a: "Electrostatic Field-Charges Due to Lightning Discharges," Quar. Jour. Roy. Met. Soc., Vol. 81, No. 348, pp. 211-228.

11. Pierce, E.T., 1955b: "The Development of Lightning Discharges," Quar. Jour. Roy. Met. Soc., Vol. 81, No. 348, pp. 229-240.

12. Smith, L.H., (ed.), 1958: Recent Advances in Atmospheric Electricity, Pergamon Press, New York.

13. Watt, A.D., 1960: "VLF Electric Fields from Thunderstorms," Jour. Res., NBS, D. Radio Propagation, Vol. 64D, No. 5. pp. 425-433.

14. Williams, D.P., and M. Brook, 1963: "Magnetic Measurements of Thunderstorm Currents, 1. Continuing Currents in Lightning," Jour. Geophys. Res., Vol. 68, No. 10, pp. 3243-3247.

15. Whitson, A.L., W.T. Sperry, and F.H. Smith, 1962: A Summary of Literature Pertaining to VLF and ELF Propagation, 2 Vols., Stanford Research Institute. (AD 406160 and 406161).

C. REFLECTION AND REFRACTION OF HYDROMAGNETIC WAVES

1. Bazer, J., 1961: Reflection and Refraction of Weak Hydromagnetic Discontinuities, Inst. Math. Sci., New York Univ., Rep. MH-11, (AFCRL-268; AD 259342).

2. Bazer, J., and J. Hurley, 1963: "Geometrical Hydromagnetics," Jour. Geophys. Res., Vol. 68, No. 1, pp. 147-174.

3. Fejer, J.A., 1963: "Hydromagnetic Reflection and Refraction at a Fluid Velocity Discontinuity," Physics of Fluids, Vol. 6, No. 4, pp. 508-512.

4. Ferraro, V.C.A., 1954: "On the Reflection and Refraction of Alfven Waves," Astrophy. Jour., Vol. 121, pp. 393-406,

5. Freeman, E.A., and R.M. Kulsrud, 1958: "Problems In Hydromagnetics," Advances in Applied Mechanics, Vol. V, H.L. Dryden and Th. Von Karman, Editors, Academic Press, Inc., New York.

6. Hruška, A., 1965: "A Note on the Reflection and Refraction of Damped Magnetodynamic Waves in the Ionosphere," Studia Geoph. et Geod., Vol. 9, pp. 53-60. (IAA A65-20884).

7. Kahalas, S.L., 1960: "Magnetohydrodynamic Wave Propagation in the Ionosphere," Phys. of Fluids, Vol. 3, No. 3, pp. 372-378.

8. Kahalas, S.L., 1963: "Coupling of Magnetohydrodynamic to Electromagnetic Waves at a Plasma Discontinuity. II. The Nonpropagating Field," Phys. of Fluids, Vol. 6, No. 3, pp. 438-446.

9. Kahalas, S.L., and D.A. McNeill, 1964: "Coupling of Magnetohydrodynamic to Electromagnetic and Acoustic Waves at a Plasma-Neutral Gas Interface," Physics of Fluids, Vol. 7, No. 8, pp. 1321-1328. (See also AFCRL-63-944, 1963, AD 431635 or AFCRL-64-813; AD 607260).

10. Kontorovich, V.M., and A.M. Glutsyuk, 1961: "Transformation of Sound and Electromagnetic Waves at the Boundary of a Conductor in a Magnetic Field," ZETF, Vol. 41, pp. 1195-1204 (Eng. trans.: Soviet Physics - JETP, Vol. 14, No. 4, pp. 852-858).

11. Kornhauser, E.T., 1961: "Electroacoustic Coupling at the Boundary of an Ionized Medium," Jour. Acoust. Soc. Amer. Vol. 33, No. 12, pp. 1764-1767. (See also: "Transmission of Waves Through Ionized Layers," Brown Univ., Sci. Rep. AF 4561/2, 1959, AD 211150).

12. Loladze, T.D., 1965: "Transformation of Waves at a Plasma-Vacuum Boundary," ZhTF, Vol. 35, No. 3, pp. 582-584. (Eng. trans.: Soviet Physics - Tech. Phys, Vol. 10, No. 3, pp. 456-457).

13. Loladze, T.D., and N.L. Tsintsadze, 1963: "Reflection and Refraction of Magnetohydrodynamic Waves at the Boundary Between Two Anisotropic Plasma Media," ZhTF, Vol. 33, No. 8, pp. 929-934. (Eng. trans.: Soviet Physics - Tech. Phys., Vol. 8, No. 8, pp. 695-698.

14. Namikawa, T., 1961: "On the Reflection and Refraction of Hydromagnetic Waves in Ionized Gas," Jour. Geomag. Geoelectr., Vol. 12, pp. 117-128.

15. Namikawa, T., 1962: "On the Reflection and Refraction of Hydromagnetic Waves in Ionized Gas II," Jour. Geomag. Geoelectr., Vol. 14, pp. 41-48.

16. Ong, R.S.B., 1962: "On the Reflection and Refraction of Hydromagnetic Waves in Interstellar Medium," Proc. K. Ned. Akad. Wetensch. B. (Netherlands), Vol. 65, No. 1, pp. 66-72.

17. Poeverlein, H., 1964: "Coupling of Magnetohydrodynamic Waves in Stratified Media," Phys. Rev., Vol. 136, No. 6A, pp. A1605-1613.

18. Pridmore-Brown, D.C., 1963: "Reflection and Refraction of Magneto-Acoustic Waves at an Interface," Phys. of Fluids, Vol. 6, No. 6, pp. 803-805.

19. Raju, P.K., and Verma, Y.K., 1960: "Reflection and Refraction of Hydromagnetic Plane Waves at the Boundary of Two Compressible Media," Z. Astrophys., Vol. 50, pp. 29-34.

20. Roberts, P.H., 1955: "On the Reflection and Refraction of Hydromagnetic Waves," Astrophys. Jour., Vol. 121, pp. 720-730.

21. Simon, R., 1958: "On the Reflection and Refraction of Hydromagnetic Waves at the Boundary of Two Compressible Gaseous Media," Astrophys. Jour., Vol. 128, pp. 392-397.

22. Smiley, R.F., 1963: Reflection and Refraction of Oblique Hydromagnetic Waves at a Plasma-Vacuum Interface, Report No. 7, Contract No. DA-36-039-SC-89177, USASRDL, Ft. Monmouth, New Jersey, Document No. ARA-T-9197-7, Allied Research Associates, Inc. (AD 409734).

23. Smiley, R.F., 1964: The Penetration of Oblique Hydromagnetic Waves Through Horizontally Stratified Plasma and Un-Ionized Media, with Applications to the Lower Ionosphere, Final Report, Vol. I, Contract No. DA-36-039-SC-89177, USAEL, Ft. Monmouth, New Jersey, Doc. No. ARA-T-9197-13, ARACON Geophysics Company. (AD 461698; NASA N65-23593).

24. Talwar, H.S., 1961: "Reflection and Refraction of Plane Hydromagnetic Waves at the Boundary of Two Compressible Media," Ann. Astrophys., Vol. 24, No. 6, pp. 536-540.

25. Totaro, C., 1958: "Sulla riflessione e rifrazione in magnetiodrodinamica," Lincei-Rend. Sc. fis. mat. e nat., Vol. 24, pp. 310-316.

26. Turcotte, D.L., and G.Schubert, 1961: "Interaction of Low-Frequency Electromagnetic Waves with a Plasma," Physics of Fluids, Vol. 4, No. 9, pp. 1156-1161.

27. Ullah, N., and S. L. Kahalas, 1963: "Coupling of Magnetohydrodynamic to Electromagnetic Waves at a Plasma Discontinuity. I. Radiation Field," Phys. of Fluids, Vol. 6, No. 2, pp. 284-289.

28. Williams, W. E., 1960: "Reflection and Refraction of Hydromagnetic Waves at the Boundary of Two Compressible Media," Astrophys. Jour., Vol. 131, No. 2, pp. 438-441.

D. HYDROMAGNETIC WAVE PROPAGATION THROUGH THE IONOSPHERE

1. Akasofu, S., 1959: "Magneto-Hydrodynamic Waves in the Ionosphere," Jour. Atmosph. Terr. Phys., Vol. 15, pp. 156-160.

2. Akasofu, S., 1965: "Attenuation of Hydromagnetic Waves in the Ionosphere," Radio Science, Vol. 69D, No. 3, pp. 361-366.

3. Bomke, H.A., et.al., 1960: "Global Hydromagnetic Wave Ducts in the Exosphere," Nature, Vol. 185, No. 4709, pp. 299-300.

4. Bostick, F.X., Jr., 1964: Propagation Characteristics of Plane Small-Amplitude Hydromagnetic Disturbances in the Earth's Upper Atmosphere, Ph.D. Thesis, University of Texas.

5. Bostick, F.X., Jr., C.E. Prince, Jr., and H.W. Smith, 1964: Propagation Characteristics of Plane Small Amplitude Hydromagnetic Disturbances in the Earth's Upper Atmosphere, EERL Rep. 135, Univ. of Texas.

6. Chang, H.H.C., 1961a: Magnetohydrodynamic Waves in the Ionosphere, Sci. Rept. No. 1, Contract AF 19(604)-7372, Hughes Research Laboratories. (AFCRL-64; AD 256588).

7. Chang, H.H.C., 1961b: Study of Magnetohydrodynamic Waves, Final Rept., Contract AF 19(604)-7372, Hughes Research Laboratories. (AFCRL-566; AD 262128).

8. Chapman, C.W., B.M. Fannin, and B.G. Gray, 1963: Calculated Refractive Indices for Small-Amplitude Geomagnetic Disturbances, EERL Rep. 6-58, Univ. of Texas. (AD 430888; AFCRL-64-228.)

9. Dungey, J.W., 1954a: The Propagation of Alfven Waves Through the Ionosphere, Scientific Report No. 56, Ionosphere Research Laboratory, State College, Pennsylvania.

10. Dungey, J.W., 1954b: Electrodynamics of the Outer Atmosphere, Scientific Report No. 69, Ionosphere Research Laboratory, State College, Pennsylvania.

11. Dungey, J.W., 1958: Cosmic Electrodynamics, Cambridge Univ. Press.

12. Fejer, J.A., 1960: "Hydromagnetic Wave Propagation in the Ionosphere," Jour. Atmosp. Terr. Phys., Vol. 18, Nos. 2/3, pp. 135-146.

13. Field, E.C., 1963: Hydromagnetic Signals in the Ionosphere, RAND RM-3830-PR. (AD 421842; NASA N64-16048.)

14. Field, E.C., and C. Greifinger, 1965: "Transmission of Geomagnetic Micropulsations Through the Ionosphere and Lower Exosphere," Jour. of Geophys. Res., Vol. 70, No. 19, pp. 4885-4899. (Also RAND RM-4494-ARPA, April 1965; AD 615164; NASA N65-27650.)

15. Field, E.C., and C. Greifinger, 1966: Equatorial Transmission of Geomagnetic Micropulsations Through the Ionosphere and Lower Exosphere, RAND RM-4858.

16. Greifinger, C., and P. Greifinger, 1964: Low-Frequency Hydromagnetic Waves in the Ionosphere, RAND RM-4225. (AD 607253.)

17. Greifinger, C., and P. Greifinger, 1965: "Transmission of Micropulsations Through the Lower Ionosphere," Jour. Geophys. Res., Vol. 70, No. 9, pp. 2217-2332. (Also RAND RM-4388, Feb. 1965; AD 610954; NASA N65-23006.)

18. Hodder, D.T., et.al., 1965: A Study of High Altitude Nuclear Blast Data, Rep No. 3, Contract No. DA-36-039-AMC-03729(E), USAEL, Ft. Monmouth, New Jersey, North American Aviation Rep. No. SID 64-143. (AD 458343.)

19. Jacobs, J.A., and T. Watanabe, 1962: "Propagation of Hydromagnetic Waves in the Lower Exosphere and the Origin of Short Period Geomagnetic Pulsations," Jour. Atmosph. Terr. Phys., Vol. 24, pp. 413-434.

20. Jenkins, A.W., Jr., and B.W. DuVall, 1965: Study of Micropulsations of About 1 Cycle Per Second, Final Report, Contract No. AF 19(628)-2477. (AD 463320.)

21. Kahalas, S.L., 1960: "Magnetohydrodynamic Wave Propagation in the Ionosphere," Phys. of Fluids, Vol. 3, No. 3, pp. 372-378.

22. Karplus, R. and W.E. Francis, 1960: "Hydromagnetic Waves in the Ionosphere," Jour. Geophs. Res., Vol. 65, No. 11, pp. 3593-3600.

23. Karplus, R., W.E. Francis, and A.J. Dragt, 1962: "The Attenuation of Hydromagnetic Waves in the Ionosphere," Planet. Space Sci., Vol. 9, pp. 771-785.

24. Kovach, R.L., and A. Ben-Menahem, 1966: "Analysis of Geomagnetic Micropulsations Due to High Altitude Nuclear Explosions," Jour. Geophys. Res., Vol. 71, No. 5, pp. 1427-1433.

25. Lehnert, B., 1956: "Magneto-hydrodynamic Waves in the Ionosphere and Their Application to Giant Pulsations," Tellus, Vol. 8, No. 2, pp. 241-251.

26. Li, T., C.E. Prince, Jr., and F.X. Bostick, Jr., 1964: Hydromagnetic Wave Propagation and Theoretical Power Spectra, EERL Rep 136, Univ. of Texas. (AD 446489.)

27. McDonald, G., 1961: "Spectrum of Hydromagnetic Waves in the Exosphere," Jour. of Geophys. Res., Vol. 66, No. 11, pp. 3639-3670. (NASA TR R-143).

28. Nishida, A., 1964: "Ionospheric Screening Effect and Storm Sudden Commencement," Jour. of Geophys. Res., Vol. 69, No. 9, pp. 1861-1874.

29. Piddington, J.H., 1959: "The Transmission of Geomagnetic Disturbances Through the Atmosphere and Interplanetary Space," Geophysic ournal (R.A.S.), Vol. 2, No. 3, pp. 173-189.

30. Prince, C.E., Jr., and F.X. Bostick, Jr., 1963: General Dispersion Relations for a Partially-Ionized Gas, EERL Rep. 129, Univ. of Texas. (AD 403127; NASA N63-20598).

31. Prince, C.E., Jr., and F.X. Bostick, Jr., 1964: "Ionospheric Transmission of Transversely Propagated Plane Waves at Micropulsation Frequencies and Theoretical Power Spectrums," Jour. of Geophys. Res., Vol. 69, pp. 3213-3234. (Also EERL Rep. 133, Univ. of Texas).

32. Prince, C.E., Jr., F.X. Bostick, Jr., and H.W. Smith, 1964: A Study of the Transmission of Plane Hydromagnetic Waves Through the Upper Atmosphere, EERL Rep. 134, Univ. of Texas. (AD 443875; NASA N64-30198).

33. Prince, C.E., Jr., F.X. Bostick, Jr., and H. W. Smith, 1965: "Impulse Response of the Magnetospheric Column," Jour. of Geophys. Res., Vol. 70, No. 19, pp. 4901-4908.

34. Smiley, R.F., 1964: The Penetration of Oblique Hydromagnetic Waves Through Horizontally Stratified Plasma and Un-Ionized Media, with Applications to the Lower Ionosphere, Final Report, Vol. I, Contract DA-36-039-SC-89177, USAEL, Ft. Monmouth, New Jersey, Doc. No. ARA-T-9197-13, Allied Research Associates, Inc., (AD 461698; NASA N65-23593).

35. Weinberg, S., 1962: "Eikonal Method in Magnetohydrodynamics," Phy. Rev., Vol. 126, No. 6, pp. 1899-1909.

Security Classification

DOCUMENT CONTROL DATA - R&D

(Security classification of title, body of abstract and indexing annotation must be entered when the overall report is classified)

1 ORIGINATING ACTIVITY (Corporate author)
Allied Research Associates, Inc.
Geophysics Division
Virginia Road, Concord, Massachusetts

2a REPORT SECURITY CLASSIFICATION
Unclassified

2b GROUP

3 REPORT TITLE
Wave Propagation Studies Related to the Theory of Near 1 cps Magnetic Effects of High Altitude Nuclear Detonations

4 DESCRIPTIVE NOTES (Type of report and inclusive dates)
Final Report - Volume II

5 AUTHOR(S) (Last name, first name, initial)
Smiley, Robert F.

6 REPORT DATE	7a TOTAL NO OF PAGES	7b NO OF REFS
October 1966	176	14

8a CONTRACT OR GRANT NO	9a ORIGINATOR'S REPORT NUMBER(S)
DA-28-043-AMC-01241(E)	9G17-14
b PROJECT NO 5011.11.854.01.33	9b OTHER REPORT NO(S) (Any other numbers that may be assigned this report) ECOM-01241-F
c	
d	

10 AVAILABILITY/LIMITATION NOTICES This document is subject to special export controls and each transmittal to foreign governments or foreign nationals may be made only with prior approval of CG, U.S. Army Electronics Command, Fort Monmouth, N.J., Attn: AMSEL-XL-S

11 SUPPLEMENTARY NOTES	12 SPONSORING MILITARY ACTIVITY
	U.S. Army Electronics Command Fort Monmouth, New Jersey 07703 Attn: AMSEL-XL-S

13 ABSTRACT

Results are presented from a group of theoretical studies of wave propagation in horizontally stratified media representative of the ionosphere and the sub-ionosphere. The report contains: four studies of the transient three-dimensional magnetic fields produced by magnetic dipoles in various combinations of horizontally stratified isotropic plasma and vacuum regions; and six studies of one-dimensional hydromagnetic wave propagation in horizontally stratified plasma and vacuum regions. Also included are bibliographies concerning natural ULF magnetotelluric effects, ULF lightning effects, reflection and refraction of hydromagnetic waves, and hydromagnetic wave propagation in the ionosphere.

DD FORM 1 JAN 64 1473

Security Classification

Unclassified

Security Classification

14 KEY WORDS	LINK A		LINK B		LINK C	
	ROLE	WT	ROLE	WT	ROLE	WT
Ionosphere Magnetohydrodynamics Wave Propagation Geophysics						

INSTRUCTIONS

1. ORIGINATING ACTIVITY: Enter the name and address of the contractor, subcontractor, grantee, Department of Defense activity or other organization *(corporate author)* issuing the report.

2a. REPORT SECURITY CLASSIFICATION: Enter the overall security classification of the report. Indicate whether "Restricted Data" is included. Marking is to be in accordance with appropriate security regulations.

2b. GROUP: Automatic downgrading is specified in DoD Directive 5200.10 and Armed Forces Industrial Manual. Enter the group number. Also, when applicable, show that optional markings have been used for Group 3 and Group 4 as authorized.

3. REPORT TITLE: Enter the complete report title in all capital letters. Titles in all cases should be unclassified. If a meaningful title cannot be selected without classification, show title classification in all capitals in parenthesis immediately following the title.

4. DESCRIPTIVE NOTES: If appropriate, enter the type of report, e.g., interim, progress, summary, annual, or final. Give the inclusive dates when a specific reporting period is covered.

5. AUTHOR(S): Enter the name(s) of author(s) as shown on or in the report. Enter last name, first name, middle initial. If military, show rank and branch of service. The name of the principal author is an absolute minimum requirement.

6. REPORT DATE: Enter the date of the report as day, month, year, or month, year. If more than one date appears on the report, use date of publication.

7a. TOTAL NUMBER OF PAGES: The total page count should follow normal pagination procedures, i.e., enter the number of pages containing information.

7b. NUMBER OF REFERENCES: Enter the total number of references cited in the report.

8a. CONTRACT OR GRANT NUMBER: If appropriate, enter the applicable number of the contract or grant under which the report was written.

8b, 8c, & 8d. PROJECT NUMBER: Enter the appropriate military department identification, such as project number, subproject number, system numbers, task number, etc.

9a. ORIGINATOR'S REPORT NUMBER(S): Enter the official report number by which the document will be identified and controlled by the originating activity. This number must be unique to this report.

9b. OTHER REPORT NUMBER(S): If the report has been assigned any other report numbers *(either by the originator or by the sponsor)*, also enter this number(s).

10. AVAILABILITY/LIMITATION NOTICES: Enter any limitations on further dissemination of the report, other than those imposed by security classification, using standard statements such as:

(1) "Qualified requesters may obtain copies of this report from DDC."

(2) "Foreign announcement and dissemination of this report by DDC is not authorized."

(3) "U. S. Government agencies may obtain copies of this report directly from DDC. Other qualified DDC users shall request through _____."

(4) "U. S. military agencies may obtain copies of this report directly from DDC. Other qualified users shall request through _____."

(5) "All distribution of this report is controlled. Qualified DDC users shall request through _____."

If the report has been furnished to the Office of Technical Services, Department of Commerce, for sale to the public, indicate this fact and enter the price, if known.

11. SUPPLEMENTARY NOTES: Use for additional explanatory notes.

12. SPONSORING MILITARY ACTIVITY: Enter the name of the departmental project office or laboratory sponsoring *(paying for)* the research and development. Include address.

13 ABSTRACT: Enter an abstract giving a brief and factual summary of the document indicative of the report, even though it may also appear elsewhere in the body of the technical report. If additional space is required, a continuation sheet shall be attached.

It is highly desirable that the abstract of classified reports be unclassified. Each paragraph of the abstract shall end with an indication of the military security classification of the information in the paragraph, represented as *(TS), (S), (C), or (U)*

There is no limitation on the length of the abstract. However, the suggested length is from 150 to 225 words.

14 KEY WORDS: Key words are technically meaningful terms or short phrases that characterize a report and may be used as index entries for cataloging the report. Key words must be selected so that no security classification is required. Identifiers, such as equipment model designation, trade name, military project code name, geographic location, may be used as key words but will be followed by an indication of technical context. The assignment of links, roles, and weights is optional.

Unclassified

Security Classification

END

DATE

FILMED

1-19-67